Dear reviewers, we have carefully reviewed the comments and revised the manuscript. We thank you for constructive remarks and took care to include all of them in the manuscript. We added a detailed reply to each point as addressed below.

Relevant changes:

- **Moved the methodology for estimating the geogenic P supply for AR from supplementary information to main text**
- **Merged the figures of geogenic P supply from the supplementary information and added them to the main text**
- **Moved the methodology for estimating the impacts on soil hydrology from supplementary information to main text**
- **Created subchapters on supplementary text for N-limited and N-unlimited AR results**
- **Changed the abstract as suggested by both reviewers**
- **Inclusion of Results chapter in the main text**
- **Changed the name of chapter Discussion to Discussion and implications**
- **Changed the figures according to reviewers suggestions**
- **Created a new figure for the hypothesis of increased harvest rates for Bioenergy grasses (Supplementary file)**

Reviewers comment

Our reply to Daniel Ibarra:

Comments 62: How does this older Gaillardet number compare to those more recently produced by co-author Hartmann's papers and Moon et al. (2014)? I would consider citing all of these sources and giving a range of the CO2 consumption rate by silicate weathering is.

In line 67 and 68 we gave the range and considered the suggested authors.

71-76: Work by Porder and Hilley, as well as Waldbauer and Chamberlain (2005) should be cited in this paragraph or previously.

The work of Porder and Hilley (2011) is cited in line 80, and Waldbauer and Chamberlain (2005) is cited in line 64.

97: Have others done this type of analysis or suggested this since von Liebig and Playfair (1843)?

We rephrased the sentence. According to Liebig's Law of the minimum(von Liebig and Playfair, 1843), biomass productivity will be limited by the scarcest nutrient in the soil. This law is widely applied to biological populations and in many ecosystem models. The new sentence is in line 103 to 106.

108: What about changes in precipitation and runoff?

The weathering rates of minerals are controlled by the following mechanisms: (i) soil pH (Lasaga et al., 1994;Grathwohl, 2014;Arshad et al., 1972); (ii) redox conditions for Fe and Mn minerals (Hering and Stum, 1990;Gilkes et al., 1973;Cánovas et al., 2019); (iii) soil solution composition (Lasaga et al., 1994;Grathwohl, 2014;Hayes et al., 2020) and soil moisture (Sverdrup et al., 1995;Appelo and Postma, 2005); (iv) temperature (Lasaga et al., 1994;Velbel et al., 1990;Hayes et al., 2020);

and (v) grain size/density of exposed structural defects on mineral surfaces (Lasaga et al., 1994;Arshad et al., 1972;Holdren Jr and Speyer, 1985;Cánovas et al., 2019). In this study we did not account for impact of changes in hydrology on weathering because model projections of hydrology in the future are not reliable. i.e. for most parts of the global model predictions it differs from each other despite similar boundary conditions (e.g. IPCC AR5). Model predictions of temperature change, on the other hand, are more reliable and all models agree on the sign (i.e. warming). Goll et al. (2014) used a simple weathering model that accounts for temperature, runoff and soil thickness controls on weathering, and illustrated that global warming was the dominating driver behind changes in weathering using climate change reconstructions from four earth system models. The reconstructions showed large differences with respect to hydrology and changes in global weathering rates to changes in temperature were rather minor. The temperature sensitivity of global weathering rates was significant and rather homogenous among four different climate models. The temperature sensitivity implicitly accounts for changes in hydrology, however it is not able to capture regional differences. Thus we only account for the T changes. This was done earlier in Sun et al. (2017) Earth's Future.

Besides the large uncertainty with respect to climate change projections, current data availability is insufficient to calibrate a complex global model, which are currently only applied on site to catchment scale (Pierret et al., 2018;Ackerer et al., 2018;Beaulieu et al., 2016). We argue that a simple model of weathering is appropriate. The used model is very simplistic but the used weathering rates were calibrated on 381 catchments in Japan (Hartmann et al., 2009) and describes the chemical weathering as a function of runoff and lithology, temperature and soil thickness (Hartmann et al., 2014). The model is increasingly used for global scale studies (Sun et al., 2017;Goll et al., 2014;Wang et al., 2018). We included part of this discussion in line 216 to line 222.

Relatedly, what are the "Parameters" in yellow in Figure 1? It might help to list them on the figure.

We rearranged Fig.1 and they are explicitly specified there.

169: In addition to Figure 1, a schematic of what is actually being done in the methods own so please specify in parentheticals and provide the median or mean estimate.

We rearranged Fig.1, so the used steps are clearer and they refer to the respective chapter sections and used equations.

191: Again, what about changes in runoff to weathering rate?

See above.

What is this 9%/degC equivalent to in an Arrhenius style calculation? While temperature increases make sense (kinetics) much of the world weathers chemostatically (equilibirium, see Winnick and Maher (2018, EPSL) and papers by Godsey for example) so changes in soil infiltration rate (P-ET = runoff) and thus soil moisture should also influence these changes.

The Arrhenius corresponding average increase is 6.5%/°C for basalt that had an average activation energy of 50 kJ/mol, ~3%/°C for carbonate activation energy of 24 kJ/mol, and ~10%/°C for a felsic rock type activation energy of 74 kJ/mol (Figure 1). Our 9%/°C value is also based on the Arrhenius calculation but represents the average value considering different lithotypes (they had mean apparent activation energies ranging from 50 to 80 kJ/mol and a deviation of ± 20 kJ/mol, based on field data and laboratory experiments (Goll et al., 2014)).

The apparent temperature sensitivity of weathering from Goll et al. (2014) implicitly includes changes in hydrology as it is derived from global model simulations using a model which describes the chemical weathering as a function of runoff and lithology, temperature and soil thickness (Hartmann et al., 2014). As lay down above we omit a more detailed representation of water effects due to high uncertainty with respect to projections of hydrology (IPCC AR5) and as temperature was found to be the dominant driver of changes (Goll et al., 2014).

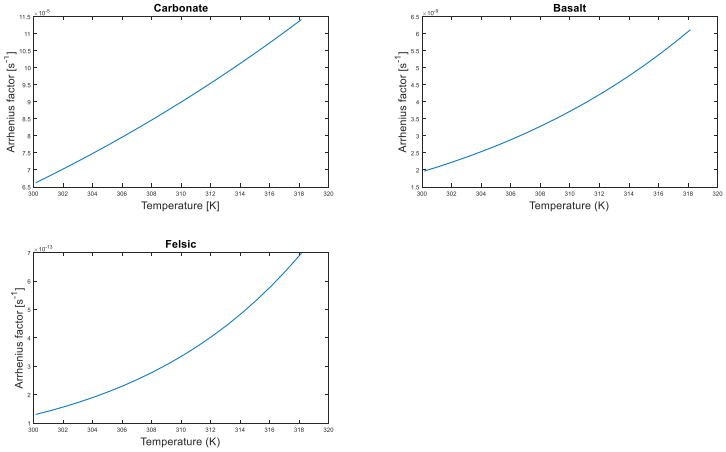

Figure 1: Increases in weathering rates for different temperatures (T), in Kelvin, estimated according to Arrhenius equation ($Arrhenius\ factor = e^{-Ae/(R*T)}$) for a gas constant R of 0.00831 kJ $K^{-1}mol^{-1}$. Average of 6.5%/°C increase for basalt that had an average activation energy (Ae) of 50 kJ/mol, average increase of ~3%/°C for carbonate activation energy of 24 kJ/mol, and average increase of ~10%/°C for a felsic rock type activation energy of 74 kJ/mol.

220-233: What about the grain size of the rock powder be applied? Does that matter at all? I assume it would be based on reactive transport simulations such as those by Maher (2010, 2011) for example. And relatedly how fine the rock is powdered will change the texture described in the next section right?

Yes, the grain size matters since it will influence on the exposed reactive surface area (generally fine textured basalt powder would have a high reactive surface area than a coarser textured basalt powder) and consequently the weathering rates. However, in our approach we considered that the grain sizes would range in between 0.6 – 90 µm (for the fine basalt powder) which is enough to completely dissolve the deployed rock powder after one year (Strefler et al., 2018). For the coarse basalt powder ~70% of its granulometry fall into the 0.6 – 90 µm range and from the other 30%, at least 20% would be dissolved in one year (Strefler et al., 2018). The finest grain size we can consider is the clay size which comprehends grains >1 µm and <3.9 µm. If a basalt powder would have only clay size granulometry, the effects on soil hydraulic conductivity would decrease in average by 37% for deployment amount of 30 kg basalt m^{-2} (for the same deployment amount and for the fine rock powder used in our work, the hydraulic conductivity would decrease by 2%). However, the finer the grain gets the higher the energy input for grinding is, which can drastically affect the costs of EW (it can reach up to 500$/t$CO_2$ sequestered; Strefler et al., 2018). Part of this discussion is included in line 254 to 255. Additionally, we make it clear that we used grain sizes not higher than 90 µm in line 279 to 283 and discussed about the assumptions of full dissolution in chapter 4.4 in line 562.

240-243: Thus, this scenario will be the maximum effect? I think that should be stated explicitly here and elsewhere.

Thanks, now it is explicitly stated in lines 283, 285, 393, and 394.

248 (equation 10) and text surrounding: Is this the 'pedotransfer function' mentioned in the above paragraph? Is the only empirical values the lambda? Further, where does the 1930 in the equation come from? A lot of this appears to be buried in the supplement, maybe it'd be more helpful if it is more explicitly stated that this is from Saxton and Rawls (2006) upfront in this section.

This is one of the used pedotransfer functions. The 1930 is a constant (i.e., a regression coefficient) which is dependent on the database used to derive the pedotransfer equation as described in the work from (Campbell, 1974). Now the pedotransfer equations are present in the main text in subchapter 2.6. No, lambda is estimated according to equation 18. The empirical values are the organic matter content and the granulometry of soil and rock powder (equations 15-17).

332: What about other soil types? Is this information in the literature? What is the most common agricultural soil type?

Considering the extension, Oxisols are the most common agricultural soil type followed by Ultisols. We added the value for Ultisol in line 450 to 453.

379: But if they are empirical wouldn't those datasets inherently have clay minerals forming in those systems? In general, I think the caveats brought up in this paragraph should be acknowledged earlier in the paper.

The used databases probably contained clay minerals in the clay-sized fraction of the soils. But the Saxton and Rawls (2006) equations accounted only for soil texture and soil organic matter content influences on water retention and hydraulic conductivity. The sentence was misleading and we changed it. You can find the improved sentence in line 523 to 531. What was meant by the old sentence was that once the rock powder will be added into the soil, the primary minerals will be weathered and genesis of clay minerals can occur. The new formed clay minerals will positively contribute to water retention in soil, since clay minerals with high cation exchange capacity were able to significantly influence soil water retention at a matric potential of -33 kPa (Gaiser et al., 2000). We have also included the potential effect of expected increase in soil organic carbon/matter on plant available water. We placed the caveats in the methodology section (lines 328 to 333) and rephrased the old sentence from line 379, which is now in line 523 to 531.

Specific Line by Line Comments 19,21 and 22: Are these ranges 95%/2 sigma ranges? Lines 147 and 172 suggests that this might be driven by the minimum and maximum harvest rates. What is the central estimate? Abstract should be able to stand on it's own so please specify in parentheticals and provide the median or mean estimate.

Now we explicitly correlate the amount sequestered for each geogenic P supply scenario and AR P demand (high, corresponding to 95th quartile of wood chemistry and low corresponding to 5th quartile of wood chemistry). You can find it in line 20 to 25.

33 and 34: Please put "i.e." and "e.g." phrases in parentheticals

We did the changes.

59: Suggest authors but "i.e., P, Mg, Ca and K" in the parenthetical before the citation. I also think some more recent work should be cited here and in the next line (60) for controls on atmospheric CO2 over geologic timescales.

We did the changes and cited the study from Singh and Schulze (2015) for weathering as the natural source nutrients (line 63) and the study from Yasunari (2020) for the weathering as control on atmospheric CO_2 (line 65)

185: Are the databases sources at most 2 by 2 degrees?

No, By common convention, fine spatial resolution data are generally upscaled to fit the coarse spatial resolution framework to minimize distortions of location (Pontius, 2000). Besides that downscaling a coarse data is not suggested since information on finer resolution is missing. We added this information in line 202 to line 203.

196: Suggest putting "cf. Wang et al. (2017)..." as a parenthetical

We accepted the suggestion, you can find it in line 211.

223: Please add citation and average P content in basalt here.

You can find the accepted suggestions in line 258 and 259. Additionally we improved the description on data selection for calculating the descriptive statistics from line 243 to 252.

262: "here estimated" is confusing.

We rephrased the sentence. Now it is explicitly said which equations were used to obtain the estimated numbers. You can check it in line 341 to 350.

282-283: Is this a citation in the parenthetical?

We corrected the citation. You can find it in line 443.

307: "under study"?

We changed the sentence, you can find the changes in line 458 to line 460.

387: please fix grammar of this sentence

We rephrased it. You can find the new sentence in chapter 4.4 line 537 to line 539.

442: I would suggest citing Uhlig's papers here rather than what I believe from the reference list list is the PhD thesis. The papers are Uhlig et al. (2017, Biogeosciences) and Uhlig and von Blanckenburg (2019, Frontiers in Earth Science).

We added the suggested citations. You can find them in line 610.

Reviewers comment

Our reply to anonymous Referee:

Major comments:

A number of uncertainties are considered in the paper, but it seems that a lot of weight is given to some uncertainties, while other potentially large uncertainties are neglected. For example, only a single CO_2/climate scenario is considered and for this particular scenario only results from a single afforestation/bioenergy model is used. What was the reason to choose this particular climate scenario?

The representative greenhouse concentration pathway 4.5 (RCP4.5) was used (Thomson et al., 2011) since it assumes a emission peak around 2040 and considers that forest lands expand from their present day extent (Thomson et al., 2011). Therefore, this CO_2 climate scenario seemed to be the most suited for our purposes since forest expansion under the RCP2.6 is lower than that for the RCP4.5 and RCP8.5 scenarios (van Vuuren et al., 2011). The RCP8.5 scenario assumes no climate policy being adopted and consequently the expansion on forest cover does not occur (van Vuuren et al., 2011). There are at least 9 different terrestrial ecosystem models for coupled C-nutrient cycle. We selected the JSBACH since it considers the same level of competition between plants and decomposing microbes for N supply, while other numerical models prioritize immobilization or plant growth (Achat et al., 2016). Based on simulations from Parida (2011), prioritizing the Plant N uptake is unrealistic because soil microbes are more competitive for soil N as compared by plants. Besides that, the selected AR model considers the impacts on biomass productivity due to natural N supply or to N fertilization at a global scale AR deployment (we considered this comment in lines 133 to 148 for AR).

Since we want to point out the influence of plant nutrition on biomass growth, using other numerical models would not change our final message (that is: Geogenic nutrient supply can limit biomass growth and consequently reduce the sequestered CO_2 potential of large scale AR).

This is seen for AR since simulations using the RCP4.5 land pattern that accounted for the RCP8.5 scenario for tree harvest rates and atmospheric CO_2 concentrations. The resulting output showed similar areas of forest growth and higher biomass productivity (Sonntag et al., 2016). However, these results did not consider natural N supply and consequently biomass productivity would be N limited, which would decrease the amount of Carbon within Biomass. Similar areas can also be observed in the study from Yousefpour et al. (2019) in Figure 2c for different RCP scenarios.

The selected bioenergy model can minimize total costs of production. It also accounts for vegetation composition and distribution for both natural and agricultural ecosystems. Additionally, it considers socio-economic conditions of a system. We selected the RCP4.5 scenario for bioenergy grasses (BG) to keep the MAgPIE simulations corresponding to the JSBACH simulations (we considered this comment in lines 155 to 156 for BG). In the case of BG, to keep high yields or maintain a selected harvest rate, it will be necessary to replenish the exported nutrients by harvest. Therefore, external source of nutrients will be necessary. Accounting for another model rather than MAgPIE would probably change the estimated minimum and maximum harvest rates for Bioenergy grasses, which would impact the necessary amount of rock powder to replenish the exported nutrients due to harvest rates. Thus, we added a hypothetical scenario assuming that the estimated maximum harvest rate by MAgPIE could be increased by one order of magnitude, even though this is unlikely to occur. Adding a scenario accounting for decrease in harvest rates is not necessary, since it is already presented in Fig. 8 from the main text by the filled horizontal lines. However, decreasing the minimum a harvest rate by a factor of two or three also represent a decrease in the minimum amount of rock powder necessary to replenish the exported nutrients by harvest.

Since the core messages of our study are: (i) Biomass productivity is limited by geogenic P supply; (ii) EW is an alternative for supplying nutrients besides the potential to keep a net positive CO_2 balance; and (iii) the effect of EW on soil hydrology can be neglected in some parts of the world, but EW has the potential to alleviate water stress, at some extent, in areas that drought occurs. Accounting for other models either for AR or bioenergy grasses would not change the general message.

A discussion on the applicability of the conclusions drawn from the paper to alternative scenarios should be included.

We included the discussion on chapter 4.1 in lines 461 to 467 considering the results from others AR model that assumes RCP8.5 for an RCP4.5 land evolution scenario. And we have also acknowledged your point (that "even using only one model induces uncertainty" the general message of the study would not change) in the last sentence.

We included a discussion for the harvest rates obtained from the MAgPIE simulations. In this discussion we assume a hypothetical one order of magnitude increase in the maximum harvest rate. The discussion is presented on chapter 4.2 in line 488 to 498.

For the carbon sequestration from afforestation you mention (line 260) that the available estimates of carbon uptake vary between 0.3 and 3.3 GtC/a, while in the paper a value of 2 GtC/a is used.

This is the value for the AR scenario from Kracher (2017), the same model shows a carbon sequestration of ~2.4 Gt C a^{-1} if N supply is unlimited. We have shown that it can fall to ~1.3 Gt C a^{-1} if geogenic P supply scenario one for mean P content within wood and leaves is selected. This number would change for another AR scenario. But the main message is that the estimated C sequestration by biomass on terrestrial carbon cycle models can fall if nutrient supply is accounted for.

On the other hand, a lot of weight in the uncertainty is given to e.g. the P concentration in basalt (5-95th percentiles). To my understanding it seems that this uncertainty is not so relevant for the present study, as I assume that for the use in EW basalt with relatively high P concentrations could in principle be selected. Would the interquartile range possible provide a more appropriate measure of the uncertainty in this parameter?

For EW, we need to firstly know rock mineralogical composition and petrography. Therefore, it is more interesting a basalt with high pyroxene group minerals content (especially the ones rich in Ca and Mg like Diopside) since these minerals would weather more rapidly (cf. Table 1 at Hartmann et al. (2013)) and less olivine or sulfide minerals content (Olivine can have high content of Nickel and Chromium that are trace elements problematic for agriculture (Edwards et al., 2017); Sulfide minerals can cause acid rock drainage if pyrite (a sulfide mineral) concentration is within 1% or 2% (Earle, 2018)). As an example, Alkali basalt can have P concentration >3000 ppm (Porder and Ramachandran, 2013), but it is rich in olivine (John, 2001;Irvine and Baragar, 1971). Therefore, in this study we have adopted a more strict data selection from the EarthChem database. We selected only the rocks exclusively named as rhyolite, dacite, andesite, and basalt. This resulted in 2985 samples for rhyolite, 3008 samples for dacite, 11099 samples for andesite, and 23816 samples for basalt. Comparing our P concentration values to other works, we see that the median P value of 916 ppm from Porder and Ramachandran (2013) is higher than ours (500 ppm of P). This occurs because Porder and Ramachandran (2013) did a broader classification, resulting in 97895 used samples, and neglected possible unwanted side-effects of trace minerals in basalt mineralogy. Therefore, the selected quartiles for rock chemistry (either for Basalt or other rock used in our study) are a conservative estimation and assuming interquartile values would decrease even more the consideration of potential rock sources for EW.

In general in the paper it is difficult to immediately associate the uncertainty ranges to uncertainty sources.

*We re-structured the paper. The results are discussed in a separate section. We also renamed the old section "results and discussion" to **Discussion and implications**, which contain the discussion for the presented results and implications to rock powder deployment.*

For AR it seems that the largest uncertainty is related to the geogenic P-supply, with scenario two showing basically no P limitation. Is there really no observation-based evidence to suggest that one or the other scenario is more realistic? This is a fundamental question for the purpose of the paper, because if P limitation is not an issue the benefit of EW in these areas will be limited to the direct CO2 consumption by weathering.

Basically, the uncertainties for the AR scenario are from biomass P demand and the geogenic P supply, with the later influencing the most our results as it was seen. Unfortunately, given current understanding of bioavailability of soil P and soil P estimates uncertainties are large with respect to how much P is available to support future plant growth (detailed analysis and discussion is found in Sun et al. (2017)) and thus AR and BG. Mineral P is likely limiting biomass production in European forests today (Jonard et al., 2015), tropical forest (Turner et al., 2018), boreal forests (Shinjini et al., 2018), as well as agricultural areas (e.g., Ringeval et al., 2019 in discussion;Kvakić et al., 2018). This situation is likely to deteriorate in the future. Therefore, considering that the inorganic and organic labile P pools will be completely available for tree nutrition is unlikely to occur. Thus, Geogenic supply Scenario 2 is a very optimistic assumption that might not correspond to reality based on the already observed P limitation on different ecosystems (Elser et al., 2007). However, we cannot rule out that gradual shifts in soil organic P fractions occur, which make comparable amounts of P as in scenario 2 available over time, We therefore opted to show both scenarios as these are a major source of uncertainty with respect to P effects on future plant growth (as has been demonstrated by Sun et al. (2017)).

In the main text there are many references to supplementary materials. References to supplementary material should be limited as much as possible for a better readability of the paper, considering also that papers in Biogeosciences are not subject to strict length limitations. Since the main paper contains only relatively few figures, I would suggest to move some of the figures from the supplementary to the main paper. For example Figs S1,S2,S3 could be merged into one figure and added to the paper. It would help to get an idea of the numbers that could then be more easily compared with e.g. the P gap in Fig. 2. I would also strongly suggest to add Fig. S8 to the main paper.

We appreciate your suggestions and have considered them. Now the Figs. S1 to S3 is the Fig. 3 in the mains text. The Fig. S8 now is the Fig. 4 in the main text (which also include the estimated P gaps for the AR scenario).

The results for the N-unlimited scenario, which are not discussed in the main text, could be presented in a separate section in the supplementary material. It is very confusing to find figures from N-unlimited experiments mixed inbetween N-limited figures.

Now in the Chapter B from the supplementary material we have the results for the AR N-limited for the 5th and 95th quartile of wood P content in the subchapter 'i'. The AR N-unlimited results are presented within the subchapter 'ii'.

Minor comments:

Figures should be numbered progressively according to where they are referenced in the text (i.e. Fig. 1 should be referenced before Fig. 2). This is valid also for figures in the supplementary.

We did the suggestion. You can find it in the supplementary file S1.docx line 47 to 53.

Line 21-22: you need to mention what scenario you are considering here, otherwise the numbers make no sense since they will be strongly dependent on future CO2/climate evolution.

Now we explicitly correlate the amount sequestered for each geogenic P supply scenario and AR P demand (high, corresponding to 95th quartile of wood chemistry and low corresponding to 5th quartile of wood chemistry). Line 20 to line 25.

Line 23: 'K' not defined here

Now it is defined (line 26).

Line 22: it would be helpful if the same unit would be used, either GtC or GtCO2. Otherwise it is difficult to compare the numbers.

Now they are in the same unit (GtC) line 25.

Line 95: '...we discuss only the N-limited AR scenario...'

We did the change, you can see it in line 102.

Line 119: please check this sentence

The sentence was deleted.

Line 147: are these numbers global averages for the areas with bioenergy plantations?

No, they are global minimum and maximum. They are necessary since for bio-energy crops the amount of exported nutrients by harvest need to be replenished to keep with the specific harvest rate. The sentence was reformulated, you can see it in line 164.

Line 186: nearest neighbour interpolation does not seem to be a very good interpolation choice for very high resolution input data (e.g. geogenic P release rates). A single 1 km^2 value will not be very representative for a 2x2_ cell.

No, according to Christman and Rogan (2012) the nearest-neighbor scaling method can keep with the overall proportions of the original fine resolution map. This is because the interpolant exhibits the smallest variation of the interpolant function while meeting the measured data. Since we are interested in P concentrations (supplied by weathering, atmospheric deposition, or different soil pools) the degree of discontinuity is very high (i.e., they are spatially and temporally heterogeneous) and using a more robust interpolation algorithm (i.e., Cubic-Spline) could result in new minima and maxima values in the original maps, which would be a wrong result. If the Best Linear Unbiased Estimator (i.e., Kriging) algorithm is selected, it would be necessary to know the proper semivariogram function or assume one based on tests to check its appropriateness or on the uncertainty estimation. Therefore, to preserve the limits of different geogenic P release rates represented by the fine resolution map from Hartmann et al. (2014) and due to its simplicity compared to the other interpolation algorithms, we selected the nearest-neighbor interpolation method. You can see these justifications in line 202 to line 204.

Line 425: where does this number come from?

We rephrased the sentence. Now you can find it in line 592.

References

Achat, D. L., Augusto, L., Gallet-Budynek, A., and Loustau, D.: Future challenges in coupled C–N–P cycle models for terrestrial ecosystems under global change: a review, Biogeochemistry, 131, 173-202, 10.1007/s10533-016-0274-9, 2016.

Ackerer, J., Chabaux, F., Lucas, Y., Clément, A., Fritz, B., Beaulieu, E., Viville, D., Pierret, M. C., Gangloff, S., and Négrel, P.: Monitoring and reactive-transport modeling of the spatial and temporal variations of the Strengbach spring hydrochemistry, Geochimica et Cosmochimica Acta, 225, 17-35, https://doi.org/10.1016/j.gca.2018.01.025, 2018.

Appelo, C. A. J., and Postma, D.: Geochemistry, Groundwater and Pollution, Second Edition, 2005.

Arshad, M., St. Arnaud, R., and Huang, P.: Dissolution of trioctahedral layer silicates by ammonium oxalate, sodium dithionite–citrate–bicarbonate, and potassium pyrophosphate, Canadian Journal of Soil Science, 52, 19-26, 1972.

Beaulieu, E., Lucas, Y., Viville, D., Chabaux, F., Ackerer, P., Goddéris, Y., and Pierret, M.-C.: Hydrological and vegetation response to climate change in a forested mountainous catchment, Modeling Earth Systems and Environment, 2, 1-15, 10.1007/s40808-016-0244-1, 2016.

Campbell, G. S.: A simple method for determining unsaturated conductivity from moisture retention data, Soil science, 117, 311-314, 1974.

Cánovas, C. R., De La Aleja, C. G., Macías, F., Pérez-López, R., Basallote, M. D., Olías, M., and Nieto, J. M.: Mineral reactivity in sulphide mine wastes: influence of mineralogy and grain size on metal release, European Journal of Mineralogy, 31, 263-273, 10.1127/ejm/2019/0031-2843, 2019.

Christman, Z. J., and Rogan, J.: Error Propagation in Raster Data Integration, Photogrammetric Engineering & Remote Sensing, 78, 617-624, 2012.

Earle, S.: Physical geology, 2018.

Edwards, D. P., Lim, F., James, R. H., Pearce, C. R., Scholes, J., Freckleton, R. P., and Beerling, D. J.: Climate change mitigation: potential benefits and pitfalls of enhanced rock weathering in tropical agriculture, Biology letters, 13, 20160715, 2017.

Elser, J. J., Bracken, M. E. S., Cleland, E. E., Gruner, D. S., Harpole, W. S., Hillebrand, H., Ngai, J. T., Seabloom, E. W., Shurin, J. B., and Smith, J. E.: Global analysis of nitrogen and phosphorus limitation of primary producers in freshwater, marine and terrestrial ecosystems, Ecology Letters, 10, 1135-1142, doi:10.1111/j.1461-0248.2007.01113.x, 2007.

Gaiser, T., Graef, F., Cordeiro, J., eacute, and Carvalho: Water retention characteristics of soils with contrasting clay mineral composition in semi-arid tropical regions, Soil Research, 38, 523-536, https://doi.org/10.1071/SR99001, 2000.

Gilkes, R., Young, R., and Quirk, J.: Artificial Weathering of Oxidized Biotite: I. Potassium Removal by Sodium Chloride and Sodium Tetraphenylboron Solutions 1, Soil Science Society of America Journal, 37, 25-28, 1973.

Goll, D. S., Moosdorf, N., Hartmann, J., and Brovkin, V.: Climate-driven changes in chemical weathering and associated phosphorus release since 1850: Implications for the land carbon balance, Geophysical Research Letters, 41, 3553-3558, doi:10.1002/2014GL059471, 2014.

Grathwohl, P.: On equilibration of pore water in column leaching tests, Waste Management, 34, 908-918, https://doi.org/10.1016/j.wasman.2014.02.012, 2014.

Hartmann, J., Jansen, N., Dürr, H. H., Kempe, S., and Köhler, P.: Global CO2-consumption by chemical weathering: What is the contribution of highly active weathering regions?, Global and Planetary Change, 69, 185-194, 2009.
Hartmann, J., Moosdorf, N., Lauerwald, R., Hinderer, M., and West, A. J.: Global chemical weathering and associated P-release - The role of lithology, temperature and soil properties, Chemical Geology, 363, 145-163, 10.1016/j.chemgeo.2013.10.025, 2014.
Hayes, N. R., Buss, H. L., Moore, O. W., Krám, P., and Pancost, R. D.: Controls on granitic weathering fronts in contrasting climates, Chemical Geology, 535, 119450, https://doi.org/10.1016/j.chemgeo.2019.119450, 2020.
Hering, J., and Stum, W.: Oxidative and reductive dissolution of minerals, Rev. Mineral., 23, 427-465, 1990.
Holdren Jr, G. R., and Speyer, P. M.: Reaction rate-surface area relationships during the early stages of weathering—I. Initial observations, Geochimica et Cosmochimica Acta, 49, 675-681, 1985.
Irvine, T., and Baragar, W.: A guide to the chemical classification of the common volcanic rocks, Canadian journal of earth sciences, 8, 523-548, 1971.
John, W.: An introduction to igneous and metamorphic petrology, 552.1 W 784552.1 W 784552.1 W 784552.1 W 784, 2001.
Kvakić, M., Pellerin, S., Ciais, P., Achat, D. L., Augusto, L., Denoroy, P., Gerber, J. S., Goll, D., Mollier, A., Mueller, N. D., Wang, X., and Ringeval, B.: Quantifying the Limitation to World Cereal Production Due To Soil Phosphorus Status, Global Biogeochemical Cycles, 32, 143-157, 10.1002/2017gb005754, 2018.
Lasaga, A. C., Soler, J. M., Ganor, J., Burch, T. E., and Nagy, K. L.: Chemical weathering rate laws and global geochemical cycles, Geochimica et Cosmochimica Acta, 58, 2361-2386, 1994.
Parida, B.: The influence of plant nitrogen availability on the global carbon cycle and N2O emissions, University of Hamburg Hamburg, 2011.
Pierret, M.-C., Cotel, S., Ackerer, P., Beaulieu, E., Benarioumlil, S., Boucher, M., Boutin, R., Chabaux, F., Delay, F., Fourtet, C., Friedmann, P., Fritz, B., Gangloff, S., Girard, J.-F., Legtchenko, A., Viville, D., Weill, S., and Probst, A.: The Strengbach Catchment: A Multidisciplinary Environmental Sentry for 30 Years, Vadose Zone Journal, 17, 10.2136/vzj2018.04.0090, 2018.
Pontius, R.: Quantification error versus location error in comparison of categorical maps, Photogrammetric Engineering and Remote Sensing, 66, 540-540, 2000.
Porder, S., and Hilley, G. E.: Linking chronosequences with the rest of the world: predicting soil phosphorus content in denuding landscapes, Biogeochemistry, 102, 153-166, 10.1007/s10533-010-9428-3, 2011.
Porder, S., and Ramachandran, S.: The phosphorus concentration of common rocks—a potential driver of ecosystem P status, Plant and soil, 367, 41-55, 2013.
Ringeval, B., Kvakić, M., Augusto, L., Ciais, P., Goll, D., Mueller, N. D., Müller, C., Nesme, T., Vuichard, N., Wang, X., and Pellerin, S.: Insights on nitrogen and phosphorus co-limitation in global croplands from theoretical and modelling fertilization experiments, Biogeosciences Discuss., 2019, 1-35, 10.5194/bg-2019-298, 2019.
Saxton, K. E., and Rawls, W. J.: Soil water characteristic estimates by texture and organic matter for hydrologic solutions, Soil science society of America Journal, 70, 1569-1578, 2006.
Shinjini, G., C., F. M., A., V. M., Mariann, G. J., D., Y. R., and J., F. T.: Phosphorus limitation of aboveground production in northern hardwood forests, Ecology, 99, 438-449, doi:10.1002/ecy.2100, 2018.
Singh, B., and Schulze, D.: Soil minerals and plant nutrition, Nature Education Knowledge, 6, 1, 2015.
Strefler, J., Amann, T., Bauer, N., Kriegler, E., and Hartmann, J.: Potential and costs of Carbon Dioxide Removal by Enhanced Weathering of rocks, Environmental Research Letters, 2018.

Sun, Y., Peng, S., Goll, D. S., Ciais, P., Guenet, B., Guimberteau, M., Hinsinger, P., Janssens, I. A., Peñuelas, J., Piao, S., Poulter, B., Violette, A., Yang, X., Yin, Y., and Zeng, H.: Diagnosing phosphorus limitations in natural terrestrial ecosystems in carbon cycle models, Earth's Future, 10.1002/2016ef000472, 2017.
Sverdrup, H., Warfvinge, P., Blake, L., and Goulding, K.: Modelling recent and historic soil data from the Rothamsted Experimental Station, UK using SAFE, Agriculture, Ecosystems & Environment, 53, 161-177, https://doi.org/10.1016/0167-8809(94)00558-V, 1995.
Turner, B. L., Brenes-Arguedas, T., and Condit, R.: Pervasive phosphorus limitation of tree species but not communities in tropical forests, Nature, 555, 367-370, 10.1038/nature25789, 2018.
Velbel, M., Taylor, A., and Romero, N.: Effect of temperature on feldspar weathering rates in alpine and non-alpine watersheds, Geol. Soc. Am. Abstr. Program, 1990, 49,
von Liebig, J. F., and Playfair, L. P. B.: Chemistry in its application to agriculture and physiology, JM Campbell, 1843.
Waldbauer, J. R., and Chamberlain, C. P.: Influence of uplift, weathering, and base cation supply on past and future CO 2 levels, in: A history of atmospheric CO2 and its effects on Plants, Animals, and Ecosystems, Springer, 166-184, 2005.
Wang, Y., Ciais, P., Goll, D., Huang, Y., Luo, Y., Wang, Y. P., Bloom, A. A., Broquet, G., Hartmann, J., Peng, S., Penuelas, J., Piao, S., Sardans, J., Stocker, B. D., Wang, R., Zaehle, S., and Zechmeister-Boltenstern, S.: GOLUM-CNP v1.0: a data-driven modeling of carbon, nitrogen and phosphorus cycles in major terrestrial biomes, Geosci. Model Dev., 11, 3903-3928, 10.5194/gmd-11-3903-2018, 2018.
Yasunari, T.: The Uplift of the Himalaya-Tibetan Plateau and Human Evolution: An Overview on the Connection Among the Tectonics, Eco-Climate System and Human Evolution During the Neogene Through the Quaternary Period, in: Himalayan Weather and Climate and their Impact on the Environment, edited by: Dimri, A. P., Bookhagen, B., Stoffel, M., and Yasunari, T., Springer International Publishing, Cham, 281-305, 2020.
Yousefpour, R., Nabel, J. E., and Pongratz, J.: Simulating growth-based harvest adaptive to future climate change, Biogeosciences, 16, 241-254, 2019.

Impacts of Enhanced Weathering on biomass production for negative emission technologies and soil hydrology

Wagner de Oliveira Garcia*[1], Thorben Amann[1], Jens Hartmann[1], Kristine Karstens[2], Alexander Popp[2], Lena R. Boysen[3], Pete Smith[4], Daniel Goll[5,6]

[1]Institute for Geology, Center for Earth System Research and Sustainability, Universität Hamburg, Germany
[2]Potsdam Institute for Climate Impact Research (PIK), Germany
[3]Max Planck Institute for Meteorology, Germany
[4]Institute of Biological and Environmental Sciences, School of Biological Sciences, University of Aberdeen
[5]Laboratoire des Sciences du Climat et de l'Environnement, CEA CNRS UVSQ, 91190 Gif-sur-Yvette, France

[6]Institute of Geography, University Augsburg, Germany

Correspondense to: Wagner de Oliveira Garcia (wagner.o.garcia@gmail.com) ORCID: https://orcid.org/0000-0001-9559-0629

Abstract. Limiting global mean temperature changes to well below 2°C likely requires a rapid and large-scale deployment of Negative Emission Technologies (NETs). Assessments so far showed a high potential for biomass based terrestrial NETs, but only few included effects of the commonly found nutrient deficient soils on biomass production. Here, we investigate the deployment of Enhanced Weathering (EW) to supply nutrients to phosphorus (P) deficient areas of Afforestation/Reforestation and naturally growing forests (AR) and bio-energy grasses (BG), besides the impacts on soil hydrology. Using stoichiometric ratios and biomass estimates from two established vegetation models, we calculated the nutrient demand of AR and BG. ~~By comparing the inferred AR P demand to different~~Insufficient geogenic P supply ~~scenarios, we estimated that 3 – 98 Gt~~ limits C ~~of the predicted~~storage in biomass ~~accumulation cannot be realized due to insufficient soil~~. For a mean P demand by AR and a low geogenic P supply ~~for an AR~~ scenario ~~considering natural N~~, AR would sequester 119 Gt C in biomass; for high geogenic P supply~~. An~~ and low AR P demand scenario, 187 Gt C would be sequestered in biomass; and for a low geogenic P supply and high AR P demand, only 92 Gt C would be accumulated by biomass. An average amount of ~~2 – 362~~~150 Gt basalt powder applied ~~by~~for EW would be needed to ~~cover~~close global P gaps and completely sequester projected amounts of 190 Gt C during years 2006 – 2099~~. The~~ for the mean AR P demand scenario (2 – 362 Gt basalt powder for the low AR P demand and for the high AR P demand scenarios would be necessary respectively). The average potential of carbon sequestration by EW until 2099 is ~12 Gt C (~0.6~~ – 97.8 Gt CO_2 for the same scenario.~~2 – ~27 Gt C) for the specified scenarios (excluding additional carbon sequestration via alkalinity production). For BG, 8 kg basalt m^{-2} a^{-1} might, on average, replenish the exported potassium (K) and P by harvest. Using pedotransfer functions, we show that the impacts of basalt powder application on soil hydraulic conductivity and plant available water, ~~for closing~~to close predicted P gaps, would depend on basalt and soil texture, but in general the impacts are marginal. We show that EW could potentially close the projected P gaps of an AR scenario, and exported nutrients by BG harvest, which would decrease or replace the use of industrial fertilizers. Besides that, EW ameliorates ~~soil~~the soils capacity to retain nutrients~~,~~ and soil pH, and ~~renew~~replenish soil nutrient pools. ~~Last~~Lastly, EW ~~applications~~application could improve plant available water capacity depending on deployed amounts of rock powder - adding a new dimension to the coupling of land-based biomass NETs with EW.

1. Introduction

To limit temperature increase due to climate change to well below 2ºC compared to pre-industrial levels by the end of the century, research efforts on negative emission technologies (NET~~),~~: i.e., ways to actively remove CO_2 from the atmosphere~~,~~), intensify. Terrestrial NETs encompass, ~~e.g.,~~ Bioenergy with Carbon Capture and Storage (BECCS), Afforestation,

Formatted: Font: Not Italic

Reforestation and natural growing forests (AR), Enhanced Weathering (EW), Biochar, restoration of wetlands, and Soil Carbon Sequestration. From these land-based NET options, BECCS, AR, Biochar, and EW can potentially be combined for increasing atmospheric carbon dioxide removal (CDR) (Smith et al., 2016;Beerling et al., 2018;Amann and Hartmann, 2019).

BECCS combines energy production from biomass and carbon capture at the power plant with subsequent storage. Sources for biomass-based energy production are crop and forestry residues (Smith, 2012;Smith et al., 2012;Tokimatsu et al., 2017), dedicated bio-energy grass (BG) plantations (Smith, 2012;Smith et al., 2012) or short rotation woody biomass from forestry (Cornelissen et al., 2012;Smeets and Faaij, 2007). Large-scale AR, as well as bio-energy plantations, require extensive landscape modifications for growing forests or natural regrowth of trees in deforested areas to increase terrestrial CDR (Kracher, 2017;Boysen et al., 2017a;Popp et al., 2017;Humpenöder et al., 2014), and huge quantities of irrigation water (Boysen et al., 2017b;Bonsch et al., 2016). The biomass yields of AR and agricultural bio-energy crops directly correlate with fertilizer application, which in turn could reduce CDR efficiency due to related emissions of N_2O (Creutzig, 2016;Popp et al., 2011) and initiate unwanted side-effects like acidification of soils (Rockström et al., 2009;Vitousek et al., 1997), streams/rivers, and lakes (Vitousek et al., 1997).

Under intensive growth scenarios, nutrient supply is a critical factor. According to Liebig's law of the minimum, supplying high amounts of nitrogen (N) might shift growth limitation to other nutrients (von Liebig and Playfair, 1843). Some U.S. forests already show changes from N-limited to a Phosphorus (P) limited system caused by increases in N atmospheric deposition (Crowley et al., 2012) along with magnesium (Mg), potassium (K) and calcium (Ca) deficiencies (Garcia et al., 2018;Jonard et al., 2012). Poor nutrient supply, related to deficient mineral nutrition, may reduce tree growth (Augusto et al., 2017). Impacts on biomass production due to poor tree nutrition is observed in European forests (Knust et al., 2016;Jonard et al., 2015) decreasing the carbon sequestration of forest ecosystems (Oren et al., 2001) – a factor rarely included in climate models leading to overestimated CDR potentials.

Specifically, global simulations with a N-enabled land surface model (Kracher, 2017) suggest that insufficient soil nitrogen availability for a RCP4.5 AR scenario (Thomson et al., 2011) could lead to a reduction in the cumulative forest carbon sequestration between year 2006 – 2099 by 15%. Goll et al. (2012) showed that carbon sequestration during the 21st century in the JSBACH land surface model was 25% lower when N and P effects were considered.

Mineral weathering is a natural and primary source of geogenic nutrients (i.e., Mg, Ca, K, P, etc.; Hopkins and Hüner, 2008;Landeweert et al., 2001;Waldbauer and Chamberlain, 2005;Singh and Schulze, 2015), and controls atmospheric CO_2 concentrations over geological timescales (Walker et al., 1981;Lenton and Britton, 2006;Berner and Garrels, 1983;Waldbauer and Chamberlain, 2005;Yasunari, 2020). Chemical dissolution of silicate minerals increases alkalinity fluxes (Kempe, 1979;Gaillardet et al., 1999;Hartmann et al., 2009), and natural weathering ~~sequesters up to 0.3 Gt C a^{-1} (Gaillardet et al., 1999).~~sequestration can range from 0.1 to 0.3 Gt C a^{-1} (Gaillardet et al., 1999;Moon et al., 2014;Hartmann et al., 2009). To sequester significant amounts of CO_2 within decades, EW aims to speed up weathering processes by increasing the ~~weatherable~~ mineral reactive surfaces through rock comminution (Hartmann et al., 2013;Schuiling and Krijgsman, 2006;Hartmann and

Kempe, 2008). Mineral-soil-microorganism interactions~~, *e.g.*, by mycorrhizal fungi~~ (e.g., by mycorrhizal fungi; Kantola et al., 2017;Landeweert et al., 2001;Taylor et al., 2009) increase the volume of soil that plant roots can extract nutrients from (Clarkson and Hanson, 1980;Hopkins and Hüner, 2008), which might enhance the weathering activity in addition to the reaction with dissolved CO_2. EW further increase soil pH by alkalinity fluxes, and could be a long-term source of macro- (e.g., Mg, Ca, K, P, and S), and micronutrients (e.g., B, Mo, Cu, Fe, Mn, Zn, Ni) (Leonardos et al., 1987;Nkouathio et al., 2008;Beerling et al., 2018;Hartmann et al., 2013;Anda et al., 2015) rejuvenating the nutrient pools of soils.

P is rather immobile soil nutrient and only a small fraction of soil P is readily available for plant uptake limiting plant growth in a wide range of ecosystem (Shen et al., 2011;Elser et al., 2007). P content in soils is a result of a process controlled by the interactions of parent material (primary rocks) with climate, tectonic uplift, and erosion history through geological time (Porder and Hilley, 2011). The processes of P transfer between biologically available and recalcitrant P pools influence at most P availability (Porder and Hilley, 2011). Orthophosphate ($H_2PO_4^-$ or HPO_4^{2-}) is the chemical species adsorbed by plants (Shen et al., 2011) and its solubility is controlled by soil pH as de-protonation occurs when pH increases. Ideal pH conditions for orthophosphate availability are from 5 to 8 (Holtan et al., 1988)~~. Soil~~ with soil moisture influencing soil P availability ~~seems to be influenced by soil moisture~~ for different crops (He et al., 2005;He et al., 2002;Shen et al., 2011), and natural ecosystems (Goll et al., 2018).

The inclusion of soil hydraulic properties in the evaluation of EW effects is important as the soil water content has a strong influence on average crop yield. Practices that increase the plant available water (PAW) are thought to mitigate drought effects on crops (Rossato et al., 2017). The water content of soils also seems to influence soil erosion rates and surface runoff (Bissonnais and Singer, 1992). In addition, soil water content influences soil pCO_2 production, which is a relevant agent for mineral dissolution (Romero-Mujalli et al., 2018).

Deploying land-based NETs would imply large changes in a local landscape nutrient and water cycles. At least 65% of worldwide soils (6.8 billion hectares of land) have unfavorable soil conditions for biomass production (Fischer et al., 2001). Therefore, we assess if applications of rock mineral based P sources could close eventual nutritional gaps in an environment with natural N supply (N-limited) and with N fertilization (N-unlimited), using a global afforestation scenario. In addition, we investigate the effects of coupling nutrient supplying (EW) to nutrient demanding (AR and BG) land-based NETs by focusing on the efficiency of different upper limits of basalt powder to supply nutrients. We hypothesize that large-scale EW deployment potentially changes soil texture. Therefore, threshold values for impacts on soil hydraulic conductivity, and plant available water will be determined.

Formatted: Font: Not Italic

Formatted: Font: Not Italic

2. Methods

Since phosphorus (P) is a limiting nutrient in a wide range of ecosystems (Elser et al., 2007), we performed a P budget for an N stock-based P demand from an AR scenario considering natural N supply (hereafter N-limited) and N fertilization (hereafter N-unlimited). We ~~chose~~selected two N supply scenarios since the related P demand is proportional to biomass N stock, but in the main text we discuss only the N-limited AR scenario. ~~Based~~We estimated the balanced supply of Mg, Ca, and K for each supplied P based on ideal Mg, Ca, and K demand of AR derived from databases of biomass ~~Mg, Ca, and K~~nutrient content~~, we estimated the balanced supply of these nutrients for each supplied P~~. Balanced nutrient supply is necessary to avoid shift of growth limitation to other nutrients, which can occur according to Liebig's Law (von Liebig and Playfair, 1843). Shift of growth limitation to other nutrients is observed for some U.S. forests that changed from a N-limited to a Phosphorus (P) limited after increase in atmospheric N deposition (Crowley et al., 2012). Based on minimum and maximum harvest rates of bio-energy grass (BG), we estimated the related ~~exported~~ P and K export by harvest from the fields. We ~~choose~~decide on these nutrients for BG since crops require large amounts of K and P, once N demand is covered. The amount of rock powder for Enhanced Weathering (EW) to cover projected P gaps and to replenish exported nutrients was estimated. The projected impacts on soil hydrology due to EW deployment were done by pedotransfer functions since they are used to estimate soil hydraulic properties (Schaap et al., 2001;Whitfield and Reid, 2013;Wösten et al., 2001) and such approximations have proven to be a suitable approach (Vienken and Dietrich, 2011).

The additional AR P demand, obtained for the 21st century for an N-unlimited and N-limited AR scenario (Kracher, 2017) was approximated by stoichiometric P:N ratios for mean and range (5th and 95th percentiles), which is a similar approach done by Sun et al. (2017). The ratios were derived from databases of hard- and softwood (Pardo et al., 2005) and foliar biome-specific nutrient content (Vergutz et al., 2012). We then compared the inferred P demand to geogenic P supply given by observation-based estimates of soil inorganic labile P and organic P (Yang et al., 2014a), observation-based estimates of P release (Hartmann et al., 2014) from weathering corrected to future temperature increase, since the uncertainty on future hydrological cycle is too high (Goll et al., 2014) and estimated atmospheric P depositions from Wang et al. (2017) to derive the potential geogenic P deficits~~,~~ (i.e. the P gap~~,~~) during the 21st century. Since the geogenic P supply cannot cope with N stock-based P demand from the different AR scenarios within P gapped areas, the biomass production and biomass C sequestration, predicted by the AR scenarios, will be lower. Based on the amount of missing P, we estimated the C-stock reduction within P gapped areas by using stoichiometric C:P ratios. The C:P ratios were derived from simulated C stock content (Kracher, 2017) and inferred N stock-based P demand.

Necessary Mg, Ca, and K supply for balanced tree nutrition based on P supply were derived from N stock-based Mg, Ca, and K additional demand normalized to the N stock-based additional P demand (Fig. 1). The nutrient demand of bio-energy grass was estimated based on stoichiometric P:N and K:N ratios, used in Bodirsky et al. (2012), for minimum and maximum exported N proportional to harvest rates of the 1995 – 2090 period obtained from the agricultural production model MAgPIE (Fig. 1).

Formatted: Font: Not Italic

Later on, the necessary amount of rock to cover the P gaps of AR scenario and to resupply the exported nutrients by BG harvest was estimated (Fig. 1). In addition, the potential impact of deploying rock powder into the topsoil ~~was done. Detailed description on used data and assumptions are given below~~hydrology was done.

2.1. Global land-system model output

2.1.1. Afforestation/Reforestation

The idealized simulations for the AR system from Kracher (2017) performed by the land surface model JSBACH (Reick et al., 2013) for a representative greenhouse concentration pathway 4.5 (RCP4.5) were used (Thomson et al., 2011). ~~The JSBACH simulations assume~~The RCP4.5 scenario assumes that the emissions peak is around 2040 and considers that forest lands expand from their present day extent (Thomson et al., 2011). The coupled terrestrial nitrogen-carbon cycle model assumes N-unlimited and N-limited conditions, and consider harvest rates, and transitions between different anthropogenic and natural land cover types (Hurtt et al., 2011) for a Gaussian grid of approximately 2°×2° resolution. Accounting for the N cycle reduces the uncertainty on atmospheric carbon sequestration prediction by AR models (Zaehle and Dalmonech, 2011). In JSBACH, the N supply for plants is controlled by competition between plants and decomposing microbes, while other numerical models prioritize immobilization or plant growth (Achat et al., 2016).

The net primary productivity (NPP) calculation was based on atmospheric CO_2 concentrations, stomatal conductance, and water availability. JSBACH considers mass conservation, a supply-demand ansatz, and fixed C:N ratios (Goll et al., 2012). ~~Kracher (2017), considered forest regrowth on abandoned croplands, which in the long term become acidic and consequently favor leaching of nutrients and heavy metals (Hesterberg, 1993), natural shift in natural vegetation, and future CO_2 increase leading to CO_2 fertilization~~The coupled terrestrial nitrogen-carbon cycle model was selected since it: (i) considered forest regrowth on abandoned croplands (which in the long term become acidic and consequently favor leaching of nutrients and heavy metals (Hesterberg, 1993)); (ii) considered natural shift in natural vegetation; (iii) considered a natural N supply scenario (N-limited) and a N fertilized scenario (N-unlimited); (iv) considered future CO_2 increase leading to CO_2 fertilization; and (v) explicitly consider large-scale afforestation.

We retrieved the annual changes in N and C content of different pools, i.e., Wood (above and below ground, also including litter) and foliar (above and below ground, also including litter) for temperate, cold, tropical, and subtropical climate growing forests and shrubs plant functional types for years 2006 – 2099 and annual model output.

2.1.2. Biomass production from bio-energy grass

Simulations of BG nutritional needs from the agricultural production model MAgPIE, a framework for modeling global land-systems (Dietrich et al., 2018;Lotze-Campen et al., 2008;Popp et al., 2010) were used. The objective of MAgPIE is to minimize total costs of production for a given amount of regional food, bio-energy demand and climate target (here RCP4.5~~).~~, to keep

Formatted: Highlight

Formatted: Font: Not Italic

correspondence to the AR simulations). In its biophysical core, the yields in the model are based on LPJmL (Bondeau et al., 2007;Beringer et al., 2011;Müller and Robertson, 2013), a dynamic global vegetation model, which is designed to simulate vegetation composition and distribution for both natural and agricultural ecosystems.

At the starting point of the simulation, the LPJmL bio-energy grass yields have been scaled using agricultural land-use intensity levels (Dietrich et al., 2012) for different world regions accounting for the yield gap between potential and observed yields for the period 1995 – 2005. For the future yields (2005 – 2090), the development is then driven by investments into yield-increasing technologies (Dietrich et al., 2014) based on the socio-economic boundary conditions of the system.

The MAgPIE output had a frequency of 10 years and the global minimum, and maximum of each output year was taken to obtain the potential bio-energy grass minimum (0.7 kg m^{-2} a^{-1}) and maximum (3.6 kg m^{-2} a^{-1}) harvest rate for the simulation period~~, which is 0.7 and 3.6 kg m^{-2} a^{-1}~~ for the areas with bio-energy plantations.

2.2. Nutrient demand

2.2.1. Afforestation/Reforestation

The P, Mg, Ca, and K additional demand is defined as the amount of P, Mg, Ca, and K needed to realize the state of ecosystem N variables in each grid cell and year according to JSBACH output (Fig. 1). It was estimated from the spatially explicit information on average forest N content of each stock and plant functional type for an N-unlimited, and an N-limited AR scenario from Kracher (2017). Since P limits forest growth in a wide range of ecosystems (Elser et al., 2007), we performed a P budget for each AR scenario. The ideal P, Mg, Ca, and K biomass- additional demand were based on the difference in the simulated change in N pools at that time with respect to the simulation year of 2006 multiplied by their corresponding Mg:N, Ca:N, K:N, or P:N ratios (r_{ij}) and were calculated following Eq. (1):

$$\Delta M_{pool,i} = \sum_{j=1}^{n} \Delta N_{ij} \times r_{ij}, \quad (1)$$

where $\Delta M_{pool,i}$ [kg m^{-2} a^{-1}] is the average N stock-based Mg, Ca, K, or P demand for a given time in the future simulation time range (2007 – 2099) within a cell for biome i. ΔN_{ij} [kg m^{-2} a^{-1}] is the average N stock change of pool j. n is the number of N pools. The N pools considered are: Wood (above and below ground, including litter) and foliar (above and below ground, including litter).

The P, Mg, Ca, K, and N content of leaves obtained from a global leaf chemistry database (Vergutz et al., 2012) was used to derive the Mg:N, Ca:N, K:N, or P:N ratios (Table 1), which was already biome classified. For wood, the tree chemical composition database of US forests (Pardo et al., 2005) was used in order to derive the global ratios, which were assumed to represent the chemical composition of all biomes (Table 1).

The AR C content (Fig. 2) from Kracher (2017) and the resulting N stock-based Mg, Ca, and K demand were normalized by the N stock-based P demand to estimate the mean and range C:P, Mg:P, Ca:P, and K:P ratios of each grid cell. The

stoichiometric C:P, Mg:P, Ca:P, and K:P ratios were used to derive the C-fixation reduction due to P deficiencies and the necessary Mg, Ca, and K supply for a balanced biomass nutrition based on supplied P (Fig. 1).

2.2.2. Biomass production from bio-energy grass

The BG yield was obtained by the spatially explicit harvest rates within a grid cell for an output frequency of 10 years and a period of 95 years (1995 – 2090). The minimum 0.7 kg m^{-2} a^{-1} and maximum 3.6 kg m^{-2} a^{-1} harvest rate were used. With the information on exported N by each harvest rate, the exported K or P from cultivation fields (~~eq~~Eq. 2) were estimated based on the P:N, and K:N stoichiometric ratios used in Bodirsky et al. (2012). We have chosen these nutrients, since crops require large amounts of K and P.

~~Differently~~The simulated forests from the AR scenario ~~forests, which~~ are perennial, differently from bio-energy grasses that are completely harvested regularly due to their use as biomass feedstock for BECCS. Thus, the natural system's nutrient supply is insufficient to maintain successive and constant yields, and the exported nutrients by harvest need to be replenished (Cadoux et al., 2012) to maintain high yields. The exported nutrient was calculated following Eq. ~~(2).~~(2):

$$Bio_x = r_x \times N_{harvest}, \quad (2)$$

where Bio_x corresponds to the exported nutrient P or K [kg m^{-2} a^{-1}] by harvest. r_x is the P:N or K:N stoichiometric ratio used in Bodirsky et al. (2012). $N_{harvest}$ is the exported N for a minimum 0.7 kg m^{-2} a^{-1} or a maximum 3.6 kg m^{-2} a^{-1} harvest rate. The harvest rate value was based on the MAgPIE output for each grid cell, representing the minimum and maximum projected global harvest rate for a period of 95 years.

2.3. Geogenic P supply for AR

~~Since the~~The geogenic P source databases have different spatial resolution (Table 2), we resampled each of them to ~~2°×2° spatial resolution fields by nearest neighbor interpolation.~~a coarser 2°×2° spatial resolution fields by nearest neighbor interpolation to minimize distortions of location (Pontius, 2000). Nearest neighbor interpolation method reliably retain the overall proportions of an original fine resolution map (Christman and Rogan, 2012). As the uncertainty on which P pool is available for long-term plant nutrition is high (Johnson et al., 2003), two scenarios for soil P supply were investigated: scenario one considering P from weathering and atmospheric P deposition. Scenario two the same as scenario one plus inorganic labile P and organic P (Yang et al., 2014a)~~(Supplement S1 Fig. S2).~~.

~~The total P supply by weathering for the 21th century (2006 – 2099) was based on Hartmann et al. (2014) maps (Supplement S1 Fig. S3). A relationship between air temperature and weathering rate was used, whereby P weathering increases by 9% per 1°C increase (Goll et al., 2014) without accounting for P concentration changes in primary and secondary P minerals.~~

The atmospheric dry and wet P deposition rates were taken from simulation outputs for the 2006 – 2013 period and for the years 2030, 2050, and 2099 for an RCP4.5 scenario for a grid cell size of 1° (Wang et al., 2017). The simulations were based

on P emissions of sea salt, dust, biogenic aerosol particles, and P emitted by combustion processes, and performed by the global aerosol chemistry-climate model LMDZ-INCA~~,~~ (cf., Wang et al. (2017) for a detailed description of model and model assumptions~~.~~). The simulation gaps were closed by linear regression and the cumulative atmospheric P deposition ~~(Supplement S1 Fig. S1)~~ was calculated by summing up the deposition rate of each cell for 2006 – 2099 period according to Eq. (3):

$$P_{tot} = \sum_{i=2006}^{2099} P_i, \quad (3)$$

where P_{tot} [kg m^{-2}] is the cumulative atmospheric P deposition of the 2006 – 2099 period~~.~~ (Fig. 3a). P [kg m^{-2} a^{-1}] is the atmospheric P deposition of each year i within a grid cell.

The total soil P map from Yang et al. (2014a) was used as estimation of the projected long term available P in the soil system (Fig. 3b). The total P supply by weathering for the 21th century (2006 – 2099) was based on Hartmann et al. (2014) maps (Fig. 3c) that describes the chemical weathering as a function of runoff and lithology, being corrected to temperature and soil thickness (Hartmann et al., 2014) and calibrated on 381 catchments in Japan (Hartmann et al., 2009). A relationship between air temperature and weathering rate was used, which was derived from reconstructed weathering rates and different climate change scenarios for the recent past (1860-2005) using the weathering model applied here. The relationship in which P weathering increases by 9% per 1ºC increase (Goll et al., 2014) implicitly accounts for changes in soil hydrology. Without accounting for P concentration changes in primary and secondary P minerals. Due to the large uncertainties in projected changes in soil hydrology we omitted a more detailed representation of hydrological effects on weathering.

2.4. Estimating geogenic P gap, related C-fixation reduction, and balanced Mg, Ca, and K supply for AR

The potential P gap (P_{gap} [kg m^{-2}]) was estimated as the difference between additional mean and range (95th and 5th percentiles) P demand estimated from the N stock for the two different AR scenarios (section on Afforestation/Reforestation nutrient demand), and the geogenic P supply from the different supply scenarios (P_{sup} [kg m^{-2}]) within the cover fraction for a grid cell of biome i (f_i [-]), for 21st century (2006 – 2099) according to Eq. ~~(4):~~(4):

$$~~P_{gapt}~~P_{gap} = P_{sup} \times f_i - \Delta P_{pool,i}, \quad (4)$$

the plant C-fixation reduction was estimated based on the P gap and calculated following Eq. (5):

$$C = r_C \times ~~P_{gapt}~~P_{gap}, \quad (5)$$

where C [kg m^{-2}] is the plant reduced C-fixation due to the projected P gap. r_C is the used stoichiometric C:P ratio based on mean and range (5th and 95th percentiles) chemistry for wood and leaves derived from the N-limited and N-unlimited AR scenario N stock as described in subsection 2.2.1.

The Mg, Ca, and K necessary supply for balanced biomass nutrition (M_x [kg m^{-2}]) should be proportional to the supplied P (P_{EW} [kg m^{-2}]) and was calculated following Eq. ~~(6):~~(6):

Formatted: Font: Not Italic

Formatted: Keep with next

Formatted: Keep with next

Formatted: Keep with next

$$M_x = r_x \times P_{EW}, \quad (6)$$

with P_{EW} being equal to the projected P_{gap} since ~~the P_{gap}~~it is covered by P from Enhanced Weathering according to Eq. (7):

$$P_{EW} = P_{gap}, \quad (7)$$

where r_x is the used stoichiometric ratio Mg:P, Ca:P, K:P obtained by normalizing the N stock based additional Mg, Ca, and K demand to the N stock based additional P demand.

2.5. Enhanced Weathering Mg, K, Ca, and P potential supply

~~To cover the potential of different igneous rocks for EW strategies, rhyolite and dacite (acid rocks), andesite (intermediate rock) and basalt (basic rock) were chosen to project used masses to cover P gap from the AR scenarios. For this, data collection of macronutrient concentrations (Mg, Ca, K, P) in weight percent within these rocks were done (Supplement S1 Fig. S4) (Earthchem web portal, http://www.earthchem.org, accessed on 2017-07-14).~~

~~The nutrient supply was estimated assuming complete rock powder dissolution in the system, which is expected over long timescales depending on the grain size (*i.e.,* one year for grain sizes between 0.6 – 90 µm (Strefler et al., 2018)). The results and discussion will focus on basalt rock powder considering median values and range (5th and 95th percentiles), as basalt is abundant worldwide (Amiotte Suchet et al., 2003;Börker et al., 2018) and has a high P content. Other rock types are included, but the results are provided in the supplementary text (Supplement S1 section S4). The necessary mass of rock powder to supply macronutrient (Mg, Ca, K, or P) was calculated following Eq. (8):~~

To cover the potential of different igneous rocks for EW strategies, rhyolite and dacite (acidic rocks), andesite (intermediate rock) and basalt (basic rock) were selected to project necessary amounts to cover P gaps from the AR scenarios. Data on macronutrient concentrations (Mg, Ca, K, P) in weight percent within these rocks were downloaded from the Earthchem web portal (Fig. 4; http://www.earthchem.org, accessed on 2017-07-14). The data was selected for rocks named as rhyolite, dacite, andesite, and basalt. Neglecting intermediate compositions between different lithotypes (i.e., a trachybasalt that has its chemical composition lying in between trachyte and basalt). Rocks that were under any metamorphism grade (e.g., meta-basalt) were neglected because metamorphism can change rock mineralogy. We neglected rocks known to have high content of minerals rich in trace elements (e.g., an alkali basalt can have P concentration >3000 ppm (Porder and Ramachandran, 2013), but it is rich in olivine (John, 2001;Irvine and Baragar, 1971) that contains elevated concentrations of nickel and chromium (Edwards et al., 2017)). Nickel and chromium are trace elements problematic for agriculture (Edwards et al., 2017). Thus, following the classification criteria, the number of selected data to calculate descriptive statistics for Mg, Ca, K, P content within rocks were 2985 chemical analysis for rhyolite, 3008 chemical analysis for dacite, 11099 chemical analysis for andesite, and 23816 chemical analysis for basalt.

The nutrient supply was estimated assuming complete rock powder dissolution in the system considering median and ranges (5^{th} or 95^{th} percentile) chemical composition. The duration of complete rock powder dissolution varies depending on the grain size (i.e., one year for grain sizes between 0.6 – 90 µm (Strefler et al., 2018) for basalt). The results and discussion will focus on basalt rock powder considering median P values (500 ppm) and range (5^{th} (157 ppm) and 95^{th} (1833 ppm) percentiles), as basalt is abundant worldwide (Amiotte Suchet et al., 2003;Börker et al., 2019) and has a high P content compared to acidic and intermediate rocks, median P concentration can be >3000 ppm for alkali basalts, but for a broader basalt classification that considered 97895 samples, it can be of 916 ppm (Porder and Ramachandran, 2013). The necessary mass of rock powder to supply macronutrients (Mg, Ca, K, or P) was calculated following Eq. (8):

$$R_d = \frac{M_{ex}}{f_{nut}}, \quad (8)$$

where R_d [kg rock m^{-2} or kg rock m^{-2} a^{-1}] represents the mass of a rock type to cover AR or BG nutritional needs, M_{ex} [kg m^{-2} or kg m^{-2} a^{-1}] is the mass of required nutrient for AR or BG~~,~~ (e.g., P to cover a ~~P gap,~~P_{gap} obtained by Eq. (4)), and f_{nut} [-] is the median and range (5^{th} or 95^{th} percentile) fractions of interest nutrient within the ~~chosen rock, *i.e,* for P in basalt a median of 500 ppm and ranges of 157 ppm for 5^{th} percentile and 1833 ppm for 95^{th} percentile is expected~~selected rock.

However, the potential nutrient supply by EW for different amounts of rock powder being deployed was also estimated following Eq. ~~(9):~~(9):

$$Nut_{in} = M_{rock} \times f_{nut}, \quad (9)$$

where Nut_{in} [kg m^{-2} or kg m^{-2} a^{-1}] represents the macronutrient input by dissolving a chosen rock. M_{rock} [kg rock m^{-2} or kg rock m^{-2} a^{-1}] is the mass of rock added to the natural system.

2.6. Related impacts on soil hydrology from Enhanced Weathering deployment

Large scale deployment of rock powder on soils is expected to influence ~~soil's~~its texture. The deployed amount and texture of rock powder will somehow affect hydraulic conductivity, water retention capacity, and specific soil surface area. Pedotransfer functions (PTFs) are used to estimate soil hydraulic properties (Schaap et al., 2001;Whitfield and Reid, 2013;Wösten et al., 2001) ~~based on~~and such approximations have proven to be a suitable approach (Vienken and Dietrich, 2011). PTFs make use of statistical analysis (Saxton and Rawls, 2006;Wösten et al., 2001), artificial neural networks, and ~~or~~ other methods applied to large soil databases of measured data (Wösten et al., 2001).

~~The impacts of basalt powder application on soil hydrology are estimated for soils corresponding to P gap areas from the N-unlimited AR scenario as a function of rock powder deployment by the use of PTFs from~~The equations from Saxton et al. (1986) performed the best estimations of soil hydraulic properties (Gijsman et al., 2002). Later on, Saxton and Rawls (2006) ~~(Supplement S1 section S5). The N-unlimited AR scenario was chosen since this scenario would have the highest P deficiencies requiring more rock powder to cover the P gaps.~~improved Saxton et al. (1986) PTFs and they are used to estimate the effects

Formatted: Font: Not Italic

on soil hydraulic properties due to deployment of basalt powder (Eqs. (10) – (18)). ~~The estimations are for a homogeneous mixture of rock powder and topsoil depth of 0.3 m. Downward transport of fine-grained material is neglected for simplification. The considered values represent upper limits of rock powder application. The impacts on plant available water (PAW) is given by the difference between water content at a pressure head of -33 kPa (Supplement S1 eq. (S7)) and -1500 kPa (Supplement S1 section S5 eq. (S6)) (Saxton and Rawls, 2006), while the impact on soil hydraulic conductivity is given by Eq. (10):~~

The potential changes in soil hydraulic properties, due to the application of a fine basalt texture (15.6% clay, 83.8% silt, and 0.6% fine sand) or a coarse basalt texture (15.6% clay, 53.8% silt, and 30.6% fine sand) were estimated as a function of rock powder deployment for soils corresponding to P gap areas from the N-unlimited AR scenario. According to the international organization for standardization, the man-made materials can be classified according to their grain sizes; therefore, here the clay comprehends grain diameters ≤ 2 µm, silt comprehends grain diameter 2 – 63 µm, and fine sand comprehends 63 – 200 µm (ISO 14688-1:2002), but since full dissolution is assumed, the ground basalt fine sand encompass grain sizes of diameter 63 – 90 µm remaining withing the ISO 14688-1:2002 classification. The N-unlimited AR scenario was selected since it would have the highest P deficiencies requiring more rock powder to cover the P gaps (i.e., it represents the maximum effect). The estimations are for a homogeneous mixture of rock powder and topsoil depth of 0.3 m. Downward transport of fine-grained material is neglected for simplification. The considered values represent upper limits of rock powder application. The impacts on plant available water (PAW) is given by the difference between water content at a pressure head of -33 kPa (Eq. (11)) and -1500 kPa (Eq. (10)), while the impact on soil hydraulic conductivity is given by (Eq. (14); Saxton and Rawls, 2006):

$$\theta_{1500} = \theta_{1500t} + (0.14 \times \theta_{1500t} - 0.02), \quad (10)$$

$$\theta_{33} = \theta_{33t} + (1.283 \times (\theta_{33t})^2 - 0.374 \times (\theta_{33t}) - 0.015), \quad (11)$$

$$\theta_{(S-33)} = \theta_{(S-33)t} + (0.636 \times \theta_{(S-33)t} - 0.107), \quad (12)$$

$$\theta_S = \theta_{33} + \theta_{(S-33)} - 0.097 \times S + 0.043, \quad (13)$$

$$K_S = 1930 \times (\theta_S - \theta_{33})^{(3-\lambda)}, \quad ~~(10)~~ (14)$$

~~where~~with:

$$\theta_{1500t} = -0.024 \times S + 0.487 \times C + 0.006 \times OM + 0.005 \times (S \times OM) - 0.013(C \times OM) + 0.068(S \times C) + 0.031, \quad (15)$$

$$\theta_{33t} = -0.251 \times S + 0.195 \times C + 0.011 \times OM + 0.006 \times (S \times OM) - 0.027 \times (C \times OM) + 0.452(S \times C) + 0.299, \quad (16)$$

$$\theta_{(S-33)t} = 0.278 \times S + 0.034 \times C + 0.022 \times OM - 0.018 \times (S \times OM) - 0.027 \times (C \times OM) - 0.584 \times (S \times C) + 0.078, \quad (17)$$

$$\lambda = \left[\frac{\ln(1500) - \ln(33)}{\ln(\theta_{33}) - \ln(\theta_{1500})}\right]^{-1}, \quad (18)$$

where S and C respectively represent the soil texture corresponding to sand and clay diameters [wt %], OM is the soil organic matter [wt %], the moisture [wt %] are estimated by θ_{1500} and θ_{33} respectively representing ~~K_S [mm h^{-1}] represents the saturated soil hydraulic conductivity, θ_{33} represents~~ the soil moisture for a pressure head of -1500 kPa (R^2 = 0.86) and of -33 kPa (R^2 = 0.63~~; Supplement S1 section S5), θ_S~~). $\theta_{(S-33)}$ and θ_S respectively corresponds to the 0 kPa to -33 kPa moisture (R^2 = 0.36), and to the saturated (0 kPa) moisture (R^2 < 0.25). K_S [mm h^{-1}] represents the saturated soil hydraulic conductivity~~; Supplement S1 section S5),~~ and λ is the slope of the logarithmic tension-moisture curve ~~(Supplement S1 section S5)~~. The numbers in front of each described variable are regression coefficients (Saxton and Rawls, 2006).

The initial hydrologic properties of topsoil were estimated for a depth of 0.3 m, as it is the average depth usual machinery can homogeneously mix topsoil (Fageria and Baligar, 2008). Greater depths can be reached but under higher energy and labor costs (Fageria and Baligar, 2008). The global data set of derived soil properties (Batjes, 2005), which had textural information (sand, silt, and clay content) for shallow soil depths (0.3 m) was used. The raster had a resolution of 0.5° and the soil properties for the interest areas of biomass growth limitation (Supplement S1 Fig. S. 7a) were included by a spatial join (using Esri ArcMap 10.8). The nutrient deficient areas encompass soils of different textures and organic matter content, which had their initial K_S estimated separately based on Eq. (14). The sum of clay, silt, and sand fractions within each cell should always be unity, and were corrected when necessary by Eq. (19):

$$G_{cor} = \frac{(G_{ini} \times M_{soil\_cell})}{\sum (G_{ini} \times M_{soil\_cell})}, \quad (19)$$

with:

$$M_{soil\_cell} = V_{cell} \times \rho_{bulk\_cell}, \quad (20)$$

where G_{ini} represents the initial topsoil texture (sand, silt, and clay content) of a specific raster cell [-]. V_{cell} [km^3] is the raster cell volume obtained by multiplying the area [km^2] to the soil depth of 0.3×10^{-3} km. ρ_{bulk_cell} [kg km^{-3}] is the raster cell topsoil bulk density. M_{soil_cell} [kg] is the total soil mass of a raster cell. G_{cor} [-] is the corrected soil texture (sand, silt, and clay content).

The necessary rock powder mass was estimated by Eq. (8) to close the P_{gap} obtained by Eq. (4). The effect of basalt powder application in soil K_S and PAW was estimated by assuming a homogeneous mixture between applied basalt powder and topsoil. The changes on initial soil organic matter (SOM) concentration within a raster grid-cell were obtained by normalizing the

SOM to the sum of applied basalt mass, mass of soil, and initial SOM mass by Eq. (21). This was necessary since the SOM concentration at the moment of basalt deployment would have a relative decrease compared to initial SOM concentration:

$$OM_c = \frac{OM_{cell}}{M_{b\_cell} + M_{soil\_cell} + OM_{cell}} \times 100, \quad (21)$$

with:

$$OM_{cell} = OM_{wt\%} \times M_{soil\_cell}, \quad (22)$$

where OM_c [wt %] is the corrected soil organic matter content, OM_{cell} [kg] is the organic matter mass within the raster cell. M_{b_cell} and M_{soil_cell}, both in [kg], are the mass of basalt and mass of soil for a specific raster cell.

The impacts in soil texture by rock powder application considered the textures of applied basalt mass added to the initial soil mass by Eq. (23). It was assumed a content of 15.6% clay, 83.8% silt, and 0.6% fine sand for fine basalt powder and 15.6% clay, 53.8% silt, and 30.6% fine sand for a coarse basalt powder.

$$G_{bs} = \frac{\left(G_{ini} \times M_{sed_{cell}} + M_{b_{cell}} \times G_{basalt}\right)}{\Sigma\left(G_{ini} \times M_{sed_{cell}} + M_{b_{cell}} \times G_{basalt}\right)}, \quad (23)$$

where G_{basalt} corresponds to the texture fractions of the fine or coarse basalt powder. G_{bs} corresponds to the texture fractions of resulting mixture of basalt plus soil. Thus, the texture fractions of resulting mixture of basalt plus soil obtained by Eq. (23) were replaced within Eq. (15) to Eq. (17) to estimate the impacts in soil hydraulic conductivity by Eq. (14) and PAW by subtracting the outcome from Eq. (11) to the outcome from Eq. (10), with clay size (grains >1 µm and <3.9 µm) being the finest grain size we can consider.

Besides texture and organic matter, intrinsic grain properties (e.g., the shape of grains and pores, tortuosity, specific surface area, and porosity) should be considered (Bear, 1972). The equations from Beyer (1964) are based on the non-uniformity of grain size distribution and density of the grain packing to estimate soil properties. Carrier III (2003) uses information on the particle grain size distribution, the particle shape, and the void ratio on his equations to estimate soil properties. However, such detailed information on a global scale is missing turning Beyer (1964) and Carrier III (2003) equations not applicable to our analysis.

3. Results ~~and discussion~~

3.1. Afforestation/Reforestation P gaps and Enhanced Weathering as nutrient source

The global C sequestration for the N-limited AR scenario is 190 Gt C, while for the N-unlimited AR scenario it is 34 Gt C higher. The AR model from Kracher (2017) shows an increase in biomass production in tropical and temperate zones (Fig. 2). The results only focus on the N-limited scenario since it considered natural N supply, but the results for the N-unlimited

scenario are presented only in the supplement (Supplement S1 section B ii). The calculated P budgets according to Eq. (4) for the AR time of 2006 – 2099 (Fig. 5) considered different geogenic supply scenarios (scenario one: P from weathering and atmospheric P deposition; scenario two: the same as scenario one plus inorganic labile P and organic P) and the average and range N stock-based P demand (calculated following Eq. 1) for the AR simulation from Kracher (2017).

The ideal P biomass additional demand (calculated from Eq. (1)), to sequester 190 Gt C (N-limited AR scenario) amounts to 200 Mt P on global scale for a mean wood and leaves P content; for 5th and 95th percentile, the estimated P demand would be 71 and 345 Mt P respectively. The P budget (estimated from Eq. (4)) for geogenic P supply scenario one suggest that P deficiency areas are distributed around the world, but with more frequent occurrences in the northern hemisphere (Fig. 5a) and the P gaps can potentially reach up to ~17 g P m^{-2} (~4 – ~30 g P m^{-2} for 5th and 95th quartiles of wood and leaves chemistry; Table 3) or a global P gap of ~77 Mt P (~9 – 181 Mt P^2 for 5th and 95th quartiles of wood and leaves chemistry; Table 3). However, for geogenic P supply scenario two, the P deficiency areas are predominantly located in the southern hemisphere (Fig. 5c) and the P gaps can potentially reach up to ~7 g P m^{-2} (~2 – ~12 g P m^{-2} for 5th and 95th quartiles of wood and leaves chemistry; Table 3) or a global P gap of ~10 Mt P (1 – ~35 Mt P^2 for 5th and 95th quartiles of wood and leaves chemistry; Table 3).

The P and N limitation cause an average C reduction of 47% for the geogenic P supply scenario one and 19% for the geogenic P supply scenario two (obtained by accounting the C reduction from N limitation, which is 34 Gt C plus the C reduction from Table 3 and then normalized by the global sequestration for the N-unlimited scenario of 224 Gt C) or ~-1.1 and ~-0.5 Gt C a^{-1}, respectively. In some areas, the C sequestration can be reduced by up to 100% compared to the predicted C sequestration of the AR models (Fig. 6). Accounting for N and P limitation on AR suggests that the biomass production will be affected, consequently decreasing the C sequestration potential of AR strategies (Table 3 and Fig. 6). Therefore, supplying the demanded P would positively contribute to biomass to reach the predicted growth of the specific AR scenario.

Besides removing carbon from the atmosphere, EW can also amend soils by supplying nutrients and increasing alkalinity fluxes (Leonardos et al., 1987;Nkouathio et al., 2008;Beerling et al., 2018;Hartmann et al., 2013;Anda et al., 2015). Since basalt has higher P content compared to acidic and intermediate rocks (Porder and Ramachandran, 2013), it could be used as raw material for EW to cover the estimated P gaps of Fig. 5a and Fig. 5c. For a median Basalt P content of 500 ppm (cf., subchapter 2.5), it would be necessary to apply ~33 and ~13 kg basalt m^{-2} (Fig. 5b and Fig. 5d) in areas of high P deficiency (~17 and ~7 g P m^{-2}, Fig. 5a and Fig. 5c respectively), considering the AR time span, the deployment rates would be less than 1 kg basal m^{-2} a^{-1}, if full congruent dissolution occurs as assumed for further given scenarios.

The total amount of basalt powder to close the estimated P gaps from Fig. 5 would depend on the assumed geogenic P supply scenario and chemical composition of wood and leaves, but for a mean P chemical composition, at least ~153 Gt basalt would be necessary for geogenic P supply scenario one and ~20 Gt basalt for geogenic P supply scenario two. Basalt has a carbon capture potential of ~0.3 t CO_2 t^{-1} basalt (Renforth, 2012), resulting in ~46 Gt CO_2 (~12.4 Gt C) and 6 Gt CO_2 (1.6 Gt C) capture by closing the P gaps from Fig. 5a and Fig. 5c, respectively. If wood and leaves P concentration correspond to 5th

percentiles (Table 1) ~2 Gt basalt would be needed for closing the P gaps from a geogenic P supply scenario two (Supplement S1 Fig. S1), which would potentially sequester ~0.6 Gt CO_2 (~0.2 Gt C) due to weathering. If wood and leaves P concentration correspond to 95th percentiles (Table 1) ~362 Gt basalt for closing the P gaps from a geogenic P supply scenario one (Supplement S1 Fig. S3) would be necessary, which would potentially sequester ~98 Gt CO_2 (~27 Gt C) due to weathering. The amount of basalt needed was estimated for a P content of 500 ppm and an increase in basalt P concentrations would represent a decrease in the necessary amounts of basalt powder. Incongruent dissolution of basalt might occur consequently increasing the necessary amounts of deployed basalt to cover the estimated P gaps.

Basalt deployment can also guarantee a balanced supply of Mg, Ca, and K for different deployment rates (Fig. 7), potentially preventing the shift of growth limitation to some of these nutrients within the P gapped areas (Fig. 5). Besides basalt, rhyolite, dacite or andesite could alternatively be used as a source of P, but these rocks generally have lower P content (Fig. 4). As a consequence, the necessary amounts of rhyolite, dacite or andesite would be higher than that for basalt. Even though, for a median rock nutrient content, if these rocks are used to close the projected P gaps, they potentially can supply the necessary amount of Ca, Mg, and K for balanced tree nutrition (Fig. 8).

3.2. Enhanced Weathering coupled to bio-energy grass production

For the simulation time spam of 1995 – 2090 the minimum and maximum biomass growth yield amounts to 0.7 and 3.6 kg m^{-2} a^{-1}, which represent a K export of 4.2 – 22 g m^{-2} and a P export of 0.7 – 3.6 g m^{-2} according to Eq. (2). To guarantee maximum bioenergy grass yield, the exported nutrients should be replaced. For a high nutrient content (95th quartile) deploying up to 1.5 kg basalt m^{-2} a^{-1} could meet the K needs of bio-energy grass (Fig. 9) and would be able to replenish up to 75% of the exported P, if the maximum bio-energy grass yield is considered (Fig. 9). Industrial fertilizer co-application would be indicated to completely replenish exported P reducing industrial fertilizers dependency. Deploying 8 kg basalt m^{-2} a^{-1} would be enough to replenish exported K and P by harvest assuming median nutrient content of basalt powder, congruent and complete dissolution (Fig. 9).

3.3. Impacts on soil hydrology

The baseline hydraulic properties for soils within the P gap areas from the N-unlimited AR scenario, since this scenario represents the maximum effect, were estimated by Eq. (10), and they show high variability. The projected hydraulic conductivity (K_S) of top soils for areas corresponding to those of P budget from geogenic P supply scenario one (Supplement S1 Fig. S7a), for the N-unlimited AR scenario encompass values ranging from 1.5 × 10^{-7} and 7.8 × 10^{-5} m s^{-1} and for PAW of 4% and 32% (Table 4). Neglecting the topography, soils having low K_S, (e.g., values of 1.5 × 10^{-7} m s^{-1}) would experience the lowest water infiltration rate. The impacts of deploying a fine basalt texture (15.6% clay, 83.8% silt, and 0.6% fine sand) or a

coarse basalt texture (15.6% clay, 53.8% silt, and 30.6% fine sand), which are in the range of commercial powders (Nunes et al., 2014), on soil hydrology were estimated by Eq. (10) for different application upper limits.

The effects of rock-powder deployment could be neglected, on average, for upper limits of 50 kg basalt m^{-2} for a fine and 205 kg basalt m^{-2} for a coarse textured rock-powder. However, deviations from what is expected for the mean might occur (Fig. 10 and Fig. 11). The average values for PAW increase together with the increase of the upper limits of rock powder application, but for a coarse basalt powder some areas might experience a decrease in the PAW (Fig. 10 and Fig. 11).

Closing the observed P gap areas from the N-unlimited AR scenario would require a maximum deployment of 34 kg basalt m^{-2} if geogenic P supply scenario one is assumed and 13 kg basalt m^{-2} if geogenic P supply scenario two is assumed (Supplement S1 Fig. S7). Filling the P gaps from scenario two by a coarse or fine basalt powder (given complete dissolution of P-bearing minerals) the related changes in soil hydrology would remain below ±10% for most of the areas (Supplement S1 Fig. S12). If the geogenic P supply from scenario one, for the N-unlimited AR scenario (Supplement S1 Fig. S7a), is assumed and a fine basalt powder is applied, the changes on hydraulic conductivity range between 58% and -11% (Fig. 12a). Decrease on PAW could be neglected for most of the deployment areas, but some would have an increase of up to 31% from 13.8% to 18.2% (Fig. 12c). A coarse basalt powder would, in general, cause fewer impacts to soil hydraulic properties (Fig. 12b and Fig. 12d).

4. Discussion and implications

~~3.1.~~4.1. Enhanced Weathering coupled to Afforestation/Reforestation

Phosphorus (P) is a limiting nutrient in a wide range of ecosystems (Elser et al., 2007)~~.~~ and in temperate and tropical climate zones (Du et al., 2020). P deficiency might affect biomass growth of tropical (Herbert and Fownes, 1995;Tanner et al., 1998;Wright et al., 2011) and northern forests (Menge et al., 2012;Shinjini et al., 2018)~~. The numerical simulations of Kracher (2017) predict biomass growth for the 21" century (Supplement S1 Fig. S5) considering natural water supply, CO_2 fertilization, and N-unlimited and N-limited scenario. In the present text, we will focus on the results from the N-limited scenario since it considers natural N supply. In the supplement, the results for the N-unlimited scenario are presented. The predicted C sequestration by the N-limited AR scenarios from~~ with mineral P already limiting biomass production in European forests (Jonard et al., 2015) and in Forests from USA (Garcia et al., 2018), as well as agricultural areas (Ringeval et al., 2019;Kvakić et al., 2018). The uncertainty on which P pool is available for long-term plant nutrition is high (Johnson et al., 2003;Sun et al., 2017) and we tackled this uncertainty assuming two potential geogenic P supply scenarios. Geogenic supply scenario two, assuming P from weathering and atmospheric deposition plus inorganic labile P and organic P, is a very optimistic assumption that might not correspond to reality based on the already observed P limitation on different ecosystems (Elser et al., 2007). However, we cannot rule out that gradual shifts in soil organic P fractions occur, which make comparable amounts of P as in scenario two available over time.

The numerical simulations of Kracher (2017) ~~is 2.0 Gt C a^{-1}.~~predicted biomass growth for the 21st century (Fig. 2) considering natural water supply, CO_2 fertilization, and N-unlimited and N-limited scenario for an RCP4.5 greenhouse gas concentration trajectory and land use transitions. The predicted C sequestration by the N-limited AR scenarios from Kracher (2017) is ~2 Gt C a^{-1}. Different authors reported the potential C sequestration by afforestation or reforestation being of 0.3 – 3.3 Gt C a^{-1} for the end of 2099 (National Research Council, 2015;Lenton, 2014, 2010;Smith et al., 2015 apud Fuss et al., 2018). However, the predicted sequestration potential estimated by Kracher (2017) can drop to ~1.3 Gt C a^{-1} if geogenic P supply scenario one for mean P content within wood and leaves is selected. If geogenic P supply scenario two for mean P content within wood and leaves is selected, it drops to ~1.9 Gt C a^{-1}.

~~The here estimated P demand based on the predicted biomass growth to sequester 190 Gt C (N-limited AR scenario) amounts to 200 Mt P on global scale for a mean wood and leaves P content. Since there are more than 60,000 tree species~~More than 60,000 tree species are recorded worldwide (Beech et al., 2017) and a precise estimation on tree chemistry represents a challenge~~. Based on global and US specific databases,~~, which we attempted to represent by the ~~range~~considered ranges of ~~N stock-based additional P demand is 71 / 345 Mt P; 5th / 95th percentile for~~ wood and leaves chemistry~~.~~

~~The P budget for geogenic P supply scenario one, with P supply by weathering and atmospheric deposition, suggest that P deficiency areas are distributed around the world, but with more frequent occurrences in the northern hemisphere (Fig. 2a).~~ from the databases. However, ~~for geogenic P supply scenario two, which is the same as geogenic P supply scenario one plus geogenic P from soil inorganic labile P and organic P pools, the P deficiency areas are predominantly located in the southern hemisphere (Fig. 2b). If N and P are limiting nutrients, it is expected a C reduction of 16.5 – 59.0%, with mean C reduction of 47.0% for the geogenic P supply scenario one and 19.0% for the geogenic P supply scenario two. Therefore, accounting for N and P limitation on AR suggests that, in average; the biomass production will be more affected, which decreases the C sequestration potential of AR strategies (Table 3). In some areas, the C sequestration can be reduced by up to 100% compared to the predicted C sequestration of the AR models (Fig. 3).~~

~~Different~~different pathways and mechanisms control soil P availability to the plant (Vitousek et al., 2010), and they are not considered in our estimations leading to conservative predictions. Adding soil P dynamics to models would allow to reliably quantify the C sequestration potential of AR~~, *e.g.,* using P enabled land surface models~~ (e.g., using P enabled land surface models; Sun et al., 2017;Wang et al., 2017;Goll et al., 2012;Goll et al., 2017;Wang et al., 2010;Yang et al., 2014b).

Kracher (2017) has shown that N can limit biomass production and consequently C sequestration. To achieve the projected C sequestration of 190 Gt C for N-limited scenario, the estimated P gaps must be closed. Potential P sources are industrial fertilizers, like diammonium phosphate (DAP) or rock powder~~,~~ (e.g., basalt~~.~~). However, DAP potentially represents an extra input of ammonium to the groundwater and it is expected, in the long-term, that DAP deployment acidifies the soil ~~(Fertilizer Technology Research Centre~~McLaughlin, 2016).

Most of the world soils are acidic, with some being strongly acidic (IGBP-DIS, 1998), which generally favors the sorption of orthophosphate onto Fe- and Al-(hydro)oxides surfaces and clay minerals, essentially demobilizing P (Shen et al., 2011).

Formatted: Font: Not Italic

Field Code Changed

Besides that, the long AR time span can undermine the effectiveness of DAP to supply P for forests due to the high soil acidification potential of DAP. Therefore, rock powder application can be an alternative as nutrients are slowly released and an increase of alkalinity fluxes is expected (Dietzen et al., 2018), which can raise and stabilize the pH of soils.

Field Code Changed

~~Correcting~~Re-establishing soil pH to ~~ideal~~(near) neutral conditions, generally between 6.6 and 7, will provide new nutrient holding sites at Fe- and Al-(hydro)oxides surfaces, and at soil organic matter ~~and~~; which turns the sorbed orthophosphate ~~will be~~ plant available. An application of 8 kg m^{-2} basalt powder can increase the CEC of oxisols by 150 – 300% (Anda et al., 2015;Anda et al., 2009) and improve the C- and N-mineralization ~~(Mersi et al., 1992).~~

~~Assuming a median P content of 500 ppm in basalt, *cf.*, subchapter 2.5~~(Mersi et al., 1992), for ultisols, the ~~maximum mass applied in 94 years would be of 33 and 13~~CEC increase by 44% after deploying ~7 kg ~~basalt~~ m^{-2} ~~respectively for P gap from both geogenic P supply scenarios. Considering the basalt deployment areas, a total amount of 2 – 362 Gt basalt applied by EW would be needed to cover the projected P gaps (5th – 95th percentile from geogenic P supply scenario two and one). Basalt has a carbon capture potential of ~ 0.3 tCO_2 t^{-1} basalt (Renforth, 2012), sequestering 0.6 – 97.8 Gt CO_2 by the end of 2099 if~~ basalt powder ~~would be deployed to cover P gaps of the N-limited AR scenario.~~(Noordin et al., 2017).

~~Rhyolite, dacite or andesite could alternatively be used as a source of P, but these rocks generally have lower P content than basalt. As a consequence, the necessary amounts of each rock to cover P gap of each P budget scenario for the AR scenarios, based on chemical composition, will be higher. Therefore, basalt powder is more effective to supply P for the estimated P gap areas due to relative high P content.~~

To avoid shifts of nutrient limitation, the supply of macronutrients like Mg, Ca, and K ~~should~~might be proportional to P supply since Mg is required as an essential element in chlorophyll, Ca has a structural role, and K is responsible for water and ionic balance (Hopkins and Hüner, 2008). Rock powder can be used as source of these nutrients, as suggested by different authors (Beerling et al., 2018;Hartmann et al., 2013;Straaten, 2007)~~. Therefore, we investigated if these macronutrients are supplied by EW for balanced tree nutrition. Assuming median rock nutrient content, the different rock types under study can supply the necessary amount of Ca, Mg, and K for balanced tree nutrition if they are used to close the projected P gaps (Supplement S1 Fig. S6). The~~ and according to our results from Fig. 7 and Fig. 8. However, the potential of basalt powder to supply K, based on chemical composition, is lower than for other analyzed rocks. For median values, rhyolite has the highest content of K; however, if occurring in K-feldspars it will not be plant available. Blending these rocks in different proportions could result in a more balanced macronutrient supply (Leonardos et al., 1987).

~~For a rock chemical composition corresponding to the 95th percentile of P content, 10 kg basalt m^{-2} would cover the maximum projected P gaps for all P supply scenarios. For a median chemical composition of rock, deploying 33 kg basalt m^{-2} would cover all the P gaps of the two geogenic P supply scenarios. For the 5th percentile, the necessary amount of rock would be even higher. Besides successfully covering the estimated P deficiencies, basalt powder seems to supply enough K, Mg, and Ca to the afforested system contributing to balanced biomass nutrition (Fig. 4) and, as expected, avoiding shift of growth limitation to other nutrients.~~

RCP8.5 scenario predicts that global agricultural areas (crop land and pastures) are going to increase in the course of 21st century due to a decrease in forested area (Sonntag et al., 2016). Assuming a future scenario of high atmospheric CO_2 levels (RCP8.5), but using the land use transitions and wood harvest rates from a RCP4.5 scenario (Sonntag et al., 2016), a similar forest cover fraction than the one presented in Fig. 2 is expected (cp. Figure 1 Sonntag et al. (2016)) and geogenic P supply would also limit the predicted biomass growth. Similar areas of forest growth were observed in Figure 2c presented in the study from Yousefpour et al. (2019) by comparing it to Fig. 2. Though using only one model induces uncertainty, however, it would not change the general message of this work.

~~3.2.~~4.2. Enhanced Weathering coupled to ~~biomass production from~~ bio-energy grass production

Generally, natural soil P content is inadequate for long-term cultivation of agricultural plants. To overcome this issue, P is supplied by fertilizers to reach or maintain optimum levels of crop productivity (Sharpley, 2000) after several harvest rotations. In order to keep a positive CO_2 balance, an alternative to industrial fertilizers ~~should~~might be used to replenish the exported nutrients by harvest. ~~Rock powder application could increase the soil macro- and micronutrient stocks, maintaining or increasing biomass yields without decreasing CDR efficiency. For a high nutrient content (95% confidence intervals) deploying up to 1.5 kg basalt m^{-2} a^{-1} could meet the K needs of bio-energy grass (Fig. 5) and would be able to replenish up to 75% of the exported P, if the maximum bio-energy grass yield is considered (Fig. 5). Industrial fertilizer co-application would be indicated to completely replenish exported P reducing industrial fertilizers dependency. Deploying 8 kg basalt m^{-2} a^{-1} would be enough to replenish exported K and P by harvest assuming median nutrient content of basalt powder (Fig. 5).~~

The chemical composition of rocks is highly variable ~~(Supplement S1 Fig. S4). Different~~(Fig. 4) and different rock types can be used for EW ~~and ideal~~. Ideal rock types need to be chosen in order to resolve a specific plant nutrient deficiency, and enhance the nutrient reservoir of a target soil besides increasing the soil pH, the CEC (Anda et al., 2015;Anda et al., 2009), improve the C- and N-mineralization ~~(Mersi et al., 1992)~~, the soil organic carbon (Doetterl et al., 2018) and the supply of Si (Beerling et al., 2018;Hartmann et al., 2013). In the case of oxisols, which are found over about 8% of the glacier-free land surface and common in tropical and subtropical agricultural regions, application of 8 kg m^{-2} basalt powder can increase the CEC by 150 – 300% ~~(Anda et al., 2015;Anda et al., 2009)~~. For ultisols, which are found over about 8% of the glacier-free land surface, application of ~7 kg m^{-2} basalt powder can increase the CEC by 44% (Noordin et al., 2017).

Overall, rock application ~~could~~has the potential to resupply the harvest exported nutrients, and partially or totally close the short- and long-term nutrient gaps in soil. Individual rock types, from basic (Mg, Ca) to acidic (K, Na), contain varying amounts of target nutrients and mixing them might increase the overall nutrient supply capacity (Leonardos et al., 1987). Intrinsic mineralogical and or petrographic structures can influence the release of nutrients (Ciceri et al., 2017), which makes them plant unavailable in some cases. K can also limit plant growth; it occurs in K-feldspars as a plant unavailable form, in the case of ~~acid~~acidic rocks, but becomes accessible after hydrothermal treatment (Liu et al., 2015;Ma et al., 2016a;Ma et al., 2016b).

However, research on release processes of other macro- and micronutrients and on nutrient-release optimization~~,~~ (e.g., by hydrothermal decomposition~~,~~) is necessary to be able to parameterize this effect in the soil environment.

Harvest rates will control the nutrient export from bioenergy grass fields. Therefore, an increase in harvest rate represent an increase in nutrient export and vice-versa. Thus, to keep with a sustainable nutritional balance of soils, the exported nutrients must be replenished, otherwise maintaining the high harvest rates become an unsustainable situation. Accounting for other simulation setup or a numerical model different from MAgPIE might change the harvest rates of this study. If we assume that the maximum harvest rate of 3.6 kg m^{-2} a^{-1} would hypothetically increase by one order of magnitude, the maximum exported nutrients would be of ~0.2 kg K m^{-2} a^{-1} and ~0.04 kg P m^{-2} a^{-1}, which would demand a basalt deployment rate of ~13 kg m^{-2} a^{-1} and ~20 kg m^{-2} a^{-1} (considering 95th percentiles of chemical composition for basalt) to respectively replenish the exported nutrients. If median K and P concentrations on basalt powder are assumed, the basalt deployment rate increase to ~48 kg m^{-2} a^{-1} and 73 kg m^{-2} a^{-1} to respectively replenish the exported nutrients (Supplement SI Fig. S11). However, such an increase in harvest rates might not correspond to reality. Harvest rates smaller than 0.7 kg m^{-2} a^{-1} (the minimum) represent less nutrient export, decreasing the basalt powder deployment rates necessary to replenish the exported nutrients by harvest.

~~3.3.~~4.3. Impacts on soil hydrology

AR and BECCS demand huge quantities of irrigation water (Boysen et al., 2017b;Bonsch et al., 2016), and it is projected that climate change will affect the water balance, and consequently influence crop yields (Kang et al., 2009). Soils with higher water holding capacity will better tolerate the impacts of drought (Kang et al., 2009). Therefore, practices that improve water availability to plants at the root system are used as strategies to mitigate drought effects (Rossato et al., 2017). We investigated if deployment of rock powder can change the top soil hydraulic conductivity, and plant available water (PAW) for different application ranges.

~~To show baseline hydraulic properties for soils with any sort of P gap, the initial hydraulic properties were estimated, and they show high variability. The projected hydraulic conductivity (K_s) of top soils for areas corresponding to those of P budget from geogenic P supply scenario one (Supplement S1 Fig. S21a), for the N-unlimited AR scenario encompass values ranging from 1.5×10^{-7} and 7.8×10^{-4} m s^{-1} and for PAW of 4% and 32% (Table 4). Neglecting the topography, soils having low K_s, *e.g.*, values of 1.5×10^{-7} m s^{-1}, would experience the lowest water infiltration rate. The impacts of deploying a fine basalt texture (15.6% clay, 83.8% silt, and 0.6% fine sand) or a coarse basalt texture (15.6% clay, 53.8% silt, and 30.6% fine sand), which are in the range of commercial powders (Nunes et al., 2014), on soil hydrology were estimated for different application upper limits.~~

~~Impact of rock powder deployment could be neglected, in average, for upper limits until 50 and 205 kg basalt m^{-2} respectively for a fine and a coarse textured rock powder being deployed. However, deviations from what is expected for the mean might occur (Fig. 6 and Supplement S1 Fig. S23 for P gap from geogenic P supply scenario two). The average values for PAW~~

Formatted: Font: Not Italic

~~increase together with the increase of the upper limits of rock powder application, but for a coarse basalt powder some areas might experience a decrease in the PAW (Fig. 6 and Supplement S1 Fig. S23 for P gap from geogenic P supply scenario two). However, overloading the soil system with rock powder can trigger plant suffocation, if gas exchange is prevented by water saturation of pores (Sairam, 2011).~~

~~Closing the observed P gap from areas presented in Supplement S1 Fig. S21 would require a maximum deployment of 34 kg basalt m^{-2} for P budget of geogenic P supply scenario one and 13 kg basalt m^{-2} for P budget of geogenic P supply scenario two (Supplement S1 Fig. S7). The P gaps from scenario two (Supplement S1 Fig. S21b) could be filled by a coarse or fine basalt powder and the related changes in soil hydrology could be neglected, remaining below 10% (for more or less) for most of the areas (Supplement S1 Fig. S26 and S27). If the geogenic P supply from scenario one, for the N-unlimited AR scenario (Supplement S1 Fig. S21a) is assumed and a fine basalt powder is applied, the maximum and minimum changes on hydraulic conductivity could be of 58% and -11.0% (Supplement S1 Fig. S24a). Decrease on PAW could be neglected for most of the deployment areas, but some would have an increase of up to 31.0% from 13.8% to 18.2% (Supplement S1 Fig. S24b). A coarse basalt powder would, in general, cause fewer impacts to soil hydraulic properties (Supplement S1 Fig. S25).~~

Concrete effects of EW on biomass productivity would depend if the changes in the initial PAW values for top soils would reach PAW threshold values to trigger biomass productivity (Sadras and Milroy, 1996). In general, the average changes on topsoil PAW related to basalt powder application would not be enough to trigger biomass growth~~, *e.g.*,~~. Therefore, areas showing PAW changes from 14% to 21% would not trigger leaf and stem expansion of maize, wheat or soybean~~, but could increase leaf and stem expansion of pearl millet~~ (Sadras and Milroy, 1996), but could increase leaf and stem expansion of pearl millet (Sadras and Milroy, 1996) after deploying 50 kg basalt m^{-2} with a fine texture. 50 kg basalt m^{-2} of coarse powder changes PAW by 19% consequently not triggering biomass productivity.

The ~~equations from~~finest grain size Saxton and Rawls (2006) ~~do not consider changes in the rock powder mineralogy, *e.g.*, by clay mineral formation, which can potentially increase the water holding capacity of soils, and subsequently change the PAW.~~equations can consider is the clay fraction (grains diameter >1 µm and <3.9 µm). Fine grain sizes influence the exposed reactive surface area of rock powder, which will affect the weathering rates. The fine basalt would have the grain sizes ranging in between 0.6 – 90 µm which might be enough to completely dissolve the deployed rock powder after one year (Strefler et al., 2018). For the coarse basalt powder, ~70% of its granulometry fall into the 0.6 – 90 µm range and from the other 30%, about 20% might be dissolved in one year (Strefler et al., 2018). Based on the used pedotransfer functions, If a basalt powder would contain only grains on the clay size fraction, the effects on soil hydraulic conductivity would decrease by 37% for deployment amount of 30 kg basalt m^{-2} (for the fine rock powder used in our work, the hydraulic conductivity would decrease by only 2%). The finer the grain gets the higher the energy input for grinding is, which can drastically affect the costs of EW (it can reach up to 500$ tCO_2^{-1} sequestered; Strefler et al., 2018). Since grains of different diameters need different times for complete dissolution, a rock powder with different grain sizes would act as a constant source of nutrients to soil.

During the weathering of rock powder, clay mineral genesis can occur and potentially increase the water holding capacity of soils (Gaiser et al., 2000), which can subsequently change the estimated PAW. The added fresh silicate minerals to the soil by EW will have high reactivity releasing a significant amount of nutrients, which increases soil nutrient pools. The increased nutrient availability will increase the potential of soils to stabilize carbon (Doetterl et al., 2018) and a positive effect on PAW is expected to occur based on Eqs. (15) to (17) and according to Olness and Archer (2005). The suitable amounts of rock powder applied depend on the target changes of the chosen soil, and on its intrinsic grain size distribution and organic matter content. Intrinsic grain properties like the shape of grains and pores, tortuosity, specific surface area, and porosity should be considered (Bear, 1972). ~~Field~~ for the evaluation of changes in soil hydraulic properties by pedotransfer functions and its consequences to dissolution kinetics. A large set of data from field and laboratory experiments covering different soil types, climatic regions, and plant species would enable a qualitatively, and quantitatively reliable assessment of soil hydrology impacts~~.~~, but also dissolution rates and changes on soil's mineralogy. The ~~impacts~~effects on soil microorganisms should be taken into account in order to correct the limits of rock powder deployment. The potential of rock powder to trigger plant suffocation, if gas exchange is prevented by water saturation of pores (Sairam, 2011), should also be considered before deployment.

~~3.4.~~4.4. Challenges of rock powder deployment

Average tillage depth ~~common machinery can reach~~ is 0.3 m and greater depths ~~cause~~can be reached with higher energy~~,~~ and labor costs (Fageria and Baligar, 2008). Since annual crops have an effective rooting depth typically in the range of 0.4 – 0.7 m (Madsen, 1985;Aslyng, 1976;Munkholm et al., 2003;Olsen, 1958), a deployment ~~depths~~depth of 0.3 m seems to be reasonable. ~~Once~~Since tillage can trigger soil carbon loss (Reicosky, 1997;La Scala et al., 2006), deploying rock powder at soil surface might be a solution. At the soil surface, the long-term water percolation, and~~-~~/or bioturbation (Fishkis et al., 2010;Taylor et al., 2015) can transport and mix fine-grained material to deeper regions within the soil profile, which potentially can change the K_S, and PAW at crop rooting zones. Groundwater recharge rates might change if clogging of pores at deeper regions of soil profile occurs~~.~~ or if the changes in soil hydraulic properties due to rock deployment can significantly influence the initial soil hydraulic conditions for a constant water precipitation. Taylor et al. (2015) argue that downward transport of a silt-textured powder deployed at a soil surface would easily reach the rooting zone of trees, which is in its majority in a depth up to 0.4 m. The authors suggest that in tropical regions higher depths might be reached due to intensive rain and bioturbation. Detailed field studies to better comprehend downward transport of grained material through the soil profile, changes on soil water residence time, PAW, mineralogy, nutrient pools, CEC (Anda et al., 2015, 2013), and bioavailability of released trace metals (Renforth et al., 2015) are necessary~~, to be able to~~. This would provide management recommendations for the diverse existing settings for EW application. In the present study, estimates for different basalt powder application upper limits are

Formatted: Highlight

done for changes in soil hydraulic properties without accounting for downward transport of fine particles through the soil profile.

Besides avoiding clogging of pores of the top soil layer by rock powder application in a certain extent, downward transport of rock powder can contribute freshly ground material being in contact with roots of trees or crops, which can enhance the weathering rates and create new sites to retain nutrients (Kantola et al., 2017;Anda et al., 2015).

Once the freshly ground material is in contact with the soil, different factors control the nutrient supply efficiency of rock powder. The nutrients from fresh material are initially inert protected within the crystallographic structures of the minerals, and would become plant-available only in solution or associated to mineral surfaces (Appelo and Postma, 2005). The release of nutrients by weathering is controlled by film and intra-particle diffusion-limited mass transfer influenced by pH, and ionic strength of the soil aqueous solution (Grathwohl, 2014), both being controlled by rooting exudates in the rhizosphere and chemical composition of infiltrating waters.

Full dissolution is a simplification based on modelled scenarios (Taylor et al., 2015;Strefler et al., 2018). Under field conditions, soil water could rapidly reach near-equilibrium concentrations (Grathwohl, 2014), which would decrease weathering rates. The opposite would occur if near-equilibrium conditions could be disturbed by a sink of nutrients by nutrient root uptake (Stefánsson et al., 2001) or by percolation of water un-equilibrated with soil porous water (Calabrese et al., 2017).

The nutrient (Mg, Ca, K, P, etc.) content of rocks can vary significantly. Besides that, deploying rock powders with grain sizes > 90 µm would decrease the reactive surface area of deployed rock powder decreasing the weathering fluxes (Goddéris et al., 2006). The median and the ranges (5^{th} or 95^{th} percentile) values for Mg, Ca, K, P content obtained from the EarthChem database considered chemical analysis of 2985 rhyolites, 3008 dacites, 11099 andesites, and 23816 basalts. Broadening the classification criteria for these rocks would change median and the ranges (5^{th} or 95^{th} percentile) for chemical composition; however, the selected median and the ranges of this study are conservative estimates. As an illustration, Porder and Ramachandran (2013) adopted another selection criteria, for the same database, which resulted in a total of 97895 samples and estimated a median P content of Basalt of 916 ppm. Additionally, the selected rock chemistry database also influences the descriptive statistics results. Recently published values for P content within basalt considering GEOROC database are 1309 ppm for median content and 428 ppm for 10^{th} percentile and 3186 ppm for 90^{th} percentile (Amann and Hartmann, 2019). Thus, before deploying EW to supply nutrients, the chemical composition of rock powder should be known to properly estimate the necessary amount of rock for supplying the demanded nutrients of a specific plant. This would allow to easily estimate the impacts on soil hydrology by the pedotransfer functions of this study or by specific laboratory experiments.

Besides the potential to be used to rejuvenate soil nutrient pools (Leonardos et al., 1987), silicate rock powder can be used to reduce the risk of nitrate mobilization, being indicated for regions in which special care to water preservation is needed. ~~However, extra input of sodium (Na) to the system, if the rock is rich in this element, could disturb this amelioration effect (Von Wilpert and Lukes, 2003)~~However, extra input of sodium (Na) to the system, if the rock is rich in this element, could disturb this amelioration effect (Von Wilpert and Lukes, 2003). Besides decreasing nitrate mobilization, co-application of rock

powder with other fertilizers can increase the biomass production of crops (Anda et al., 2013;Leonardos et al., 1987;Theodoro et al., 2013).

An additional challenge of the application of rock products will be the assessment of the fate of weathering products, which might be transported eventually into river systems and alter geochemical baselines as evidenced by past land use changes in some large rivers (Hartmann et al., 2007;Raymond and Hamilton, 2018).

4.5. Conclusions

Our results illustrate the potential of Enhanced Weathering (EW) to act as a nutrient source to nutrient demanding AR and BG. This is an important, yet often overlooked, aspect of EW besides CO_2 sequestration. The investigated scenarios show that areas with undersupply of P exist, and a C-stock reduction is expected to occur if P is the only limiting nutrient. Considering N, and P deficiency together for a low geogenic P supply and high biomass P demand, the C-stock reduction ~~increases~~will be up to 59% of the projected total global C sequestration potential of 224 Gt C from the N-unlimited AR scenario. Potential P deficiencies were here based on the soil P availability and P demand scenarios, indicating that the inclusion of P cycles in AR models is necessary to accurately project the C sequestration of forests. Industrial fertilizers can be used to alleviate the P deficiency but the extra input of ammonium along with it can undermine the carbon budget and acidify the soils. Furthermore, acidic soil conditions generally favors the sorption of orthophosphate onto Fe- and Al-(hydro)oxides surfaces and clay minerals, essentially demobilizing P (Shen et al., 2011).

Besides the high chemical P content and relative fast weathering rates, the equilibrated supply of Ca, K, and Mg put the use of basalt powder one step ahead as a potential alternative to industrial fertilizers~~.~~ than other rocks. Regrowth of forests on abandoned agricultural land is a passive landscape restoration method (Bowen et al., 2007). In most of the cases soils become acidic in abandoned agricultural land in the long term (Hesterberg, 1993), which favors the leaching of nutrients (Haynes and Swift, 1986) and heavy metals (Hesterberg, 1993). As a consequence, the regrowth rate of forests might be limited in acidic soils. The use of basalt powder will keep a positive carbon budget, increase the soil pH (Anda et al., 2015;Anda et al., 2009), as basalt powder would act as a buffer maintaining soil pH under neutral to slight alkaline conditions, close nutritional needs of AR and BG, and rock powder can be used to reduce the risk of nitrate mobilization ~~(Von Wilpert and Lukes, 2003).~~(Von Wilpert and Lukes, 2003). However, to be able to assess the global potential of the combination of land-based biomass NETs with EW~~;~~, it is necessary to ~~compile knowledge on the~~explore related physico-chemical changes of soil influenced by ~~a variety of~~varying EW deployment rates, ~~from the~~based on already available data, and then develop improved EW models. They should be tested with field-based approaches. For example, tracking added elements through the ecosystem's soil and plant reservoirs probably needs test sites using advanced methods of nutrient balance and isotope studies, as recently developed (Uhlig, 2019;Uhlig et al., 2017;Uhlig and von Blanckenburg, 2019).

In addition to the use for replenishing soil nutrient content, our research suggests that deployment of rock powder on the top soil can enhance Plant Available Water (PAW) for different upper limits. Apart from controlling the nutrient release rates, the texture of deployed rock powder would influence the impacts on soil hydrology together with the initial soil texture. In general, EW appears to have considerable potential for water retention management of top soils. This is an important characteristic not explored before, since under a future scenario of climate change EW can potentially mitigate or alleviate drought effects ~~in~~to a certain extent within areas used for AR and BG plantation. Field and laboratory experiments are needed to quantify soil hydraulic changes under a natural and controlled environment. Besides that, investigation of potential changes of coupling EW with other terrestrial NETs such as Biochar is necessary, since Biochar and EW can increase the amount of soil organic matter, a variable also responsible for increasing water retention of soils.

We show that EW can be an important part of the solution to the problem of nutrient limitation AR and BG might suffer from. Specifically, the potential for hydrological management of soils was shown and it could be used in areas where seasonality and droughts might affect the biomass growth. The use of Enhanced Weathering for hydrological management coupled to land based NETs is worth to investigate. A global management of the carbon pools will need a full ecosystem understanding, addressing nutrient fluxes, and related soil mineralogy changes, soil hydrology, impacts on soil microorganisms, and responses of plants on the diverse array of soil types and climates. Applied ecosystem engineering is likely a future nexus discipline which needs to link local ecosystem processes with a global perspective on carbon pools within a universal effort to manage the carbon cycle.

~~5.~~6. ORCID iDs

Wagner de Oliveira Garcia https://orcid.org/0000-0001-9559-0629
Jens Hartmann https://orcid.org/0000-0003-1878-9321
Thorben Amann https://orcid.org/0000-0001-9347-0615
Pete Smith https://orcid.org/0000-0002-3784-1124
Lena R. Boysen http://orcid.org/0000-0002-6671-4984
Daniel Goll https://orcid.org/0000-0001-9246-9671

~~6.~~7. Acknowledgements

This study was funded by the German Research Foundation's priority program DFG SPP 1689 on "Climate Engineering–Risks, Challenges and Opportunities?" and specifically the CEMICS2 project. In addition this work was supported by the Deutsche Forschungsgemeinschaft (DFG, German Research Foundation) under Germany´s Excellence Strategy – EXC 2037

'Climate, Climatic Change, and Society' – Project Number: 390683824, contribution to the Center for Earth System Research and Sustainability (CEN) of Universität Hamburg. DSG is funded by the "IMBALANCE-P" project of the European Research Council (ERC-2013-SyG-610028). We are grateful for the constructive comments and suggestions from the reviewers and editor.

8. Review statement.

This paper was edited by Alexey Eliseev and reviewed by Daniel Ibarra and an anonymous referee.

~~7.~~9. Author contribution

This article was conceived by the joint work of all authors, which participated in the discussions and writing, with the lead of WOG. The study was designed by W.O.G., J.H., and T.A~~.~~. W.O.G. compiled all the used data and conducted the calculations. K.K and A.P. supplied the MAgPIE model simulations and the stoichiometric ratios used for bioenergy grass. L.R.B. contributed to handling the JSBACH model outputs and D.G. contributed to the methodology to obtain the P-stock based demand for AR.

~~8.~~10. Competing interests

The authors declare that they have no conflict of interest.

~~9.~~11. References

, !!! INVALID CITATION !!! .

14688-1:2002, I.: 14688-1: 2002: Geotechnical investigation and testing–Identification and classification of soil–Part 1: Identification and description, International Organization for Standardization, Geneva, 2002.

Achat, D. L., Augusto, L., Gallet-Budynek, A., and Loustau, D.: Future challenges in coupled C–N–P cycle models for terrestrial ecosystems under global change: a review, Biogeochemistry, 131, 173-202, 10.1007/s10533-016-0274-9, 2016.

Amann, T., and Hartmann, J.: Ideas and perspectives: Synergies from co-deployment of negative emission technologies, Biogeosciences, 16, 2949-2960, 10.5194/bg-16-2949-2019, 2019.

Amiotte Suchet, P., Probst, J. L., and Ludwig, W.: Worldwide distribution of continental rock lithology: Implications for the atmospheric/soil CO2 uptake by continental weathering and alkalinity river transport to the oceans, Global Biogeochemical Cycles, 17, 2003.

Anda, M., Shamshuddin, J., Fauziah, C. I., and Omar, S. R. S.: Dissolution of Ground Basalt and Its Effect on Oxisol Chemical Properties and Cocoa Growth, Soil Science, 174, 264-271, 10.1097/SS.0b013e3181a56928, 2009.
Anda, M., Shamshuddin, J., and Fauziah, C. I.: Increasing negative charge and nutrient contents of a highly weathered soil using basalt and rice husk to promote cocoa growth under field conditions, Soil & Tillage Research, 132, 1-11, 10.1016/j.still.2013.04.005, 2013.
Anda, M., Shamshuddin, J., and Fauziah, C. I.: Improving chemical properties of a highly weathered soil using finely ground basalt rocks, Catena, 124, 147-161, 10.1016/j.catena.2014.09.012, 2015.
Appelo, C. A. J., and Postma, D.: Geochemistry, Groundwater and Pollution, Second Edition, 2005.
Aslyng, H.: Klima, jord og planter, Kulturteknik I, 5, 1976.
Augusto, L., Achat, D. L., Jonard, M., Vidal, D., and Ringeval, B.: Soil parent material-A major driver of plant nutrient limitations in terrestrial ecosystems, Glob Chang Biol, n/a-n/a, 10.1111/gcb.13691, 2017.
Batjes, N.: ISRIC-WISE global data set of derived soil properties on a 0.5 by 0.5 degree grid (version 3.0), ISRIC – World Soil Information, 2005.
Bear, J.: Dynamics of fluids in porous media, American Elsevier., New York, 1972.
Beech, E., Rivers, M., Oldfield, S., and Smith, P.: GlobalTreeSearch: The first complete global database of tree species and country distributions, Journal of Sustainable Forestry, 36, 454-489, 2017.
Beerling, D. J., Leake, J. R., Long, S. P., Scholes, J. D., Ton, J., Nelson, P. N., Bird, M., Kantzas, E., Taylor, L. L., Sarkar, B., Kelland, M., DeLucia, E., Kantola, I., Müller, C., Rau, G., and Hansen, J.: Farming with crops and rocks to address global climate, food and soil security, Nature Plants, 4, 138-147, 10.1038/s41477-018-0108-y, 2018.
Beringer, T., Lucht, W., and Schaphoff, S.: Bioenergy production potential of global biomass plantations under environmental and agricultural constraints, Gcb Bioenergy, 3, 299-312, 2011.
Berner, A. R. L., A. C., and Garrels, R. M.: The carbonate-silicate geochemical cycle and its effect on atmospheric carbon dioxide over the past 100 million years, Am J Sci, 283, 641-683, 1983.
Beyer, W.: Zur bestimmung der wasserdurchlässigkeit von kiesen und sanden aus der kornverteilungskurve, WWT, 14, 165-168, 1964.
Bissonnais, Y. L., and Singer, M. J.: Crusting, Runoff, and Erosion Response to Soil Water Content and Successive Rainfalls, Soil Science Society of America Journal, 56, 1898-1903, 10.2136/sssaj1992.03615995005600060042x, 1992.
Bodirsky, B. L., Popp, A., Weindl, I., Dietrich, J. P., Rolinski, S., Scheiffele, L., Schmitz, C., and Lotze-Campen, H.: N2O emissions from the global agricultural nitrogen cycle – current state and future scenarios, Biogeosciences, 9, 4169-4197, 10.5194/bg-9-4169-2012, 2012.
Bondeau, A., Smith, P. C., Zaehle, S., Schaphoff, S., Lucht, W., Cramer, W., Gerten, D., LOTZE-CAMPEN, H., Müller, C., and Reichstein, M.: Modelling the role of agriculture for the 20th century global terrestrial carbon balance, Global Change Biology, 13, 679-706, 2007.
Bonsch, M., Humpenöder, F., Popp, A., Bodirsky, B., Dietrich, J. P., Rolinski, S., Biewald, A., Lotze-Campen, H., Weindl, I., Gerten, D., and Stevanovic, M.: Trade-offs between land and water requirements for large-scale bioenergy production, GCB Bioenergy, 8, 11-24, doi:10.1111/gcbb.12226, 2016.
Börker, J., Hartmann, J., Romero-Mujalli, G., and Li, G.: Aging of basalt volcanic systems and decreasing CO2 consumption by weathering, Earth Surface Dynamics, 1-9, 2018.
Börker, J., Hartmann, J., Romero-Mujalli, G., and Li, G.: Aging of basalt volcanic systems and decreasing CO2 consumption by weathering, Earth Surf. Dynam., 7, 191-197, 10.5194/esurf-7-191-2019, 2019.

Bowen, M. E., McAlpine, C. A., House, A. P. N., and Smith, G. C.: Regrowth forests on abandoned agricultural land: A review of their habitat values for recovering forest fauna, Biological Conservation, 140, 273-296, https://doi.org/10.1016/j.biocon.2007.08.012, 2007.
Boysen, L. R., Lucht, W., and Gerten, D.: Trade-offs for food production, nature conservation and climate limit the terrestrial carbon dioxide removal potential, Global Change Biology, 23, 4303-4317, 10.1111/gcb.13745, 2017a.
Boysen, L. R., Lucht, W., Gerten, D., Heck, V., Lenton, T. M., and Schellnhuber, H. J.: The limits to global-warming mitigation by terrestrial carbon removal, Earth's Future, 5, 463-474, 10.1002/2016EF000469, 2017b.
Cadoux, S., Riche, A. B., Yates, N. E., and Machet, J.-M.: Nutrient requirements of Miscanthus x giganteus: Conclusions from a review of published studies, Biomass and Bioenergy, 38, 14-22, https://doi.org/10.1016/j.biombioe.2011.01.015, 2012.
Calabrese, S., Porporato, A., and Parolari, A. J.: Hydrologic transport of dissolved inorganic carbon and its control on chemical weathering, Journal of Geophysical Research: Earth Surface, 122, 2016-2032, 2017.
Carrier III, W. D.: Goodbye, hazen; hello, kozeny-carman, Journal of geotechnical and geoenvironmental engineering, 129, 1054-1056, 2003.
Christman, Z. J., and Rogan, J.: Error Propagation in Raster Data Integration, Photogrammetric Engineering & Remote Sensing, 78, 617-624, 2012.
Ciceri, D., de Oliveira, M., Stokes, R. M., Skorina, T., and Allanore, A.: Characterization of potassium agrominerals: Correlations between petrographic features, comminution and leaching of ultrapotassic syenites, Minerals Engineering, 102, 42-57, 10.1016/j.mineng.2016.11.016, 2017.
Clarkson, D. T., and Hanson, J. B.: The Mineral Nutrition of Higher Plants, Annual Review of Plant Physiology, 31, 239-298, 10.1146/annurev.pp.31.060180.001323, 1980.
Cornelissen, S., Koper, M., and Deng, Y. Y.: The role of bioenergy in a fully sustainable global energy system, Biomass and Bioenergy, 41, 21-33, https://doi.org/10.1016/j.biombioe.2011.12.049, 2012.
Council, N. R.: Climate Intervention: Carbon Dioxide Removal and Reliable Sequestration, The National Academies Press, Washington, DC, 154 pp., 2015.
Creutzig, F.: Economic and ecological views on climate change mitigation with bioenergy and negative emissions, GCB Bioenergy, 8, 4-10, 10.1111/gcbb.12235, 2016.
Crowley, K. F., McNeil, B. E., Lovett, G. M., Canham, C. D., Driscoll, C. T., Rustad, L. E., Denny, E., Hallett, R. A., Arthur, M. A., Boggs, J. L., Goodale, C. L., Kahl, J. S., McNulty, S. G., Ollinger, S. V., Pardo, L. H., Schaberg, P. G., Stoddard, J. L., Weand, M. P., and Weathers, K. C.: Do Nutrient Limitation Patterns Shift from Nitrogen Toward Phosphorus with Increasing Nitrogen Deposition Across the Northeastern United States?, Ecosystems, 15, 940-957, 10.1007/s10021-012-9550-2, 2012.
Dietrich, J. P., Schmitz, C., Müller, C., Fader, M., Lotze-Campen, H., and Popp, A.: Measuring agricultural land-use intensity–A global analysis using a model-assisted approach, Ecological Modelling, 232, 109-118, 2012.
Dietrich, J. P., Schmitz, C., Lotze-Campen, H., Popp, A., and Müller, C.: Forecasting technological change in agriculture—an endogenous implementation in a global land use model, Technological Forecasting and Social Change, 81, 236-249, 2014.
Dietrich, J. P., Bodirsky, B. L., Weindl, I., Humpenöder, F., Stevanovic, M., Kreidenweis, U., Wang, X., Karstens, K., Mishra, A., Klein, D., Ambrósio, G., Araujo, E., Biewald, A., Lotze-Campen, H., and Popp, A.: MAgPIE – An Open Source land-use modeling framework – Version 4.0, doi:10.5281/zenodo.1418752, 2018.
Doetterl, S., Berhe, A. A., Arnold, C., Bodé, S., Fiener, P., Finke, P., Fuchslueger, L., Griepentrog, M., Harden, J. W., Nadeu, E., Schnecker, J., Six, J., Trumbore, S., Van Oost, K., Vogel, C., and Boeckx, P.: Links among warming, carbon

and microbial dynamics mediated by soil mineral weathering, Nature Geoscience, 11, 589-593, 10.1038/s41561-018-0168-7, 2018.
Du, E., Terrer, C., Pellegrini, A. F. A., Ahlström, A., van Lissa, C. J., Zhao, X., Xia, N., Wu, X., and Jackson, R. B.: Global patterns of terrestrial nitrogen and phosphorus limitation, Nature Geoscience, 10.1038/s41561-019-0530-4, 2020.
Edwards, D. P., Lim, F., James, R. H., Pearce, C. R., Scholes, J., Freckleton, R. P., and Beerling, D. J.: Climate change mitigation: potential benefits and pitfalls of enhanced rock weathering in tropical agriculture, Biology letters, 13, 20160715, 2017.
Elser, J. J., Bracken, M. E. S., Cleland, E. E., Gruner, D. S., Harpole, W. S., Hillebrand, H., Ngai, J. T., Seabloom, E. W., Shurin, J. B., and Smith, J. E.: Global analysis of nitrogen and phosphorus limitation of primary producers in freshwater, marine and terrestrial ecosystems, Ecology Letters, 10, 1135-1142, doi:10.1111/j.1461-0248.2007.01113.x, 2007.
Fageria, N. K., and Baligar, V. C.: Chapter 7 Ameliorating Soil Acidity of Tropical Oxisols by Liming For Sustainable Crop Production, in: Advances in Agronomy, Academic Press, 345-399, 2008.
Fischer, G., Shah, M., van Velthuizen, H., and Nachtergaele, F. O.: Global agro-ecological assessment for agriculture in the 21st century, 2001.
Fishkis, O., Ingwersen, J., Lamers, M., Denysenko, D., and Streck, T.: Phytolith transport in soil: A field study using fluorescent labelling, Geoderma, 157, 27-36, https://doi.org/10.1016/j.geoderma.2010.03.012, 2010.
Gaillardet, J., Dupré, B., Louvat, P., and Allegre, C.: Global silicate weathering and CO2 consumption rates deduced from the chemistry of large rivers, Chemical geology, 159, 3-30, 1999.
Gaiser, T., Graef, F., Cordeiro, J., eacute, and Carvalho: Water retention characteristics of soils with contrasting clay mineral composition in semi-arid tropical regions, Soil Research, 38, 523-536, https://doi.org/10.1071/SR99001, 2000.
Garcia, d. O. W., Amann, T., and Hartmann, J.: Increasing biomass demand enlarges negative forest nutrient budget areas in wood export regions, Scientific Reports, 8, 5280, 10.1038/s41598-018-22728-5, 2018.
Gijsman, A. J., Jagtap, S. S., and Jones, J. W.: Wading through a swamp of complete confusion: how to choose a method for estimating soil water retention parameters for crop models, European Journal of Agronomy, 18, 77-106, https://doi.org/10.1016/S1161-0301(02)00098-9, 2002.
Goddéris, Y., François, L. M., Probst, A., Schott, J., Moncoulon, D., Labat, D., and Viville, D.: Modelling weathering processes at the catchment scale: The WITCH numerical model, Geochimica et Cosmochimica Acta, 70, 1128-1147, 10.1016/j.gca.2005.11.018, 2006.
Goll, D. S., Brovkin, V., Parida, B., Reick, C. H., Kattge, J., Reich, P. B., Van Bodegom, P., and Niinemets, Ü.: Nutrient limitation reduces land carbon uptake in simulations with a model of combined carbon, nitrogen and phosphorus cycling, Biogeosciences, 9, 3547-3569, 2012.
Goll, D. S., Moosdorf, N., Hartmann, J., and Brovkin, V.: Climate-driven changes in chemical weathering and associated phosphorus release since 1850: Implications for the land carbon balance, Geophysical Research Letters, 41, 3553-3558, doi:10.1002/2014GL059471, 2014.
Goll, D. S., Winkler, A., Raddatz, T., Dong, N., Prentice, I. C., Ciais, P., and Brovkin, V.: Carbon-nitrogen interactions in idealized simulations with JSBACH (version 3.10), Geoscientific Model Development, 10, 2009-2030, 2017.
Goll, D. S., Joetzjer, E., Huang, M., and Ciais, P.: Low Phosphorus Availability Decreases Susceptibility of Tropical Primary Productivity to Droughts, Geophysical Research Letters, 45, 8231-8240, 10.1029/2018gl077736, 2018.

Grathwohl, P.: On equilibration of pore water in column leaching tests, Waste Management, 34, 908-918, https://doi.org/10.1016/j.wasman.2014.02.012, 2014.
Hartmann, J., Jansen, N., Kempe, S., and Dürr, H. H.: Geochemistry of the river Rhine and the upper Danube: Recent trends and lithological influence on baselines, Journal of Environmental Science for Sustainable Society, 1, 39-46, 2007.
Hartmann, J., and Kempe, S.: What is the maximum potential for CO2 sequestration by "stimulated" weathering on the global scale?, Naturwissenschaften, 95, 1159-1164, 10.1007/s00114-008-0434-4, 2008.
Hartmann, J., Jansen, N., Dürr, H. H., Kempe, S., and Köhler, P.: Global CO2-consumption by chemical weathering: What is the contribution of highly active weathering regions?, Global and Planetary Change, 69, 185-194, 2009.
Hartmann, J., West, A. J., Renforth, P., Köhler, P., De La Rocha, C. L., Wolf-Gladrow, D. A., Durr, H. H., and Scheffran, J.: Enhanced chemical weathering as a geoengineering strategy to reduce atmospheric carbon dioxide, supply nutrients, and mitigate ocean acidification, Reviews of Geophysics, 51, 113-149, 10.1002/rog.20004, 2013.
Hartmann, J., Moosdorf, N., Lauerwald, R., Hinderer, M., and West, A. J.: Global chemical weathering and associated P-release - The role of lithology, temperature and soil properties, Chemical Geology, 363, 145-163, 10.1016/j.chemgeo.2013.10.025, 2014.
Haynes, R. J., and Swift, R. S.: Effects of soil acidification and subsequent leaching on levels of extractable nutrients in a soil, Plant and Soil, 95, 327-336, 10.1007/bf02374613, 1986.
He, Y., Zhu, Y., Smith, S., and Smith, F.: Interactions between soil moisture content and phosphorus supply in spring wheat plants grown in pot culture, 2002.
He, Y., Shen, Q., Kong, H., Xiong, Y., and Wang, X.: Effect of soil moisture content and phosphorus application on phosphorus nutrition of rice cultivated in different water regime systems, Journal of plant nutrition, 27, 2259-2272, 2005.
Herbert, D. A., and Fownes, J. H.: Phosphorus limitation of forest leaf area and net primary production on a highly weathered soil, Biogeochemistry, 29, 223-235, 10.1007/bf02186049, 1995.
Hesterberg, D.: Effects of stopping liming on abandoned agricultural land, Land Degradation & Development, 4, 257-267, 10.1002/ldr.3400040409, 1993.
Holtan, H., Kampnielsen, L., and Stuanes, A. O.: Phosphorus in Soil, Water and Sediment - an Overview, Hydrobiologia, 170, 19-34, Doi 10.1007/Bf00024896, 1988.
Hopkins, W. G., and Hüner, N. P. A.: Introduction to plant physiology, Ed. 4, John Wiley and Sons, 2008.
Humpenöder, F., Popp, A., Dietrich, J. P., Klein, D., Lotze-Campen, H., Bonsch, M., Bodirsky, B. L., Weindl, I., Stevanovic, M., and Müller, C.: Investigating afforestation and bioenergy CCS as climate change mitigation strategies, Environmental Research Letters, 9, 064029, 2014.
Hurtt, G. C., Chini, L. P., Frolking, S., Betts, R. A., Feddema, J., Fischer, G., Fisk, J. P., Hibbard, K., Houghton, R. A., Janetos, A., Jones, C. D., Kindermann, G., Kinoshita, T., Klein Goldewijk, K., Riahi, K., Shevliakova, E., Smith, S., Stehfest, E., Thomson, A., Thornton, P., van Vuuren, D. P., and Wang, Y. P.: Harmonization of land-use scenarios for the period 1500–2100: 600 years of global gridded annual land-use transitions, wood harvest, and resulting secondary lands, Climatic Change, 109, 117, 10.1007/s10584-011-0153-2, 2011.
IGBP-DIS, S.: A program for creating global soil-property databases, IGBP Global Soils Data Task, France, 1998.
Irvine, T., and Baragar, W.: A guide to the chemical classification of the common volcanic rocks, Canadian journal of earth sciences, 8, 523-548, 1971.
John, W.: An introduction to igneous and metamorphic petrology, 552.1 W 784552.1 W 784552.1 W 784552.1 W 784, 2001.

Johnson, A. H., Frizano, J., and Vann, D. R.: Biogeochemical implications of labile phosphorus in forest soils determined by the Hedley fractionation procedure, Oecologia, 135, 487-499, 10.1007/s00442-002-1164-5, 2003.
Jonard, M., Legout, A., Nicolas, M., Dambrine, E., Nys, C., Ulrich, E., Perre, R., and Ponette, Q.: Deterioration of Norway spruce vitality despite a sharp decline in acid deposition: a long-term integrated perspective, Global Change Biology, 18, 711-725, doi:10.1111/j.1365-2486.2011.02550.x, 2012.
Jonard, M., Furst, A., Verstraeten, A., Thimonier, A., Timmermann, V., Potocic, N., Waldner, P., Benham, S., Hansen, K., Merila, P., Ponette, Q., de la Cruz, A. C., Roskams, P., Nicolas, M., Croise, L., Ingerslev, M., Matteucci, G., Decinti, B., Bascietto, M., and Rautio, P.: Tree mineral nutrition is deteriorating in Europe, Glob Chang Biol, 21, 418-430, 10.1111/gcb.12657, 2015.
Kang, Y., Khan, S., and Ma, X.: Climate change impacts on crop yield, crop water productivity and food security – A review, Progress in Natural Science, 19, 1665-1674, https://doi.org/10.1016/j.pnsc.2009.08.001, 2009.
Kantola, I. B., Masters, M. D., Beerling, D. J., Long, S. P., and DeLucia, E. H.: Potential of global croplands and bioenergy crops for climate change mitigation through deployment for enhanced weathering, Biology Letters, 13, 10.1098/rsbl.2016.0714, 2017.
Kempe, S.: Carbon in the rock cycle, The global carbon cycle, 380, 343-375, 1979.
Knust, C., Schua, K., and Feger, K.-H.: Estimation of Nutrient Exports Resulting from Thinning and Intensive Biomass Extraction in Medium-Aged Spruce and Pine Stands in Saxony, Northeast Germany, Forests, 7, 302, 2016.
Kracher, D.: Nitrogen-Related Constraints of Carbon Uptake by Large-Scale Forest Expansion: Simulation Study for Climate Change and Management Scenarios, Earth's Future, 5, 1102-1118, 10.1002/2017EF000622, 2017.
Kvakić, M., Pellerin, S., Ciais, P., Achat, D. L., Augusto, L., Denoroy, P., Gerber, J. S., Goll, D., Mollier, A., Mueller, N. D., Wang, X., and Ringeval, B.: Quantifying the Limitation to World Cereal Production Due To Soil Phosphorus Status, Global Biogeochemical Cycles, 32, 143-157, 10.1002/2017gb005754, 2018.
La Scala, N., Bolonhezi, D., and Pereira, G. T.: Short-term soil CO2 emission after conventional and reduced tillage of a no-till sugar cane area in southern Brazil, Soil and Tillage Research, 91, 244-248, https://doi.org/10.1016/j.still.2005.11.012, 2006.
Landeweert, R., Hoffland, E., Finlay, R. D., Kuyper, T. W., and van Breemen, N.: Linking plants to rocks: ectomycorrhizal fungi mobilize nutrients from minerals, Trends in Ecology & Evolution, 16, 248-254, https://doi.org/10.1016/S0169-5347(01)02122-X, 2001.
Lenton, T. M., and Britton, C.: Enhanced carbonate and silicate weathering accelerates recovery from fossil fuel CO2 perturbations, Global Biogeochemical Cycles, 20, 2006.
Lenton, T. M.: The potential for land-based biological CO2 removal to lower future atmospheric CO2 concentration, Carbon Management, 1, 145-160, 2010.
Lenton, T. M.: The global potential for carbon dioxide removal, Geoengineering of the Climate System, 52-79, 2014.
Leonardos, O. H., Fyfe, W. S., and Kronberg, B. I.: The use of ground rocks in laterite systems: An improvement to the use of conventional soluble fertilizers?, Chemical Geology, 60, 361-370, https://doi.org/10.1016/0009-2541(87)90143-4, 1987.
Liu, S., Han, C., Liu, J., and Li, H.: Hydrothermal decomposition of potassium feldspar under alkaline conditions, Rsc Advances, 5, 93301-93309, 2015.
Lotze-Campen, H., Müller, C., Bondeau, A., Rost, S., Popp, A., and Lucht, W.: Global food demand, productivity growth, and the scarcity of land and water resources: a spatially explicit mathematical programming approach, Agricultural Economics, 39, 325-338, 2008.

Ma, X., Ma, H., and Yang, J.: Sintering Preparation and Release Properties of K2MgSi3O8 Slow-Release Fertilizer Using Biotite Acid-Leaching Residues as Silicon Source, Industrial & Engineering Chemistry Research, 55, 10926-10931, 2016a.
Ma, X., Yang, J., Ma, H., and Liu, C.: Hydrothermal extraction of potassium from potassic quartz syenite and preparation of aluminum hydroxide, International Journal of Mineral Processing, 147, 10-17, 2016b.
Madsen, H. B.: Distribution of spring barley roots in Danish soils, of different texture and under different climatic conditions, Plant and Soil, 88, 31-43, 10.1007/bf02140664, 1985.
Menge, D. N. L., Hedin, L. O., and Pacala, S. W.: Nitrogen and Phosphorus Limitation over Long-Term Ecosystem Development in Terrestrial Ecosystems, PLoS ONE, 7, e42045, 10.1371/journal.pone.0042045, 2012.
Mersi, W. V., Kuhnert-Finkernagel, R., and Schinner, F.: The influence of rock powders on microbial activity of three forest soils, Z Pflanz Bodenkunde, 155, 29-33, doi:10.1002/jpln.19921550107, 1992.
Moon, S., Chamberlain, C. P., and Hilley, G. E.: New estimates of silicate weathering rates and their uncertainties in global rivers, Geochimica et Cosmochimica Acta, 134, 257-274, https://doi.org/10.1016/j.gca.2014.02.033, 2014.
Müller, C., and Robertson, R. D.: Projecting future crop productivity for global economic modeling, Agricultural Economics, 45, 37-50, 10.1111/agec.12088, 2013.
Munkholm, L. J., Schjønning, P., and Sørensen, H.: Jordpakning og mekanisk løsning på grovsandet jord, Ministeriet for Fødevarer, Landbrug og Fiskeri,, Viborg, 6, 2003.
Nkouathio, D. G., Wandji, P., Bardintzeff, J. M., Tematio, P., Kagou Dongmo, A., and Tchoua, F.: Utilisation des roches volcaniques pour la remineralisation des sols ferrallitiques des regions tropicales. Cas des pyroclastites basaltiques du graben de Tombel (Ligne volcanique du Cameroun), Bull. Soc. Vaudoise Sci. Nat., 14, 2008.
Noordin, W., Zulkefly, S., Shamshuddin, J., and Hanafi, M.: IMPROVING SOIL CHEMICAL PROPERTIES AND GROWTH PERFORMANCE OF Hevea brasiliensis THROUGH BASALT APPLICATION, International Proceedings of IRC 2017, 1, 308-323, 2017.
Nunes, J. M. G., Kautzmann, R. M., and Oliveira, C.: Evaluation of the natural fertilizing potential of basalt dust wastes from the mining district of Nova Prata (Brazil), Journal of Cleaner Production, 84, 649-656, 10.1016/j.jclepro.2014.04.032, 2014.
Olness, A., and Archer, D.: EFFECT OF ORGANIC CARBON ON AVAILABLE WATER IN SOIL, Soil Science, 170, 90-101, 2005.
Olsen, M.: Orienterende forsøg vedrørende jordes dybdebehandling, Hedeselskabets Forskningsvirksomhed, Viborg, 41, 1958.
Oren, R., Ellsworth, D. S., Johnsen, K. H., Phillips, N., Ewers, B. E., Maier, C., Schafer, K. V., McCarthy, H., Hendrey, G., McNulty, S. G., and Katul, G. G.: Soil fertility limits carbon sequestration by forest ecosystems in a CO2-enriched atmosphere, Nature, 411, 469-472, 10.1038/35078064, 2001.
Pardo, L. H., Robin-Abbott, M., Duarte, N., and Miller, E., K.: Tree Chemistry Database (Version 1.0), United States Department of Agriculture, NE-324. Newtown Square PA, Gen. Tech. Rep., 45, 2005.
Pontius, R.: Quantification error versus location error in comparison of categorical maps, Photogrammetric Engineering and Remote Sensing, 66, 540-540, 2000.
Popp, A., Lotze-Campen, H., and Bodirsky, B.: Food consumption, diet shifts and associated non-CO2 greenhouse gases from agricultural production, Global Environmental Change, 20, 451-462, 2010.

Popp, A., Lotze-Campen, H., Leimbach, M., Knopf, B., Beringer, T., Bauer, N., and Bodirsky, B.: On sustainability of bioenergy production: Integrating co-emissions from agricultural intensification, Biomass and Bioenergy, 35, 4770-4780, https://doi.org/10.1016/j.biombioe.2010.06.014, 2011.
Popp, A., Calvin, K., Fujimori, S., Havlik, P., Humpenöder, F., Stehfest, E., Bodirsky, B. L., Dietrich, J. P., Doelmann, J. C., Gusti, M., Hasegawa, T., Kyle, P., Obersteiner, M., Tabeau, A., Takahashi, K., Valin, H., Waldhoff, S., Weindl, I., Wise, M., Kriegler, E., Lotze-Campen, H., Fricko, O., Riahi, K., and Vuuren, D. P. v.: Land-use futures in the shared socio-economic pathways, Global Environmental Change, 42, 331-345, https://doi.org/10.1016/j.gloenvcha.2016.10.002, 2017.
Porder, S., and Hilley, G. E.: Linking chronosequences with the rest of the world: predicting soil phosphorus content in denuding landscapes, Biogeochemistry, 102, 153-166, 10.1007/s10533-010-9428-3, 2011.
Porder, S., and Ramachandran, S.: The phosphorus concentration of common rocks—a potential driver of ecosystem P status, Plant and soil, 367, 41-55, 2013.
Raymond, P. A., and Hamilton, S. K.: Anthropogenic influences on riverine fluxes of dissolved inorganic carbon to the oceans, Limnology and Oceanography Letters, 3, 143-155, 2018.
Reick, C. H., Raddatz, T., Brovkin, V., and Gayler, V.: Representation of natural and anthropogenic land cover change in MPI-ESM, Journal of Advances in Modeling Earth Systems, 5, 459-482, 10.1002/jame.20022, 2013.
Reicosky, D. C.: Tillage-induced CO2 emission from soil, Nutrient Cycling in Agroecosystems, 49, 273-285, 10.1023/A:1009766510274, 1997.
Renforth, P.: The potential of enhanced weathering in the UK, International Journal of Greenhouse Gas Control, 10, 229-243, 10.1016/j.ijggc.2012.06.011, 2012.
Renforth, P., von Strandmann, P. A. E. P., and Henderson, G. M.: The dissolution of olivine added to soil: Implications for enhanced weathering, Applied Geochemistry, 61, 109-118, 10.1016/j.apgeochem.2015.05.016, 2015.
Ringeval, B., Kvakić, M., Augusto, L., Ciais, P., Goll, D., Mueller, N. D., Müller, C., Nesme, T., Vuichard, N., Wang, X., and Pellerin, S.: Insights on nitrogen and phosphorus co-limitation in global croplands from theoretical and modelling fertilization experiments, Biogeosciences Discuss., 2019, 1-35, 10.5194/bg-2019-298, 2019.
Rockström, J., Steffen, W., Noone, K., Persson, Å., Chapin Iii, F. S., Lambin, E. F., Lenton, T. M., Scheffer, M., Folke, C., Schellnhuber, H. J., Nykvist, B., de Wit, C. A., Hughes, T., van der Leeuw, S., Rodhe, H., Sörlin, S., Snyder, P. K., Costanza, R., Svedin, U., Falkenmark, M., Karlberg, L., Corell, R. W., Fabry, V. J., Hansen, J., Walker, B., Liverman, D., Richardson, K., Crutzen, P., and Foley, J. A.: A safe operating space for humanity, Nature, 461, 472, 10.1038/461472a, 2009.
Romero-Mujalli, G., Hartmann, J., Börker, J., Gaillardet, J., and Calmels, D.: Ecosystem controlled soil-rock pCO2 and carbonate weathering – Constraints by temperature and soil water content, Chemical Geology, https://doi.org/10.1016/j.chemgeo.2018.01.030, 2018.
Rossato, L., Alvalá, R. C. d. S., Marengo, J. A., Zeri, M., Cunha, A. P. M. d. A., Pires, L. B. M., and Barbosa, H. A.: Impact of Soil Moisture on Crop Yields over Brazilian Semiarid, Frontiers in Environmental Science, 5, 10.3389/fenvs.2017.00073, 2017.
Sadras, V. O., and Milroy, S. P.: Soil-water thresholds for the responses of leaf expansion and gas exchange: A review, Field Crop Res, 47, 253-266, https://doi.org/10.1016/0378-4290(96)00014-7, 1996.
Sairam, R.: PHYSIOLOGY OF WATERLOGGING TOLERANCE IN PLANTS, National Seminar on Sustainable Crop Productivity through Physiological Interventions, 2011, 9,

Saxton, K., Rawls, W. J., Romberger, J., and Papendick, R.: Estimating generalized soil-water characteristics from texture 1, Soil Science Society of America Journal, 50, 1031-1036, 1986.
Saxton, K. E., and Rawls, W. J.: Soil water characteristic estimates by texture and organic matter for hydrologic solutions, Soil science society of America Journal, 70, 1569-1578, 2006.
Schaap, M. G., Leij, F. J., and van Genuchten, M. T.: rosetta: a computer program for estimating soil hydraulic parameters with hierarchical pedotransfer functions, Journal of Hydrology, 251, 163-176, https://doi.org/10.1016/S0022-1694(01)00466-8, 2001.
Schuiling, R. D., and Krijgsman, P.: Enhanced Weathering: An Effective and Cheap Tool to Sequester Co2, Climatic Change, 74, 349-354, 10.1007/s10584-005-3485-y, 2006.
Sharpley, A.: Phosphorus availability. CRC Press. Boca Raton Florida. pp. D18-D37, 2000.
Shen, J., Yuan, L., Zhang, J., Li, H., Bai, Z., Chen, X., Zhang, W., and Zhang, F.: Phosphorus Dynamics: From Soil to Plant, Plant Physiology, 156, 997-1005, 10.1104/pp.111.175232, 2011.
Shinjini, G., C., F. M., A., V. M., Mariann, G. J., D., Y. R., and J., F. T.: Phosphorus limitation of aboveground production in northern hardwood forests, Ecology, 99, 438-449, doi:10.1002/ecy.2100, 2018.
Singh, B., and Schulze, D.: Soil minerals and plant nutrition, Nature Education Knowledge, 6, 1, 2015.
Smeets, E. M. W., and Faaij, A. P. C.: Bioenergy potentials from forestry in 2050, Climatic Change, 81, 353-390, 10.1007/s10584-006-9163-x, 2007.
Smith, P.: Agricultural greenhouse gas mitigation potential globally, in Europe and in the UK: what have we learnt in the last 20 years?, Global Change Biology, 18, 35-43, 10.1111/j.1365-2486.2011.02517.x, 2012.
Smith, P., Davis, S. J., Creutzig, F., Fuss, S., Minx, J., Gabrielle, B., Kato, E., Jackson, R. B., Cowie, A., Kriegler, E., van Vuuren, D. P., Rogelj, J., Ciais, P., Milne, J., Canadell, J. G., McCollum, D., Peters, G., Andrew, R., Krey, V., Shrestha, G., Friedlingstein, P., Gasser, T., Grübler, A., Heidug, W. K., Jonas, M., Jones, C. D., Kraxner, F., Littleton, E., Lowe, J., Moreira, J. R., Nakicenovic, N., Obersteiner, M., Patwardhan, A., Rogner, M., Rubin, E., Sharifi, A., Torvanger, A., Yamagata, Y., Edmonds, J., and Yongsung, C.: Biophysical and economic limits to negative CO2 emissions, Nature Climate Change, 6, 42, 10.1038/nclimate2870

https://www.nature.com/articles/nclimate2870#supplementary-information, 2015.
Smith, P., Davis, S. J., Creutzig, F., Fuss, S., Minx, J., Gabrielle, B., Kato, E., Jackson, R. B., Cowie, A., Kriegler, E., van Vuuren, D. P., Rogelj, J., Ciais, P., Milne, J., Canadell, J. G., McCollum, D., Peters, G., Andrew, R., Krey, V., Shrestha, G., Friedlingstein, P., Gasser, T., Grubler, A., Heidug, W. K., Jonas, M., Jones, C. D., Kraxner, F., Littleton, E., Lowe, J., Moreira, J. R., Nakicenovic, N., Obersteiner, M., Patwardhan, A., Rogner, M., Rubin, E., Sharifi, A., Torvanger, A., Yamagata, Y., Edmonds, J., and Yongsung, C.: Biophysical and economic limits to negative CO2 emissions, Nature Clim. Change, 6, 42-50, 10.1038/nclimate2870

http://www.nature.com/nclimate/journal/v6/n1/abs/nclimate2870.html#supplementary-information, 2016.
Smith, W. K., Zhao, M., and Running, S. W.: Global Bioenergy Capacity as Constrained by Observed Biospheric Productivity Rates, BioScience, 62, 911-922, 10.1525/bio.2012.62.10.11, 2012.
Sonntag, S., Pongratz, J., Reick, C. H., and Schmidt, H.: Reforestation in a high-CO2 world—Higher mitigation potential than expected, lower adaptation potential than hoped for, Geophysical Research Letters, 43, 6546-6553, 10.1002/2016gl068824, 2016.
Stefánsson, A., Gíslason, S. R., and Arnórsson, S.: Dissolution of primary minerals in natural waters: II. Mineral saturation state, Chemical Geology, 172, 251-276, 2001.

Straaten, P. v.: Agrogeology: the use of rocks for crops, 631.4 S894, Enviroquest, 2007.
Strefler, J., Amann, T., Bauer, N., Kriegler, E., and Hartmann, J.: Potential and costs of Carbon Dioxide Removal by Enhanced Weathering of rocks, Environmental Research Letters, 2018.
Sun, Y., Peng, S., Goll, D. S., Ciais, P., Guenet, B., Guimberteau, M., Hinsinger, P., Janssens, I. A., Peñuelas, J., Piao, S., Poulter, B., Violette, A., Yang, X., Yin, Y., and Zeng, H.: Diagnosing phosphorus limitations in natural terrestrial ecosystems in carbon cycle models, Earth's Future, 10.1002/2016ef000472, 2017.
Tanner, E. V. J., Vitousek, P. M., and Cuevas, E.: Experimental investigation of nutrient limitation of forest growth on wet tropical mountains, Ecology, 79, 10-22, 1998.
Taylor, L. L., Leake, J. R., Quirk, J., Hardy, K., Banwart, S. A., and Beerling, D. J.: Biological weathering and the long-term carbon cycle: integrating mycorrhizal evolution and function into the current paradigm, Geobiology, 7, 171-191, 10.1111/j.1472-4669.2009.00194.x, 2009.
Taylor, L. L., Quirk, J., Thorley, R. M. S., Kharecha, P. A., Hansen, J., Ridgwell, A., Lomas, M. R., Banwart, S. A., and Beerling, D. J.: Enhanced weathering strategies for stabilizing climate and averting ocean acidification, Nature Climate Change, 6, 402-406, 10.1038/nclimate2882, 2015.
Theodoro, S. H., de Souza Martins, E., Fernandes, M. M., and de Carvalho, A. M. X.: II Congresso Brasileiro de Rochagem, 2013.
Thomson, A. M., Calvin, K. V., Smith, S. J., Kyle, G. P., Volke, A., Patel, P., Delgado-Arias, S., Bond-Lamberty, B., Wise, M. A., Clarke, L. E., and Edmonds, J. A.: RCP4.5: a pathway for stabilization of radiative forcing by 2100, Climatic Change, 109, 77, 10.1007/s10584-011-0151-4, 2011.
Tokimatsu, K., Yasuoka, R., and Nishio, M.: Global zero emissions scenarios: The role of biomass energy with carbon capture and storage by forested land use, Applied Energy, 185, 1899-1906, https://doi.org/10.1016/j.apenergy.2015.11.077, 2017.
Uhlig, D., Schuessler, J. A., Bouchez, J., Dixon, J. L., and von Blanckenburg, F.: Quantifying nutrient uptake as driver of rock weathering in forest ecosystems by magnesium stable isotopes, Biogeosciences, 14, 3111-3128, 10.5194/bg-14-3111-2017, 2017.
Uhlig, D.: The deep Critical Zone as a source of mineral nutrients to montane, temperate forest ecosystems, 2019.
Uhlig, D., and von Blanckenburg, F.: How Slow Rock Weathering Balances Nutrient Loss During Fast Forest Floor Turnover in Montane, Temperate Forest Ecosystems, Frontiers in Earth Science, 7, 10.3389/feart.2019.00159, 2019.
Vergutz, L., Manzoni, S., Porporato, A., Novais, R. F., and Jackson, R. B.: A Global Database of Carbon and Nutrient Concentrations of Green and Senesced Leaves. ORNL Distributed Active Archive Center, 2012.
Vienken, T., and Dietrich, P.: Field evaluation of methods for determining hydraulic conductivity from grain size data, Journal of Hydrology, 400, 58-71, 2011.
Vitousek, P. M., Aber, J. D., Howarth, R. W., Likens, G. E., Matson, P. A., Schindler, D. W., Schlesinger, W. H., and Tilman, D. G.: Human alteration of the global nitrogen cycle: sources and consequences, Ecological applications, 7, 737-750, 1997.
Vitousek, P. M., Porder, S., Houlton, B. Z., and Chadwick, O. A.: Terrestrial phosphorus limitation: mechanisms, implications, and nitrogen–phosphorus interactions, Ecological Applications, 20, 5-15, 10.1890/08-0127.1, 2010.
von Liebig, J. F., and Playfair, L. P. B.: Chemistry in its application to agriculture and physiology, JM Campbell, 1843.
Von Wilpert, K., and Lukes, M.: Ecochemical effects of phonolite rock powder, dolomite and potassium sulfate in a spruce stand on an acidified glacial loam, Nutrient Cycling in Agroecosystems, 65, 115-127, 2003.

Waldbauer, J. R., and Chamberlain, C. P.: Influence of uplift, weathering, and base cation supply on past and future CO 2 levels, in: A history of atmospheric CO2 and its effects on Plants, Animals, and Ecosystems, Springer, 166-184, 2005.

Walker, J. C., Hays, P., and Kasting, J. F.: A negative feedback mechanism for the long-term stabilization of Earth's surface temperature, Journal of Geophysical Research: Oceans, 86, 9776-9782, 1981.

Wang, R., Goll, D., Balkanski, Y., Hauglustaine, D., Boucher, O., Ciais, P., Janssens, I., Penuelas, J., Guenet, B., Sardans, J., Bopp, L., Vuichard, N., Zhou, F., Li, B., Piao, S., Peng, S., Huang, Y., and Tao, S.: Global forest carbon uptake due to nitrogen and phosphorus deposition from 1850 to 2100, Global Change Biology, 23, 4854-4872, doi:10.1111/gcb.13766, 2017.

Wang, Y. P., Law, R. M., and Pak, B.: A global model of carbon, nitrogen and phosphorus cycles for the terrestrial biosphere, Biogeosciences, 7, 2261-2282, 10.5194/bg-7-2261-2010, 2010.

Whitfield, C. J., and Reid, C.: Predicting surface area of coarse-textured soils: Implications for weathering rates, Canadian Journal of Soil Science, 93, 621-630, 2013.

Wösten, J. H. M., Pachepsky, Y. A., and Rawls, W. J.: Pedotransfer functions: bridging the gap between available basic soil data and missing soil hydraulic characteristics, Journal of Hydrology, 251, 123-150, https://doi.org/10.1016/S0022-1694(01)00464-4, 2001.

Wright, S. J., Yavitt, J. B., Wurzburger, N., Turner, B. L., Tanner, E. V., Sayer, E. J., Santiago, L. S., Kaspari, M., Hedin, L. O., and Harms, K. E.: Potassium, phosphorus, or nitrogen limit root allocation, tree growth, or litter production in a lowland tropical forest, Ecology, 92, 1616-1625, 2011.

Yang, X., Post, W. M., Thornton, P. E., and Jain, A. K.: Global Gridded Soil Phosphorus Distribution Maps at 0.5-degree Resolution. ORNL Distributed Active Archive Center, 2014a.

Yang, X., Thornton, P. E., Ricciuto, D. M., and Post, W. M.: The role of phosphorus dynamics in tropical forests – a modeling study using CLM-CNP, Biogeosciences, 11, 1667-1681, 10.5194/bg-11-1667-2014, 2014b.

Yasunari, T.: The Uplift of the Himalaya-Tibetan Plateau and Human Evolution: An Overview on the Connection Among the Tectonics, Eco-Climate System and Human Evolution During the Neogene Through the Quaternary Period, in: Himalayan Weather and Climate and their Impact on the Environment, edited by: Dimri, A. P., Bookhagen, B., Stoffel, M., and Yasunari, T., Springer International Publishing, Cham, 281-305, 2020.

Yousefpour, R., Nabel, J. E., and Pongratz, J.: Simulating growth-based harvest adaptive to future climate change, Biogeosciences, 16, 241-254, 2019.

Zaehle, S., and Dalmonech, D.: Carbon–nitrogen interactions on land at global scales: current understanding in modelling climate biosphere feedbacks, Current Opinion in Environmental Sustainability, 3, 311-320, 2011.

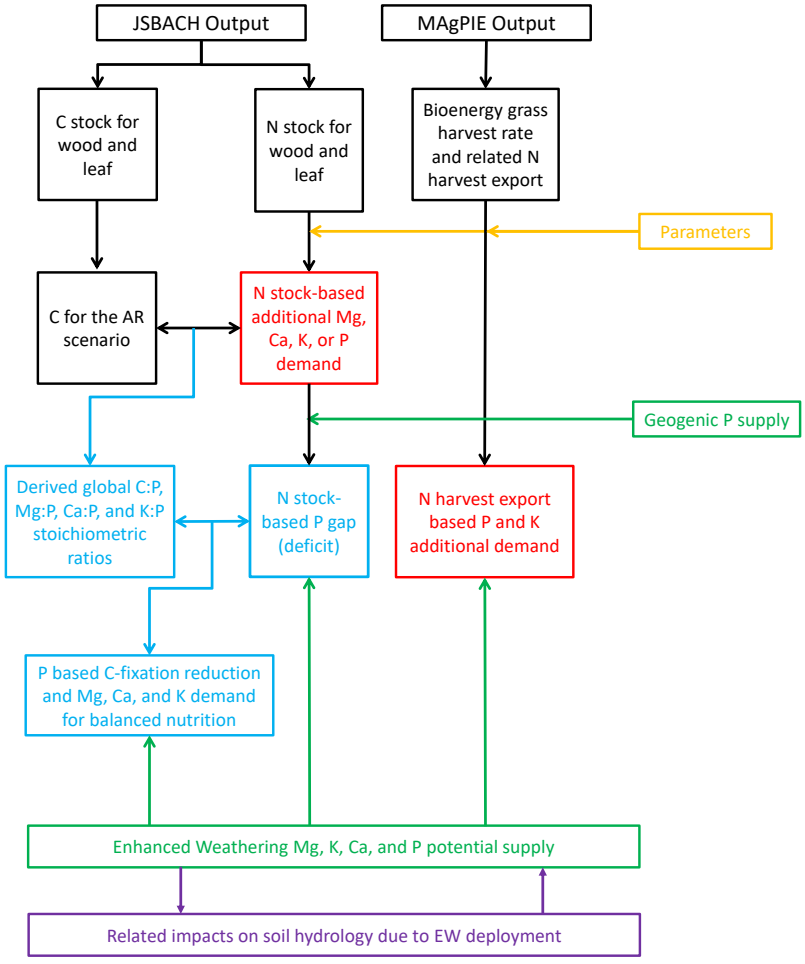
JSBACH Output
MAgPIE Output
C stock for wood and leaf
N stock for wood and leaf
Bioenergy grass harvest rate and related N harvest export
Parameters
C for the AR scenario
N stock-based additional Mg, Ca, K, or P demand
Geogenic P supply
Derived global C:P, Mg:P, Ca:P, and K:P stoichiometric ratios
N stock-based P gap (deficit)
N harvest export based P and K additional demand
P based C-fixation reduction and Mg, Ca, and K demand for balanced nutrition
Enhanced Weathering Mg, K, Ca, and P potential supply
Related impacts on soil hydrology due to EW deployment

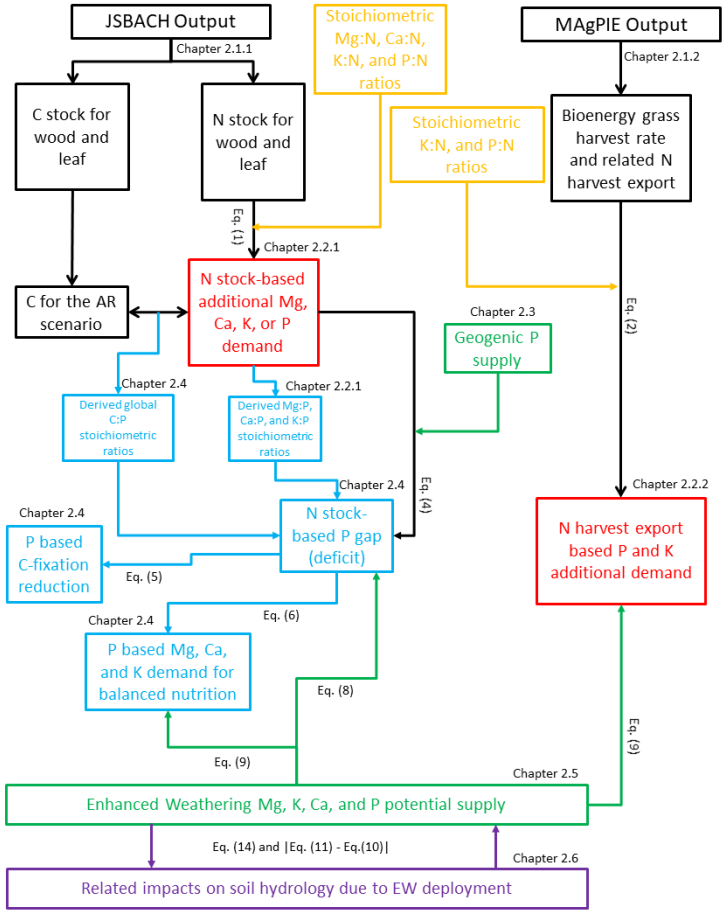

Fig. 1: Schematic steps and datasets used to derive geogenic nutrient demand from simulated biomass changes, P gaps, reduced C sequestration, and Ca, K, and Mg supply for balanced tree nutrition. Black colors: Outputs from land surface model JSBACH and agricultural production model MAgPIE. Yellow colors: stoichiometric Mg:N, Ca:N, K:N, and P:N ratios used to obtain the N stock-based nutrient demand. Red colors: N stock-based P, Mg, Ca, and K demand for wood and leaf (AR) or N harvest export based P and K demand (BG). Green colors: nutrient supply from geogenic sources (atmospheric P deposition and different soil P pools) or from Enhanced Weathering. Blue colors: derived P gap for AR, derived stoichiometric C:P, Mg:P, Ca:P, and K:P ratios, P based C-fixation reduction, and P based Mg, Ca, and K supply for balanced tree nutrition. Purple colors: Related EW deployment impacts on soil hydrology estimated by pedotransfer functions. AR: Afforestation/reforestation, BG: Bio-energy grass.

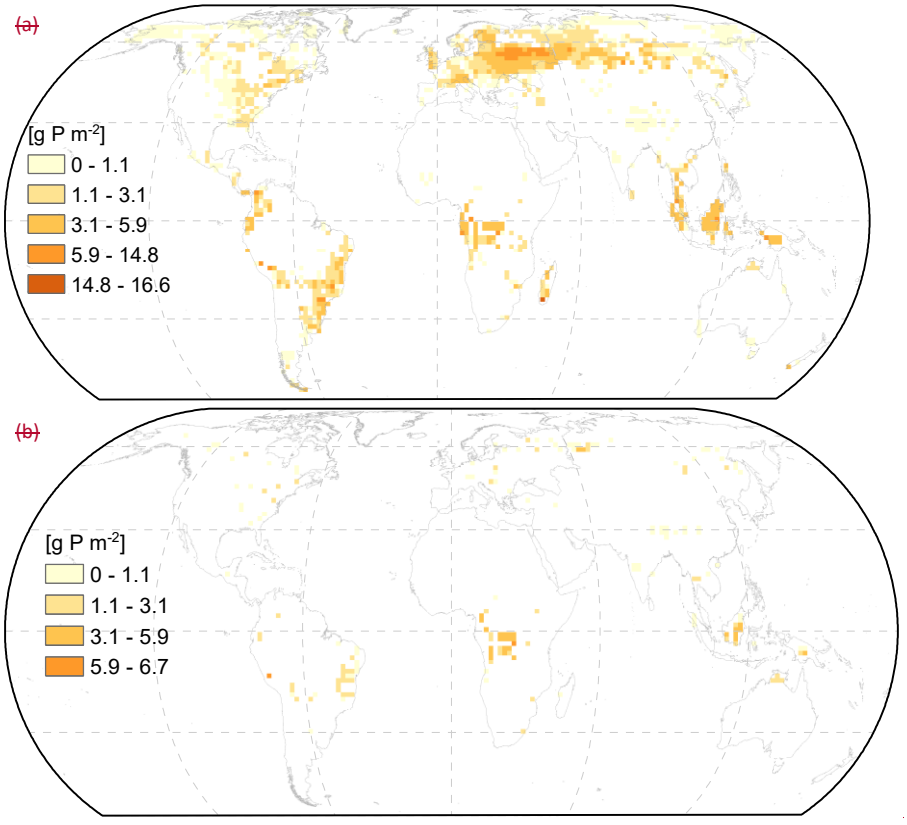

1700

(a)

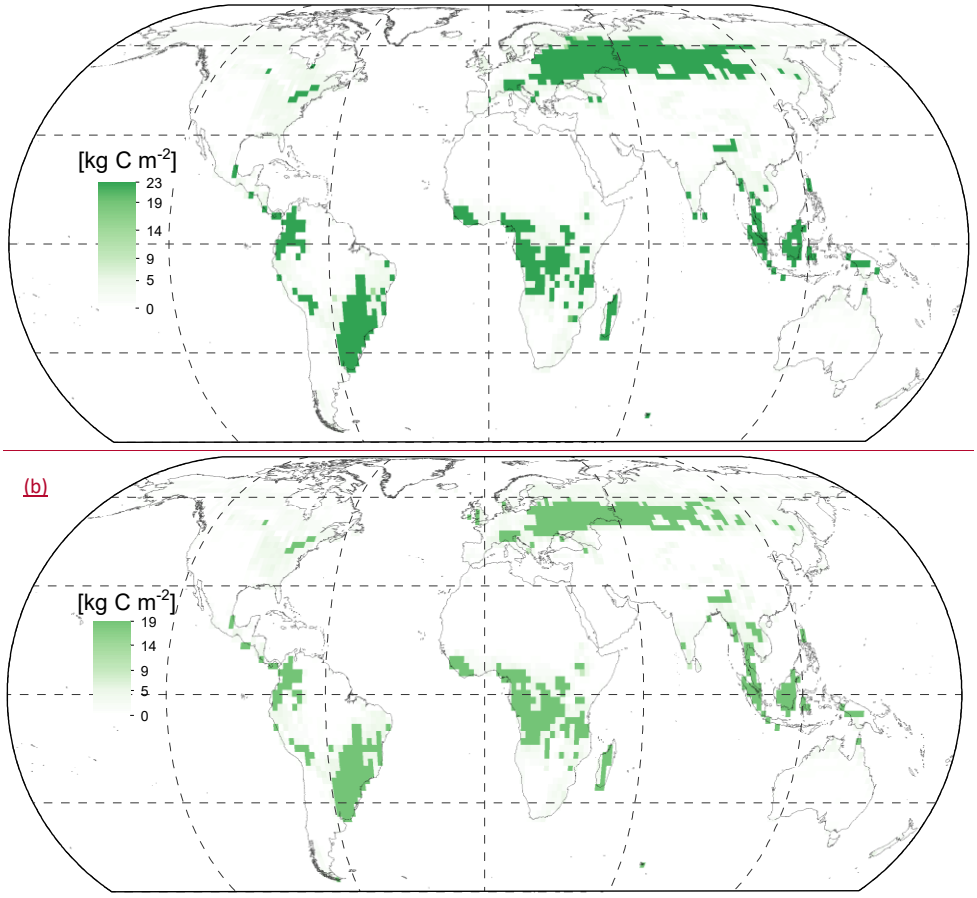

Fig. 2: Carbon sequestered in different afforestation reforestation scenarios for the 21st century (2006 – 2099) period for a RCP4.5 scenario, according to Kracher (2017). a) For an N-unlimited AR scenario the global C sequestration is 224 Gt C. b) For an N-limited AR scenario the global C sequestration is 190 Gt C. Map generated with ESRI ArcGIS ver. 10.6 (http://www.esri.com).

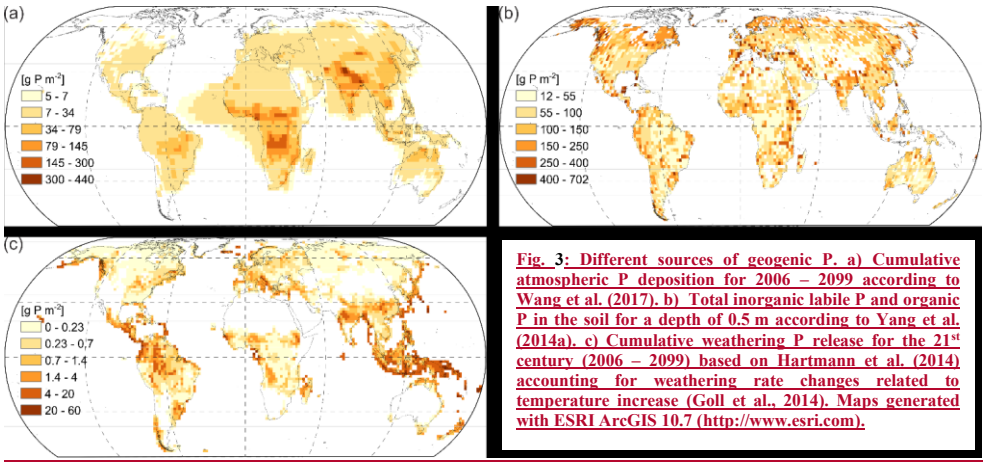

Fig. 3: Different sources of geogenic P. a) Cumulative atmospheric P deposition for 2006 – 2099 according to Wang et al. (2017). b) Total inorganic labile P and organic P in the soil for a depth of 0.5 m according to Yang et al. (2014a). c) Cumulative weathering P release for the 21st century (2006 – 2099) based on Hartmann et al. (2014) accounting for weathering rate changes related to temperature increase (Goll et al., 2014). Maps generated with ESRI ArcGIS 10.7 (http://www.esri.com).

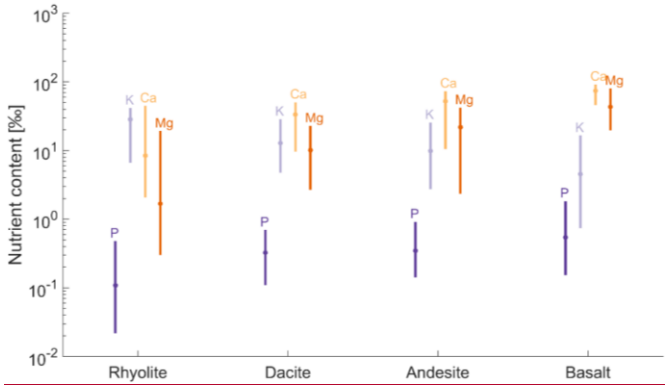

Fig. 4: Statistical data of major element concentration in rocks, median values (filled circles) and range (5th and 95th percentiles, whiskers). Values from Earthchem webportal (http://www.earthchem.org). The number of chemical analysis used to calculate the descriptive statistics were: 2985 chemical analysis for rhyolite, 3008 chemical analysis for dacite, 11099 chemical analysis for andesite, and 23816 chemical analysis for basalt.

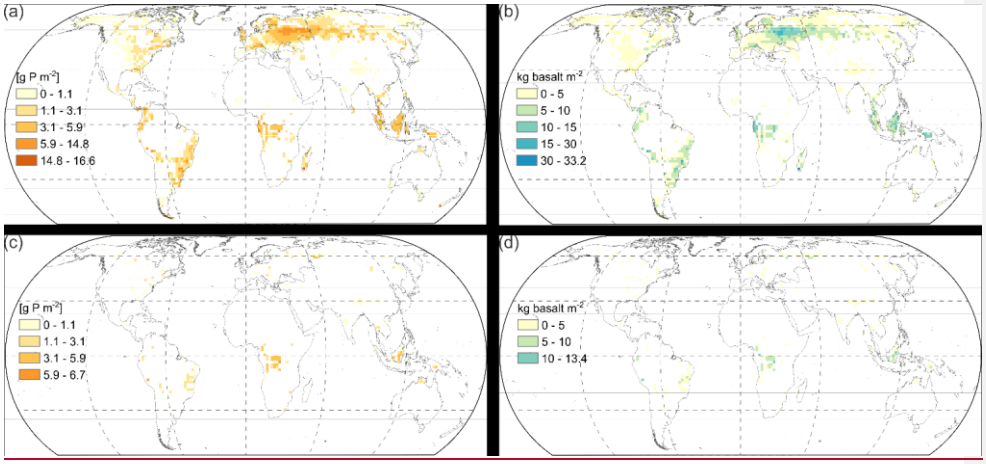

Fig. 5: Areas with potential P gap for the nutrient budget of the N-limited AR scenario (after 94 years of simulation) assuming P concentrations within foliar and wood material corresponding to mean values (Table 1). a) Geogenic P supply scenario one (geogenic P from weathering plus atmospheric P deposition as source of P). ~~b~~b) Basalt deployment necessary to close P gaps from P budget scenario of Fig. 5a. c) Geogenic P supply scenario two (geogenic P from soil inorganic labile P and organic P pools plus atmospheric P deposition and P from weathering as source of P). d) Basalt deployment necessary to close P gaps from P budget scenario of Fig. 5c. Map generated with ESRI ArcGIS 10.67 (http://www.esri.com).

Formatted: Font: Not Italic, Font color: Black

Formatted: Font: Calibri, 11 pt

Formatted: Space After: 8 pt

~~(a)~~

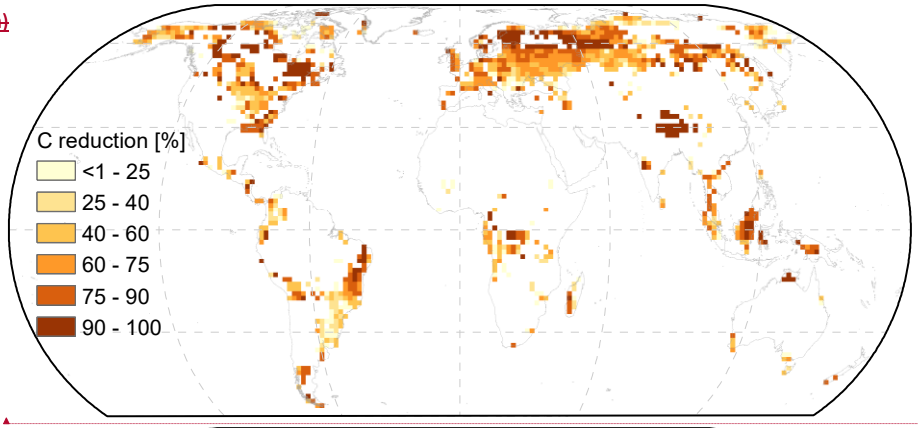

~~(b)~~

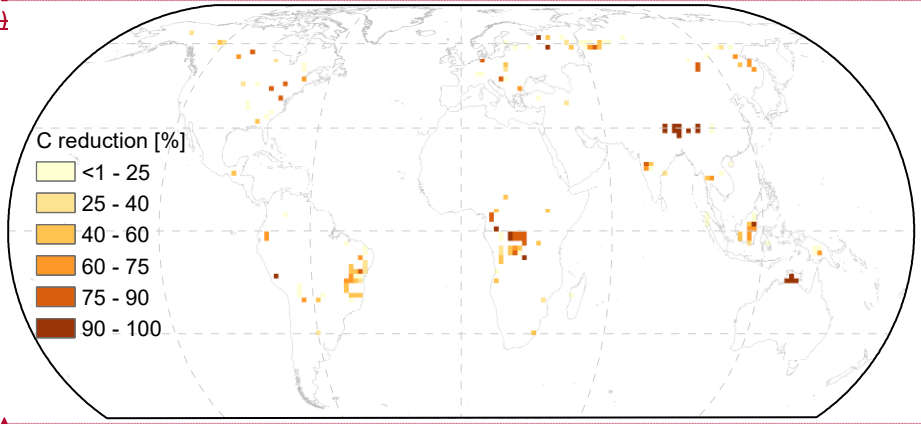

Fig. 6: Reduction on forest C sequestration due to geogenic P limitation. C-reduction estimated from stoichiometric C:P ratios for the N-limited AR scenario assuming P concentrations within foliar and wood material corresponding to mean values (Table 1). On Fig. 2b we present the C sequestration potential if geogenic P supply is not limiting biomass growth. a) C-reduction based on P gaps of ~~Fig. 2~~Fig. 5a, obtained for geogenic P supply scenario one (geogenic P from weathering plus atmospheric P deposition as source of P). b) C-reduction based on P gaps of ~~Fig. 2b~~Fig. 5c, obtained for geogenic P supply scenario two (geogenic P from soil inorganic labile P and organic P pools plus atmospheric P deposition and P from weathering as source of P). For resulting global C reduction check Table 3. Map generated with ESRI ArcGIS 10.67 (http://www.esri.com).

Formatted: Indent: Left: 0.25"

Formatted: Font: Calibri, 11 pt

Formatted: Font: Calibri, 11 pt

~~(a)~~

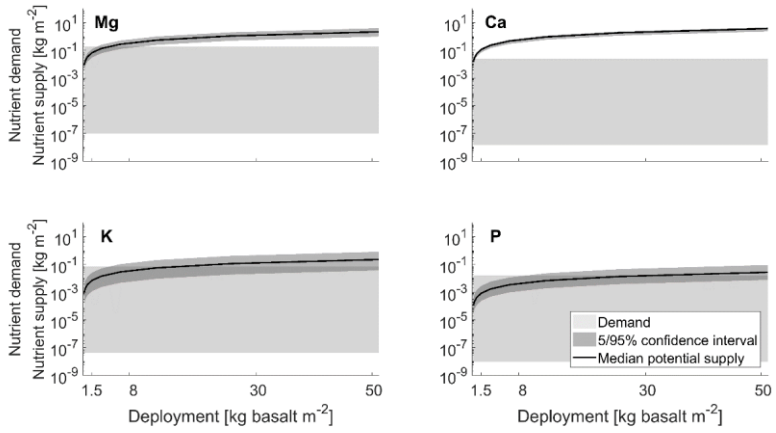
Mg
Ca
K
P
Nutrient demand
Nutrient supply [kg m-2]
Demand
5/95% confidence interval
Median potential supply
1.5
8
30
50
Deployment [kg basalt m-2]

~~(b)~~

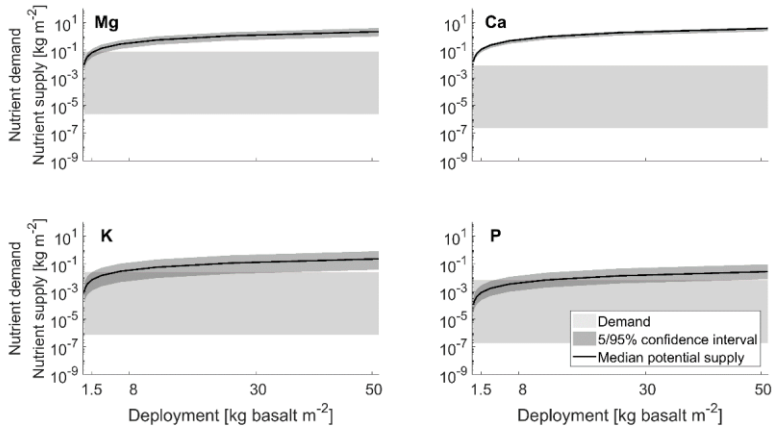
Mg
Ca
K
P
Nutrient demand
Nutrient supply [kg m-2]
Demand
5/95% confidence interval
Median potential supply
1.5
8
30
50
Deployment [kg basalt m-2]

(a)

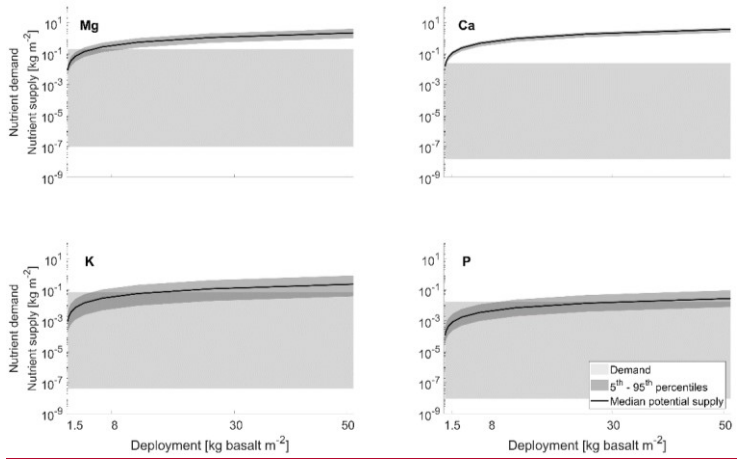

(b)

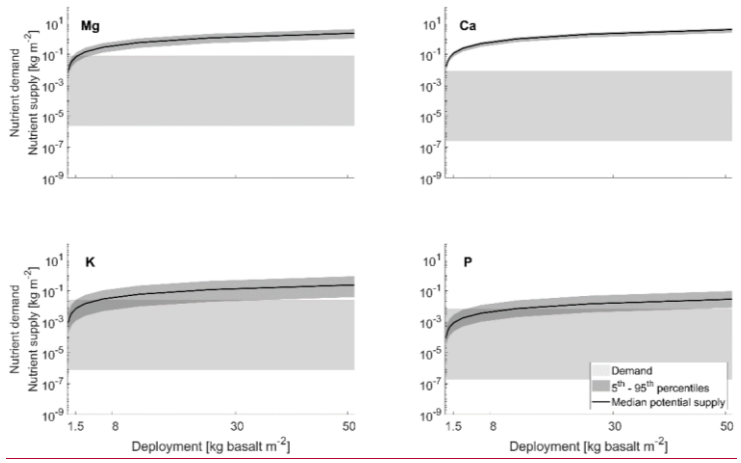

Fig. 7: Mg, Ca, K, and P supply by basalt dissolution (logarithmic curve) given as median and ~~5/95% confidence intervals~~ranges (5th and 95th percentiles) (dark grey areas). Horizontal filled boxes indicate the nutrient demand for maximum (17.1 g P m^{-2}) and minimum (<<1 g P m^{-2}) gap of each geogenic P supply scenario for P and derived Mg, Ca, and K demand for balanced tree nutrition assuming mean foliar and wood material chemistry (Table 1). a) Based on minimum and maximum P gap values of <1 g P m^{-2} and ~~17.1~~16.6 g P m^{-2}, which were obtained for a geogenic P supply scenario one (geogenic P from weathering plus atmospheric P deposition as source of P). b) Based on minimum and maximum P gap values of <1 g P m^{-2} and 6.67 g P m^{-2}, which were obtained for a geogenic P supply scenario two (geogenic P from soil inorganic labile P and organic P pools plus atmospheric P deposition and P from weathering as source of P).

Formatted: Indent: Left: 0.25"

Formatted: Font: Italic

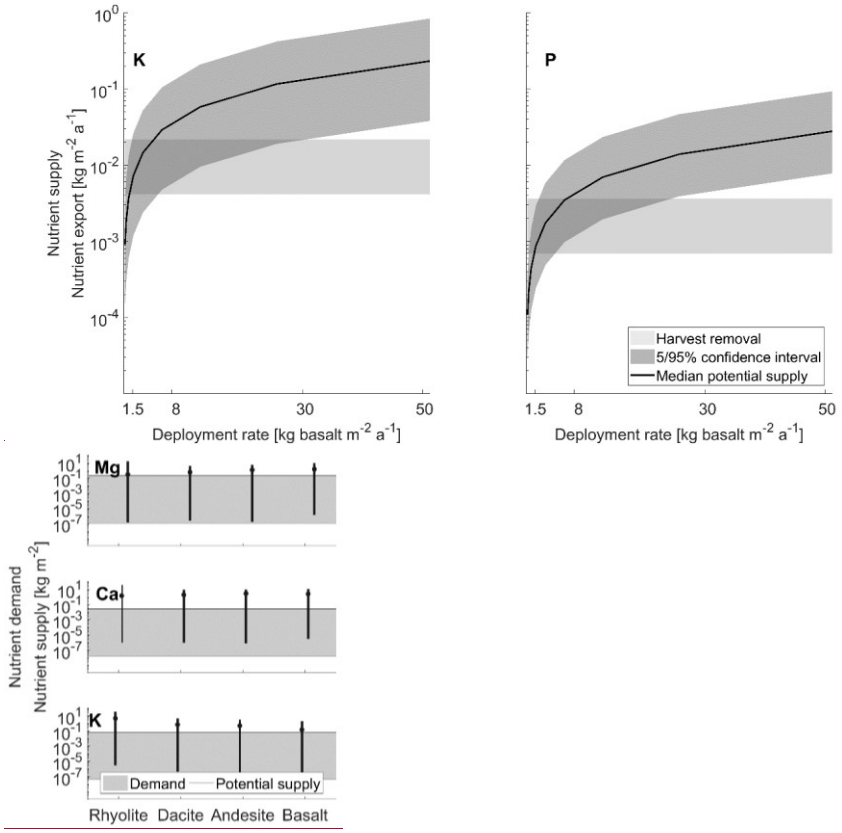

Fig. 8: Potential macronutrient (Mg, Ca, and K) supply of different rocks for closing projected P gaps of <<1 to 17.1 g P m^{-2}. Median and ranges (5^{th} and 95^{th} percentiles) of potential supply based on rock chemistry.

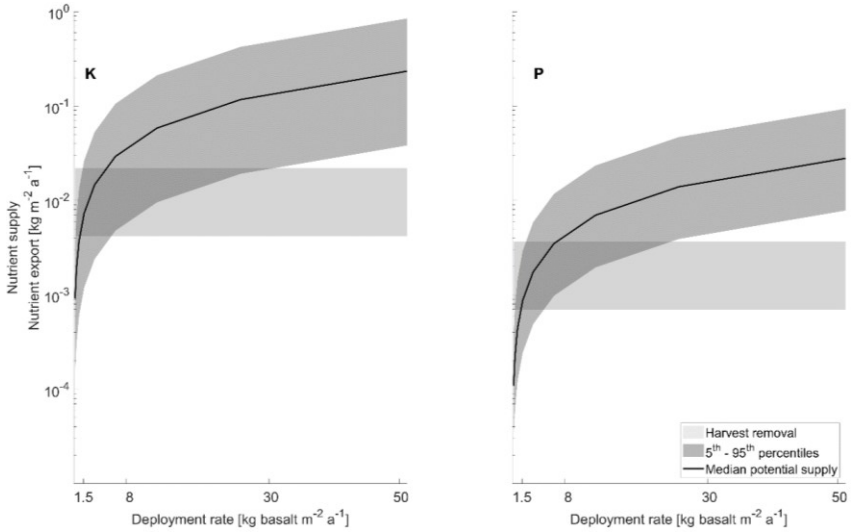

Fig. 9: Projected K and P supply (logarithmic curve) by basalt dissolution given as median ranges (5th and ~~5/95% confidence interval~~95th percentiles) for bio-energy grasses K and P demand (horizontal filled boxes) based on global minimum 0.7 kg m^{-2} a^{-1} and maximum 3.6 kg m^{-2} a^{-1} harvest rates for simulation years of 1995 – 2090. The amount of exported nutrients by several harvest rates higher than the minimum and lower than the maximum harvest rates are represented by the vertical filled boxes.

Formatted: Space After: 8 pt

Formatted: Superscript

Formatted: Superscript

Formatted: Superscript

Formatted: Superscript

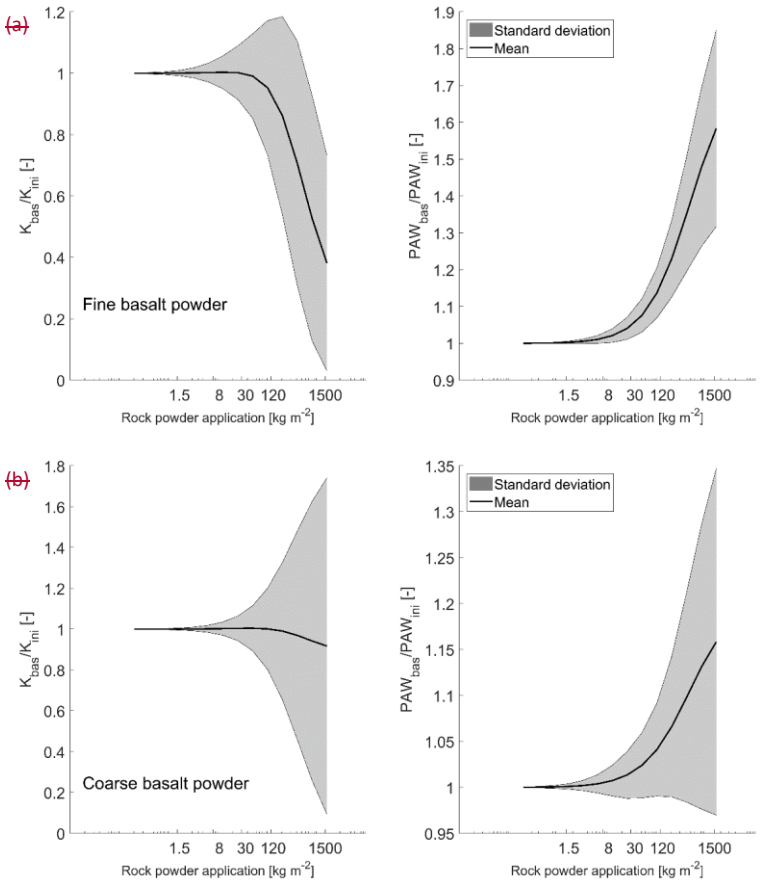
(a)
Fine basalt powder
K_{bas}/K_{ini} [-]
PAW_{bas}/PAW_{ini} [-]
Standard deviation
Mean
1.5 8 30 120 1500
Rock powder application [kg m^{-2}]
(b)
Coarse basalt powder
K_{bas}/K_{ini} [-]
PAW_{bas}/PAW_{ini} [-]
Standard deviation
Mean
1.5 8 30 120 1500
Rock powder application [kg m^{-2}]

1755

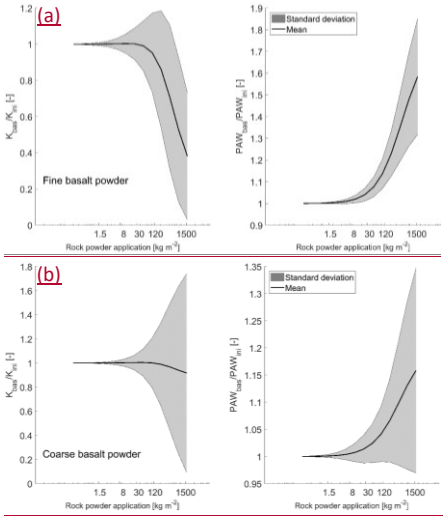

Fig. 10: Relative impacts on soil saturated hydraulic conductivity (K_S) and Plant Available Water (PAW). K_{bas} and PAW_{bas} respectively represent the estimated soil K_S and PAW after basalt application. K_{ini} is the estimated initial soil K_S and PAW_{ini} is the estimated initial PAW of different soils. a) Application of a fine basalt texture (15.6% clay, 83.8% silt, and 0.6% fine sand). b) Application of a coarse basalt texture (15.6% clay, 53.8% silt, and 30.6% fine sand) for areas corresponding to P gaps of geogenic P supply scenario one, for the N-unlimited AR scenario (Supplement S1 Fig. S7a). Mean and standard deviations for n=15318 grid cells. cf., Supplement S1 section D for impacts on initial K_S and PAW of fine or coarse basalt powder texture on soils of P gap areas from (Supplement S1 Fig. S7c).

1760

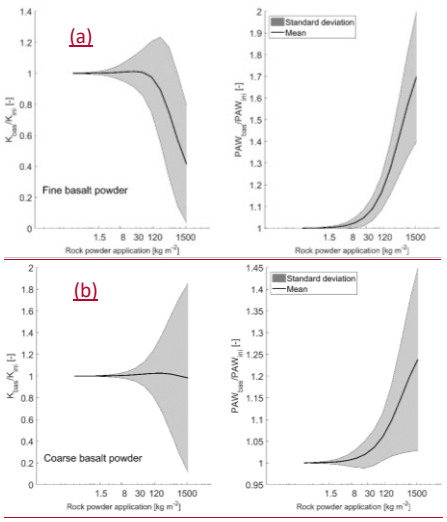

Fig. 11: Relative impacts on soil saturated hydraulic conductivity (K_S) and Plant Available Water (PAW). K_{bas} and PAW_{bas} respectively represents the estimated soil K_S and PAW after basalt application. K_{ini} is the estimated initial soil K_S and PAW_{ini} is the estimated initial PAW of different soils. a) Application of a fine basalt texture (15.6% clay, 83.8% silt, and 0.6% fine sand). b) Application of a coarse basalt texture (15.6% clay, 53.8% silt, and 30.6% fine sand) for areas corresponding to P budget scenario two, for the N-unlimited AR scenario (Supplement S1 Fig. S7c). Mean and standard deviations for n=2525 grid cells.

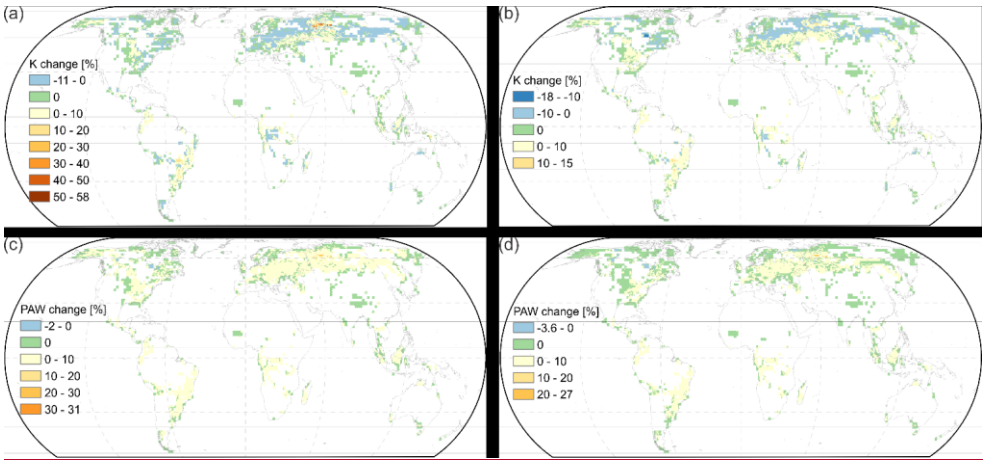

Fig. 12~~: Relative impacts on soil saturated hydraulic conductivity (K_S) and Plant Available Water (PAW). K_{bas} and PAW_{bas} respectively represent the estimated soil K_S and PAW after basalt application. K_{ini} is the estimated initial soil K_S and PAW_{ini} is the estimated initial PAW of different soils. a) Application of a fine basalt texture (15.6% clay, 83.8% silt, and 0.6% fine sand). b) Application of a coarse basalt texture (15.6% clay, 53.8% silt, and 30.6% fine sand) for areas corresponding to P gaps of geogenic P supply scenario one, for the N-unlimited AR scenario (Supplement S1 Fig. S21a). Mean and standard deviations for n=1525 grid cells. *cf.*, Supplement S1 section S5 for impacts on initial K_S and PAW of fine or coarse basalt powder texture on soils of P gap areas from b.~~: Impacts on soil hydrology estimated according to Saxton and Rawls (2006) equations for basalt deployment mass coincident to areas with potential P gap for the nutrient budget of the N-unlimited AR scenario assuming P concentrations within foliar and wood material corresponding to mean values (Supplement Fig. S7a). a) Hydraulic conductivity (K) changes relative to initial soil values for a fine basalt texture (15.6% clay, 83.8% silt, and 0.6% sand) being deployed. b) Hydraulic conductivity (K) changes relative to initial soil values for a coarse basalt texture (15.6% clay, 53.8% silt, and 30.6% fine sand) being deployed. c) Plant available water (PAW) changes relative to initial soil values for a fine basalt texture (15.6% clay, 83.8% silt, and 0.6% sand) being deployed. d) Plant available water (PAW) changes relative to initial soil values for a coarse basalt texture (15.6% clay, 53.8% silt, and 30.6% fine sand) being deployed. Map generated with ESRI ArcGIS 10.7 (http://www.esri.com).

Formatted: Font: Not Italic

Table 1: Stoichiometric parameters for different pools and biomes used in this study.

Biome		Tropical evergreen					Tropical deciduous					Temperate evergreen				
Leaf[a]		mean	Std	n	5th percentile	95th percentile	mean	Std	n	5th percentile	95th percentile	mean	Std	n	5th percentile	95th percentile
C:N		29.72	15.01	4	16.33	46.49	26.96*	10.53*	171*	14.50*	46.7*	49.11	12.15	8	33.54	65.69
P:N		0.06	0.02	59	0.04	0.10	0.07	0.03	43	0.04	0.13	0.09	0.03	23	0.05	0.13
K:N	[-]	0.97	0.80	2	0.46	1.48	1.26	0.93	22	0.23	2.45	0.47	0.09	12	0.33	0.58
Ca:N		2.73	3.44	2	0.54	4.91	1.55	0.78	22	0.52	2.90	0.73*	0.67*	150*	0.16*	1.94*
Mg:N		0.40	0.52	2	0.07	0.73	0.37	0.29	22	0.10	0.83	0.21*	0.21*	115*	0.05*	0.66*
Wood[b]		mean	Std	n	5th percentile	95th percentile	mean	Std	n	5th percentile	95th percentile	mean	Std	n	5th percentile	95th percentile
C:N		235	244	9	56	610	235	244	9	56	610	235	244	9	56	610
P:N		0.15	0.20	684	0.04	0.30	0.15	0.20	684	0.04	0.30	0.15	0.20	684	0.04	0.30
K:N	[-]	0.60	0.40	700	0.20	1.20	0.60	0.40	700	0.20	1.20	0.60	0.40	700	0.20	1.20
Ca:N		1.80	1.30	705	0.40	4.30	1.80	1.30	705	0.40	4.30	1.80	1.30	705	0.40	4.30
Mg:N		0.20	0.10	681	0.10	0.40	0.20	0.10	681	0.10	0.40	0.20	0.10	681	0.10	0.40

Biome		Temperate deciduous					Shrubs raingreen					Shrubs deciduous				
Leaf[a]		mean	Std	n	5th percentile	95th percentile	mean	Std	n	5th percentile	95th percentile	mean	Std	n	5th percentile	95th percentile
C:N		55.30	12.02	2	47.65	62.95	26.31	6.83	2	21.97	30.65	26.96*	10.53*	171*	14.5*	46.70*
P:N		0.08	0.03	32	0.04	0.13	0.07	0.01	2	0.06	0.08	0.08*	0.05*	662*	0.04*	0.16*
K:N	[-]	0.43	0.13	23	0.24	0.61	0.38	0.02	2	0.37	0.39	0.59*	0.45*	207*	0.24*	1.50*
Ca:N		0.73*	0.67*	150*	0.16*	1.94*	0.44	0.08	2	0.39	0.50	0.73*	0.67*	150*	0.16*	1.94*
Mg:N		0.21*	0.21*	115*	0.05*	0.66*	0.09	0.04	2	0.06	0.12	0.21*	0.21*	115*	0.05*	0.66*
Wood[b]		mean	Std	n	5th percentile	95th percentile	mean	Std	n	5th percentile	95th percentile	mean	Std	n	5th percentile	95th percentile
C:N		235	244	9	56	610	235	244	9	56	610	235	244	9	56	610
P:N		0.15	0.20	684	0.04	0.30	0.15	0.20	684	0.04	0.30	0.15	0.20	684	0.04	0.30
K:N	[-]	0.60	0.40	700	0.20	1.20	0.60	0.40	700	0.20	1.20	0.60	0.40	700	0.20	1.20
Ca:N		1.80	1.30	705	0.40	4.30	1.80	1.30	705	0.40	4.30	1.80	1.30	705	0.40	4.30
Mg:N		0.20	0.10	681	0.10	0.40	0.20	0.10	681	0.10	0.40	0.20	0.10	681	0.10	0.40

*Values obtained from all biomes. [a] Stoichiometric ratios derived from a global leaf chemistry database (Vergutz et al., 2012). [b] Stoichiometric ratios derived from a US soft- and hardwood database (Pardo et al., 2005). cf., SI-table.xlsx file for used database.

Formatted: Font: Not Italic

Table 2: Geogenic P sources used for each geogenic P supply scenario.

P source	Resolution	Geogenic P supply scenario one	Geogenic P supply scenario two	Reference
Soil organic P and inorganic labile P	0.5°		X	(Yang et al., 2014a)
Atmospheric P deposition	1°	X	X	(Wang et al., 2017)
~~Geogenic P release rates~~P from weathering	1 km^2	X	X	(Hartmann et al., 2014)

Formatted Table

Formatted Table

Table 3: Global P gap, maximum estimated P gap, maximum C sequestration reduction, and global C reduction for the natural N supply (N-limited) AR scenario (projected C sequestration of 190 Gt C).

N supply	Geogenic P supply	Maximum estimated P gap [g P m^{-2}]			Global P gap [Mt P]			Maximum C sequestration reduction [kg C m^{-2}]			Global C reduction [Gt C]		
								Wood and leaves P content					
		5th percentile	Mean	95th percentile	5th percentile	Mean	95th percentile	5th percentile	mean	95th percentile	5th percentile	mean	95th percentile
Limited	Scenario one	4.1	16.6	30.2	9.2	76.6	181.0	9.7	14.5	15.6	23.0	71.0	98.0
	Scenario two	1.6	6.7	12.2	1.0	9.9	34.7	4.7	6.2	6.5	3.0	9.5	19.0

Table 4: Minimum and maximum soil hydraulic conductivity for areas coincident to the P gap areas of each geogenic P supply scenario one, for the N-unlimited AR scenario (Supplement S1 Fig. ~~S21a~~S7a).

	Geogenic P supply scenario one	Geogenic P supply scenario two
	Hydraulic conductivity (K) [m s^{-1}]	
Min	1.5×10^{-7}	2.7×10^{-7}
Max	1.7×10^{-4}	7.8×10^{-5}
	Plant available water (PAW) [%]	
Min	4	6
Max	32	28

1785